Forschungszentrum Karlsruhe
in der Helmholtz-Gemeinschaft

Wissenschaftliche Berichte
FZKA 7433

Thermo Mechanical Fatigue Testing on EUROFER 97 and Selected Reduced Activation Ferritic Martensitic (RAFM) Steels

RAFM Steels: Metallurgical and Mechanical Characterisation

Final Report for Task TW2-TTMS-002-D19

C. Petersen

Institut für Materialforschung
Programm Kernfusion
Association Forschungszentrum Kalrsruhe/EURATOM

Oktober 2009

Forschungszentrum Karlsruhe

in der Helmholtz-Gemeinschaft

Wissenschaftliche Berichte

FZKA 7433

FUSION 301

Thermo mechanical fatigue testing on EUROFER 97 and selected Reduced Activation Ferritic Martensitic (RAFM) Steels

RAFM Steels: Metallurgical and Mechanical Characterisation

Final Report for

Task TW2-TTMS-002 - D19

C. Petersen

Institut für Materialforschung II
Programm Kernfusion
Association Forschungszentrum Karlsruhe / EURATOM

Forschungszentrum Karlsruhe GmbH, Karlsruhe

2009

The results obtained within the studies performed under this task did not yield any specific innovation or intellectual property

This work, supported by the European Communities under the contract of Association between EURATOM and Forschungszentrum Karlsruhe, was carried out within the framework of the European Fusion Development Agreement. The views and opinions expressed herein do not necessarily reflect those of the European Commission.

Forschungszentrum Karlsruhe GmbH
Postfach 3640, 76021 Karlsruhe

Mitglied der Hermann von Helmholtz-Gemeinschaft
Deutscher Forschungszentren (HGF)

ISSN 0947-8620

urn:nbn:de:0005-074331

Thermomechanische Ermüdung an EUROFER 97 und ausgesuchten niedrig aktivierbaren ferritisch martensitischen Stählen

Zusammenfassung

Blanket Module eines zukünftigen Kernfusionsreaktors werden während ihres Einsatzes, als Folge des pulsierenden Reaktorbetriebes, wechselnden thermischen und mechanischen Spannungen ausgesetzt. Deshalb müssen die als Strukturmaterialien in Frage kommenden niedrig aktivierbaren ferritisch-martensitischen Stähle auf diese thermomechanische Ermüdungsbelastung hin überprüft werden. Dazu sind nach der Entwicklung der Prüfmethode und dem Aufbau der Thermozyklieranlagen Versuche an einer Reihe von Werkstoffen durchgeführt worden.

Nach einem sorgfältigen Plausibilitätsprozess wurden Datensätze von ca. 350 thermomechanischen Ermüdungsexperimenten, mit und ohne Haltezeiten, die in den vergangenen 15 Jahren durchgeführt worden waren, nach der Entwicklung von Datenreduktionsprogrammen in die Mat-DB, das Datenbanksystem des Joint Research Centers, Petten, übertragen:

MANET I, wie angeliefert, 42 Versuche ohne Haltezeiten, 44 Versuche mit 100s Haltezeit, 4 Versuche mit 1000s Haltezeit.
MANET II, wie angeliefert, 32 Versuche ohne Haltezeiten, 38 Versuche mit 100s Haltezeit, 5 Versuche mit 1000s Haltezeit.
OPTIFER IV, wie angeliefert, 20 Versuche ohne Haltezeiten, 6 Versuche mit 100s Haltezeit.
F82H mod., wie angeliefert, 23 Versuche ohne Haltezeiten, 18 Versuche mit 100s Haltezeit, 13 Versuche mit 1000s Haltezeit.
EUROFER 97, wie angeliefert, 9 Versuche ohne Haltezeiten, 17 Versuche mit 100s Haltezeit, 23 Versuche mit 1000s Haltezeit
EUROFER 97, wärmebehandelt, 7 Versuche ohne Haltezeiten, 18 Versuche mit 1000s Haltezeit

sowie dem austenitischen Stahl:
AISI 316 L, wie angeliefert, 33 Versuche ohne Haltezeiten, 22 Versuche mit 100s Haltezeit.

Die Ergebnisse aller thermomechanischen Ermüdungsversuche zeigen für alle untersuchten Stähle eine ausgeprägte Lebensdauerreduktion im Vergleich zu Ergebnissen aus isothermen Ermüdungsexperimenten dieser Stähle. Auch die thermomechanischen Ermüdungsversuche mit Haltezeiten führen zu anderen Ergebnissen als isotherme Haltezeit-Ermüdungsversuche. Mikrostrukturelle Untersuchungen an verformten Proben aus beiden Versuchsführungen geben keinen Hinweis auf unterschiedliches Schädigungsverhalten.

Abstract

Blanket Modules of a future nuclear fusion reactor are subjected during service to alternating thermal and mechanical stresses as a consequence of the pulsed reactor operation. Therefore the Thermo-Mechanical Fatigue (TMF) behaviour of reduced activation ferrite/martensite stainless steels, as its structural material, is examined. After the development of the testing method and the setup of the facilities for TMF testing a series of different materials had been examined.

After a peer selection process evaluated data of about 350 TMF-experiments, with and without hold times, performed in the last 15 years, have been transferred into the Mat-DB, the data bank system of the Joint Research Center, Petten:

MANET I, as received, 42 tests without hold times, 44 tests with 100s hold times, 4 tests with 1000s hold times.
MANET II, as received, 32 tests without hold times, 38 tests with 100s hold times, 5 tests with 1000s hold times.
OPTIFER IV, as received, 20 tests without hold times, 6 tests with 100s hold times.
F82H mod., as received, 23 tests without hold times, 18 tests with 100s hold times, 13 tests with 1000s hold times.
EUROFER 97, as received, 9 tests without hold times, 17 tests with 100s hold times, 23 tests with 1000s hold times.
EUROFER 97, heat treated, 7 tests without hold times, 18 tests with 1000s hold times.

as well as of the austenitic steel:
AISI 316 L, as received, 33 tests without hold times, 22 tests with 100s hold times.

TMF results of examined steels show a remarkable reduction in life time compared to isothermal low cycle fatigue (LCF) tests. The application of hold times in TMF-experiments leads to different damage reactions than during LCF loading. Micro structural evaluation during both cyclic loading procedures is very similar and gives no indication of the different damage behaviour.

CONTENTS

LIST OF TABLES

LIST OF FIGURES

1 Introduction

Scientists and engineers from China, Europe, Japan, Korea, Russia, and the United States are working in an unprecedented cooperation on the next major step for the development of nuclear fusion i.e. International Thermonuclear Experimental Reactor (ITER, which means "the way" in Latin language). ITER's mission is to demonstrate the scientific and technological feasibility of nuclear fusion energy for peaceful purposes. To do this, ITER will demonstrate moderate power multiplication and essential fusion energy technologies in a system integrating the appropriate physics and technology, and test key elements required to use nuclear fusion as a practical energy source [1]. On June 28th 2005 it was decided to built ITER at the EU - Cadarache site in southern France.

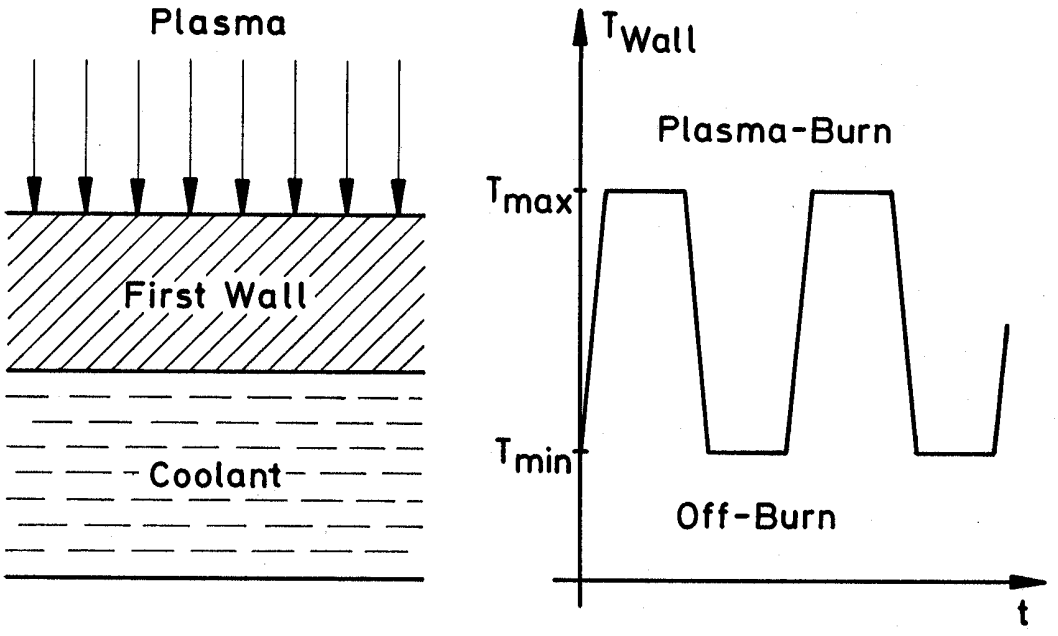

Fig. 1-1 Principle of thermal loading of the first wall during operation of a Tokamak Fusion reactor.

In Fig. 1-1 the principle of the thermal loading of the first wall of a Tokamak Fusion reactor during operation is shown. Actually the plasma burn times in the range of seconds are still very short, but to generate energy these times must be extended. Therefore we realised in our thermal-mechanical fatigue tests already hold times up to 1000 s.
The long term aim of the plasma physicists is to generate a so called quasi continuous burning plasma that is still far away from reality.

But also the next generation of Fusion reactors of the Tokamak-type, like DEMO, will operate in a cyclic mode with extended hold times.

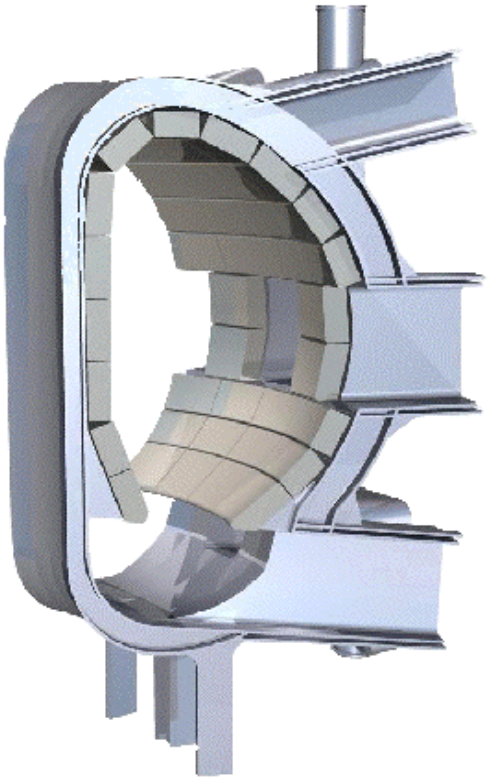

Fig. 1-2 Three dimensional arrangement of toroidal ITER-section with blanket modules

Blanket Modules (BM), schematically shown in Fig. 1-2, of a thermonuclear fusion reactor are subjected during service to alternating thermal and mechanical stresses as consequence of the pulsed reactor operation. Of particular concern is the thermo-mechanical fatigue (TMF) endurance of 9% Cr low activation Ferrite/Martensite steels. To design such blankets operating under the above loading conditions, for the time being fatigue life is predicted using design codes based on isothermal fatigue material data, but these codes will be verified with TMF-data. Of particular concern is the fatigue endurance of Test Blanket Modules (TBM) manufactured of Reduced Activation Ferrite/Martensite (RAF/M) steels. In our experiments the preceding heats of Ferrite/Martensite steels as MANET I and MANET II as well as RAF/M-steels like the Japanese F82H mod., the German OPTIFER IV and the European EUROFER 97 had been subjected to cyclic strains and stresses produced by these temperature changes. [2],[3],[4],[5],[6],[7],[8].

2 Experimental

2.1 Test facility

In Thermo Mechanical Fatigue (TMF) experiments, internal constraints inside the component caused by in stationary temperature gradients are replaced by an external uniaxial constraint resulting in partial or total suppression of thermal strains. The TMF test rig (Figs. 2-1 and 2-2) consists of a self developed stiff load frame for mechanical clamping of the sample, which was directly heated by the digitally controlled ohmic heating device [9]. The grips have been water cooled. Temperature was controlled and measured by a SCHUNTERMANN & BENNINGHOFEN temperature programmer with a 0.1 mm thick NiCr-Ni-thermocouple, spot welded 5 mm above mid plane of the specimen, to avoid an influence on the fracture zone. For each test this thermocouple was attached to the specimen at exactly the same position. Load was measured by a load cell of 20 kN full scale and the deflection of the sample by an extensometer with a gauge length of 8 mm pulled against the sample from the opposite side by springs. Load and strain data are directly registered by a PC data acquisition system. In respect with strain behaviour this simple TMF test includes complications not normally encountered with controlled TMF-tests, because the mechanical strain is not a controlled quantity and therefore a variable. Another restriction of these facilities is the fact that only so called out of phase experiments can be performed. But this procedure is identical to the loading scenarios during service of a blanket module in a fusion reactor.

In case of TMF the temperature cycling of the specimen has been performed between the lower temperature T_L and the higher temperature T_H. The temperature rate is mostly kept constant at 5.8 K/s for all TMF testing conditions and therefore variable strain rates are resulting from the temperature range changes. Tests are automatically terminated after reaching a preset electric current value indicating that a crack has covered half of the cross section of the specimen. All tests were conducted in air until failure.

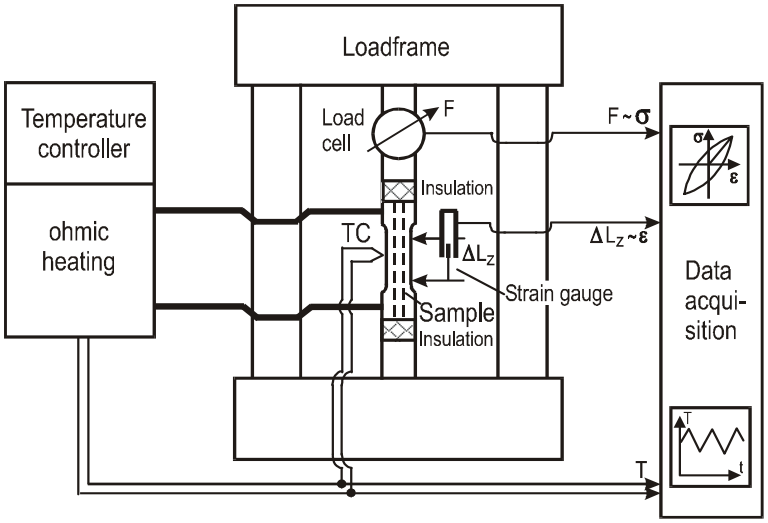

Fig. 2-1 Scheme of TMF-testing facility

Fig. 2-2 Photograph of TMF-load frame

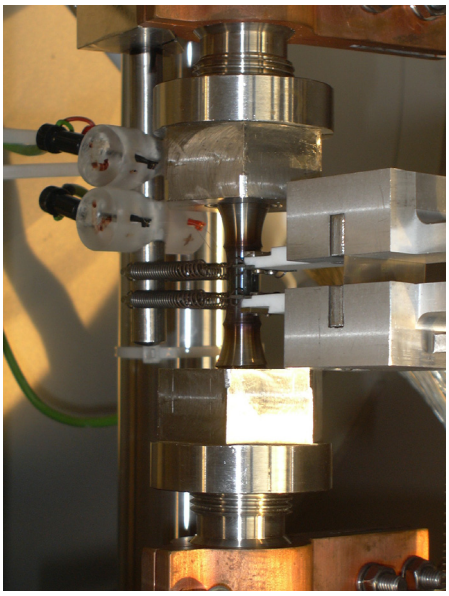

Fig. 2-3 Partly view of the TMF test section, strain measurement

Due to the fact that TMF experiments, especially with hold times, are very long lasting – the end criterion for an experiment without failure was 70000 cycles – we installed a TMF laboratory with nine facilities as it can be depicted from Fig. 2-3.

2.2 Test procedure

During initial heating from room temperature to the minimum temperature T_{min}, specimens were allowed to expand freely in direction of the specimens axis at zero stress. After reach-

ing T_{min}, the defined triangular thermal cycle between e.g. 200 °C and 600 °C with a heating and cooling rate of ±5.8 K/s was imposed about 15 – 20 times to reach steady state conditions in the grips and pullrods and to measure the actual thermal strain of the sample. Than the specimen is mechanically clamped at mean temperature T_{mean} (T_{mittel}) and the experiment started towards T_{min}.

2.2.1 TMF-Data recording

The quantities, force, mechanical deformation and time had been recorded continuously. Depending on time or a defined change of the measured quantity data scans are performed. In Fig. 2-4 are plotted as an example selected hysteresis loops during thermal-mechanical cycling between 200°C and 625°C of the austenitic steel AISI 316L where the numbers on the hysteresis indicate the cycle.

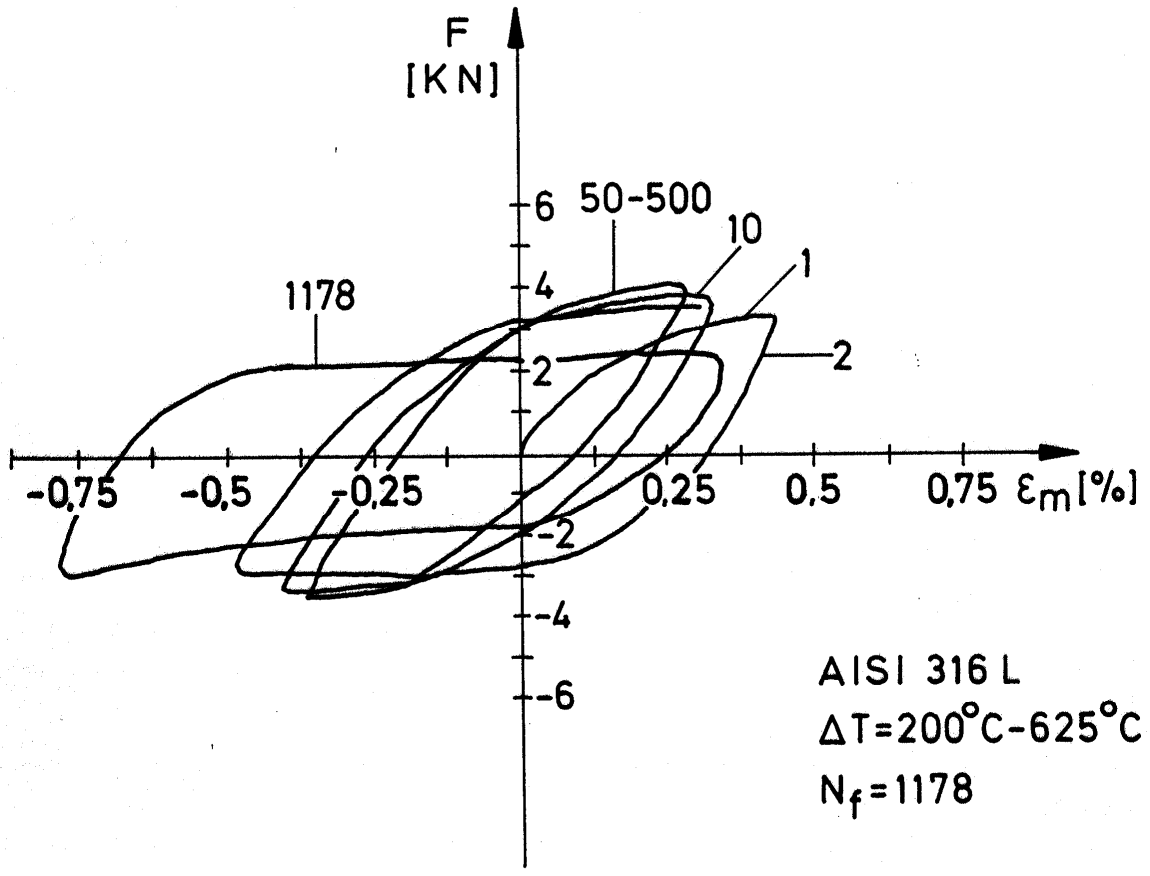

Fig. 2-4 Selected hysteresis loops during thermal-mechanical cycling of the austenitic steel AISI 316L

In the digital data recording system the following quantities of each TMF-test had been recorded: Force (German: Kraft) in [N], mechanical deformation (German: Mechanische Verformung) in [μm] and plastic deformation (German: Mechanische Verformung (F=0)) in [μm].

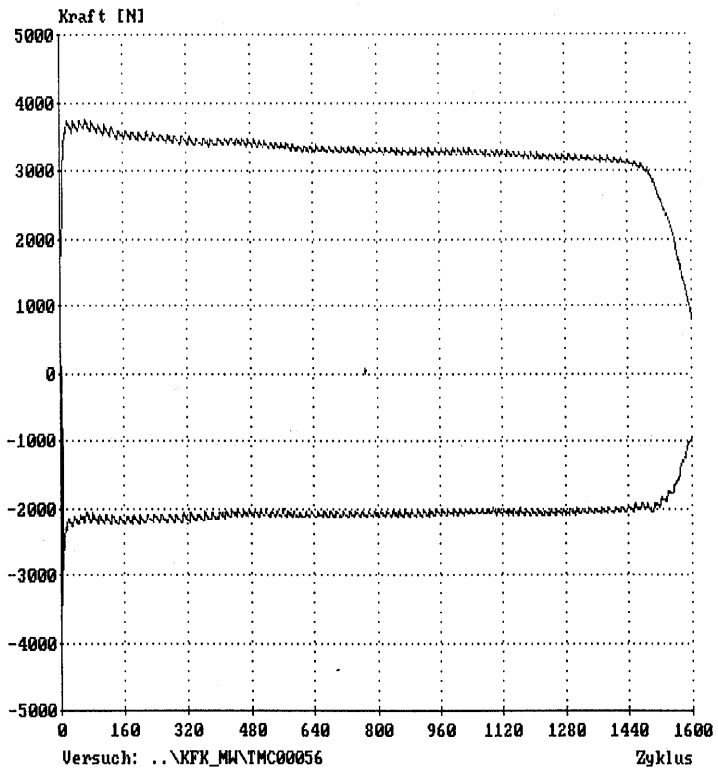

Fig. 2-5 Maximum and minimum Force versus cycles

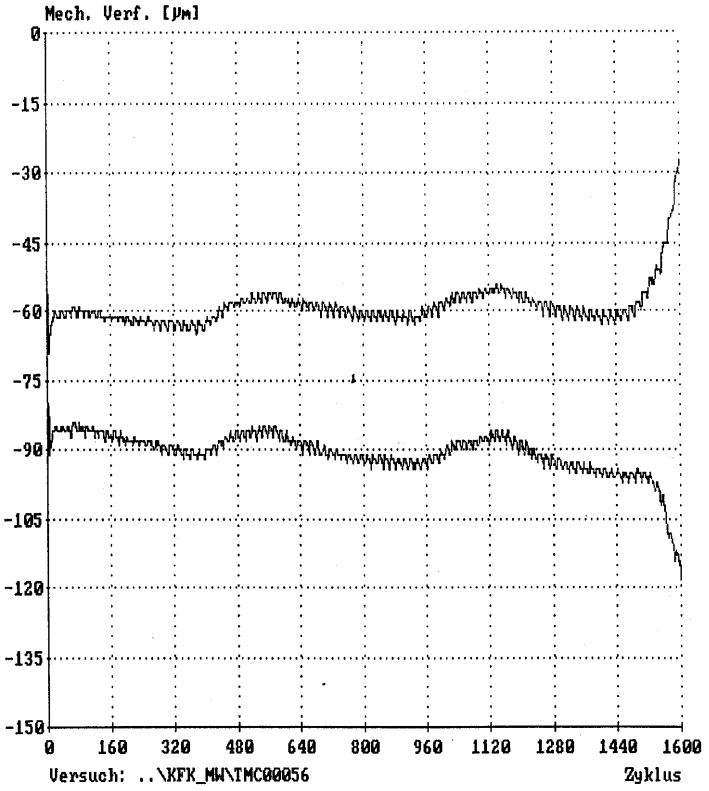

Fig. 2-6 Maximum and minimum mechanical strain versus cycles

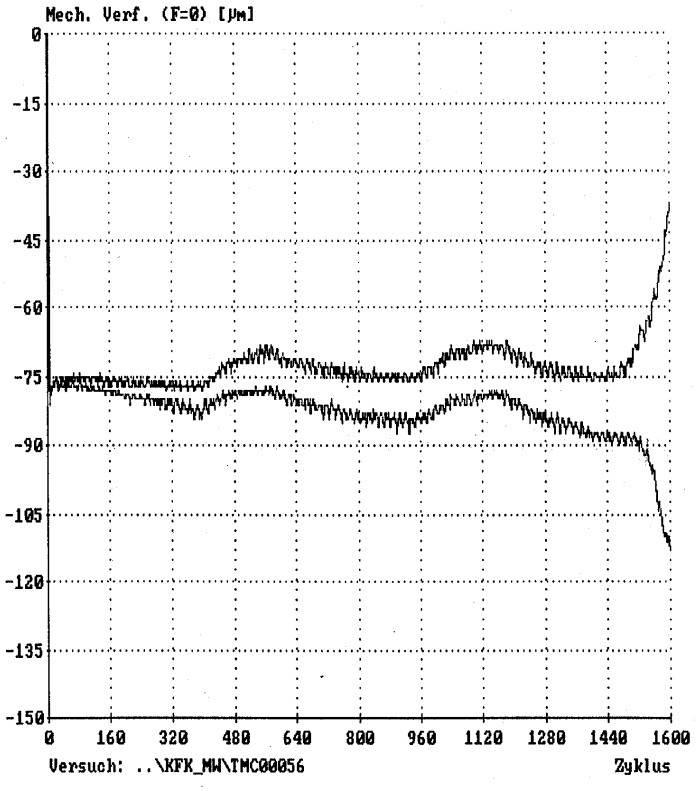

Fig. 2-7 Maximum and minimum plastic strain versus cycles

But also the maximum and minimum peak values of force, mechanical strain and plastic strain were recorded as it is shown in Figs. 2-5 to 2-7.

2.2.2 TMF-Data analysis

The sum of the thermal strain ε_{th} and the mechanical strain ε_{me} was kept constant, due to the fact, that $\Delta\varepsilon_{me} = -\Delta\varepsilon_{th}$, the appearing cyclic mechanical strains are out of phase with the selected triangular temperature-time cycles. Thus, at the high temperature of each cycle a compressive stress-level is reached and at the low temperature a tensile stress-level. T_{min} was fixed on 100°C or 200 °C and T_{max} varying from 450°C to 750°C. $R_\varepsilon = -\infty$ could have been realized, therefore the frequency range was from 0.32 to 0.5 cpm.

By definition, the net strain ε_{net}, at $T = T_{mean}$ was set to zero and therefore

$$\varepsilon_{net} = \varepsilon_{me} + \varepsilon_{th} = \varepsilon_{in,me} + \varepsilon_{el,me} + \varepsilon_{th} = 0 \qquad (1) \qquad \text{or}$$

$$\varepsilon_{me} = \varepsilon_{in,me} + \varepsilon_{el,me} = -\varepsilon_{th} \qquad (2)$$

but in the real TMF-experiment the condition $\varepsilon_{net} = 0$ was difficult to obtain, therefore a negligeble amount of net strain was detected. From Eq. 2, the mechanical and also the sum of the inelastic and elastic strain generated by the total suppression of thermal strains were determined. During all performed TMF-experiments, temperature T, thermal strain ε_{th}, net strain ε_{net}, mechanical strain ε_{me}, inelastic mechanical strain $\varepsilon_{in,me}$, elastic mechanical strain

$\varepsilon_{el,me}$ and nominal stress σ, are measured or calculated as a function of time. This is plotted qualitatively for the 1st and the 2nd cycle in Fig. 2-8.

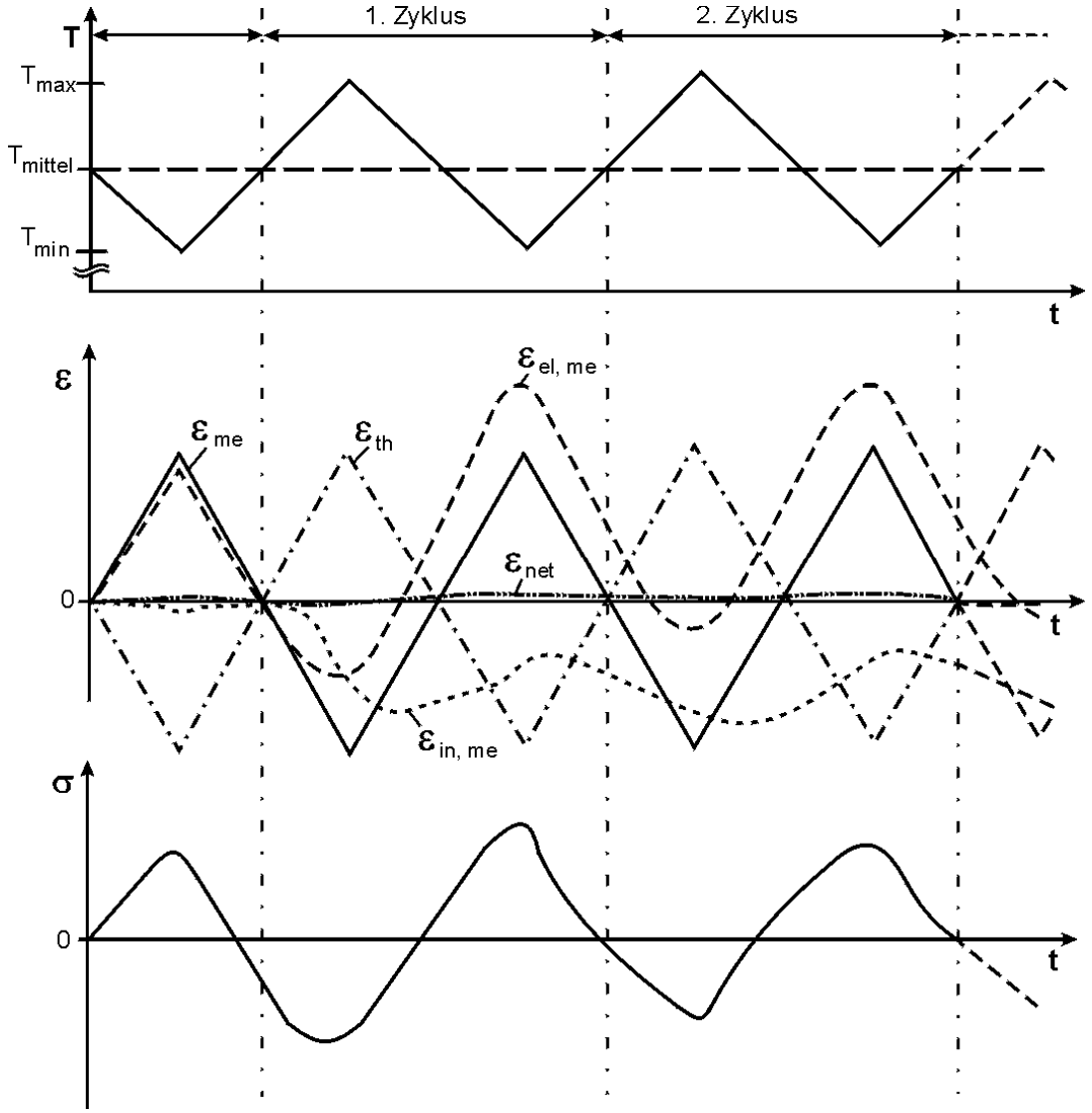

Fig. 2-8 Time dependence of measured quantities in a TMF experiment during the 1. and 2. cycle: Temperature *T*, thermal strain ε_{th}, net strain ε_{net}, mechanical strain ε_{me}, inelastic-mechanical strain $\varepsilon_{in,me}$, elastic-mechanical strain $\varepsilon_{el,me}$ and nominal stress σ.

In the TMF-experiment the nominal stress is measured as a function of temperature (Fig. 2-9, left hand side) and the stress-temperature hysteresis is evaluated. Because the thermal strain range $\Delta\varepsilon_{th}$ (T) = α(T) · ΔT, with α = thermal expansion coefficient, is completely compensated by the mechanical strain range $\Delta\varepsilon_{me}$, a stress-strain hysteresis loop as shown on the right hand side of the figure may be determined. This hysteresis loops can be used, to draw the total strain range $\Delta\varepsilon_{me,}$ the inelastic strain range $\Delta\varepsilon_{in,me,}$ and the stress range $\Delta\sigma$ (Fig. 2-9, right hand side).

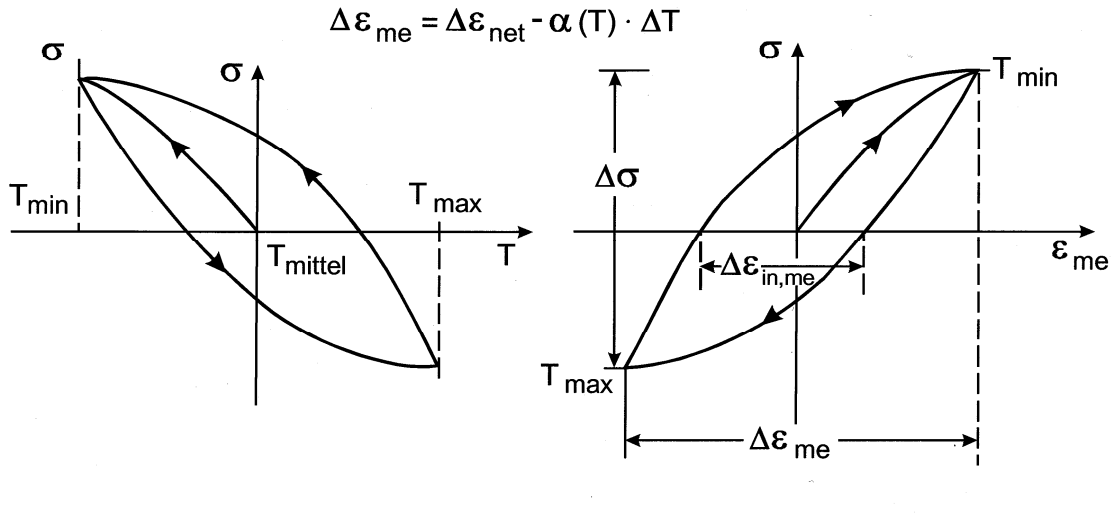

Fig. 2-9 Evaluation of the out-of-phase thermo-mechanical test

Crack initiation was determined as the first deviation from linear best fitting of the “steady-state” stress region (Fig. 2-10), giving the number of cycles to crack initiation. As a measure of the fatigue life N_f, the number of cycles to a 5 % drop from the stable linear cyclic softening behavior in tensile stress of ferrite martensite stainless steels was used. The total separation of the specimen, the traditional measurement of fatigue life, was not considered suitable since it depends on the spacial distribution of initiated cracks which can lead to a larger scatter in number of cycles to failure.

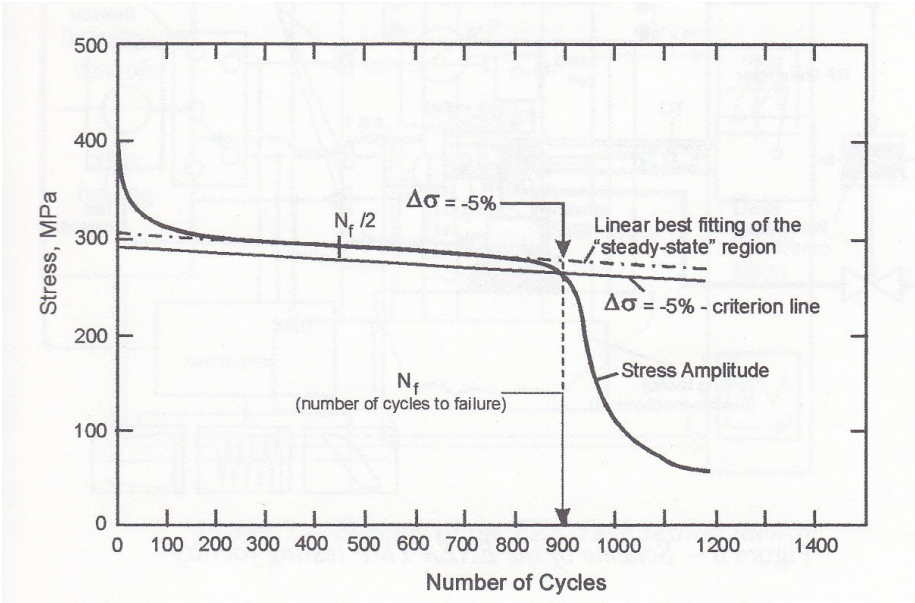

Fig. 2-10 Example of evaluation of fatigue life from peak tensile stress versus number of cycles plot of ferrite martensite stainless steels

2.3 Specimen

From all tested materials hollow TMF-specimens with the same dimensions had been manufactured within a very precise specification. The specimen with the overall dimensions of 77 mm in length and of 8.8 mm diameter in case of hour glass or in the cylindrical gauge length of 10 mm has a wall thickness of 0.4 mm. A hollow specimen (Figs. 2-11 and 2-12) has been

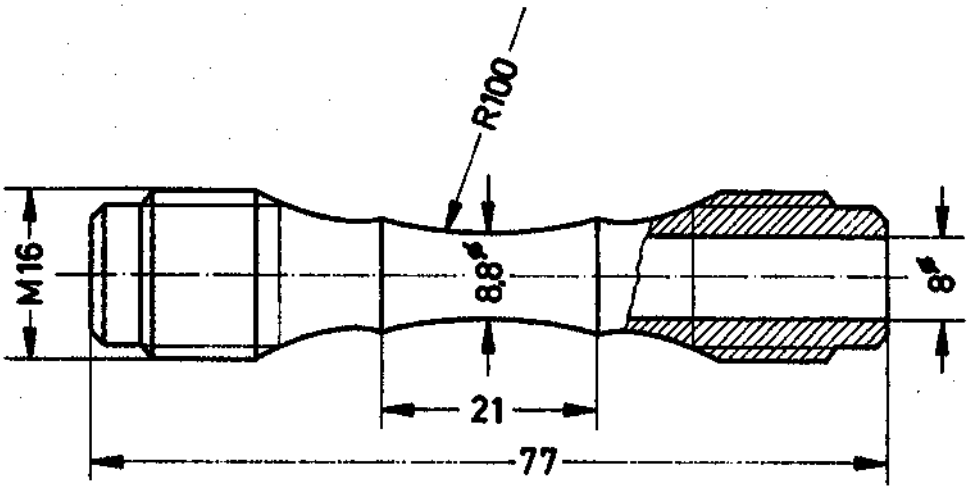

Fig. 2-11 Sketch of hourglass TMF-specimen

selected to keep the radial thermal expansion as low as possible. But due to this very thin wall thickness the danger of buckling limited the total strain in the TMF experiments on 1,2 %.

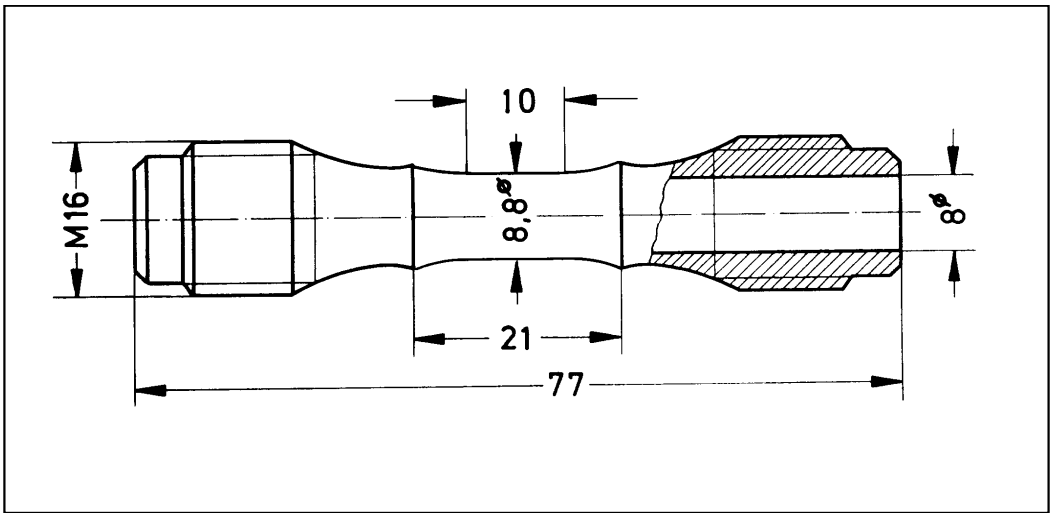

Fig. 2-12 Sketch of cylindrical TMF-specimen

The 25 mm plates of all materials had been cut perpendicular to the rolling direction into bars of 80 x 20 x 25 mm and from these pieces cylinders of 18 mm in diameter were turned. In a next step the longitudinal hole was drilled by precision deep hole drilling and the internal surface was honed. Than this rod has been drawn on a test mandrel and the outer shape was machined by turning. Finally the gauge length was grinded (Fig. 2-13). From each specimen

a protocol with tolerances inside the specification had been prepared. On each specimen a NiCr – Ni thermocouple (TC) of 0,1 mm wire diameter had been spot welded 5 mm above midline of the specimen to control the thermal cycle. In preparatory calibration experiments these TC positions were calibrated to control the middle of the specimen in the desired temperature range.

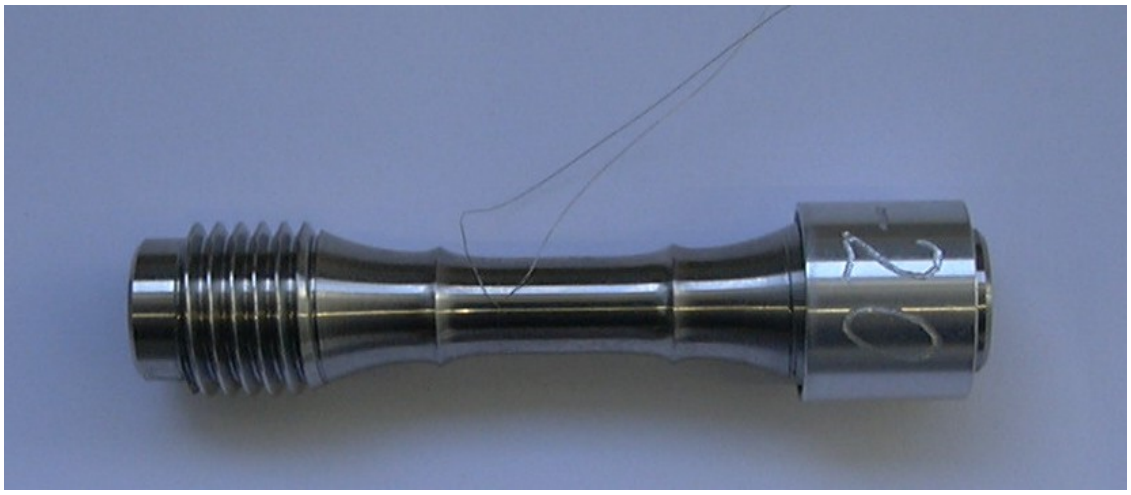

Fig. 2-13 Photograph of cylindrical TMF-specimen and spot welded thermocouple

In the first years of TMF testing we utilized hollow specimens with an hour glass shape (Fig. 2-11) of a radius of 100 mm in the gauge length of 10 mm and all TMF experiments on AISI 316L and MANET I as well as few of MANET II have been performed on this type of specimen. Most TMF experiments on MANET II and all on F82Hmod., OPTIFER IV and EUROFER 97 in both tempering modifications have been performed with TMF-specimens with cylindrical gauge length (Fig. 2-12).

2.4 Materials

The first TMF experiments had been performed on the austenitic steel AISI 316L, the chemical composition of all materials is given in Table 7-1. The following examined materials had been conventional ferritic-martensitic 10% Cr stainless steels, tested in tempered condition (see Table 7-2). These steels, named MANET I and II (MArtensitic steel for the Next European Torus), had been selected at that time by the EC Fusion Program as one of the prime candidate materials for applications as a first wall of the blanket structure. Than the development of so called Reduced Activation Ferritic/Martensitic (RAF/M) steels had been successful and we continued with one material developed at FZK of this family, named OPTIFER IV. The next material examined was from a 5-ton heat of a modified Japanese RAF/M steel F82H-mod. produced by Nippon Kokan K.K. (NKK) and distributed for collaborative research coordinated by an International Energy Agency (IEA) committee [10],[11],[12],[13].

Finally an industrial batch of the European RAF/M steel EUROFER 97 was produced by Böhler Austria GmbH. For specimen preparation plates, with a thickness of 25 mm have been used. Normalization was performed at 980 °C/0.5 h and tempering, followed by air cooling was done at 760 °C/1.5 h. For TMF testing the specimens were machined in the as

received state (labeled EUROFER 1). To study the influence of the higher austenitizing temperature on the laboratory scale, another part of the specimens (labeled EUROFER 2) was machined from 25 mm thick EUROFER 97 plates subjected to a pre-testing heat treatment at a higher austenitizing temperature of 1040 °C.

3 TMF-Results

Different series of TMF experiments were performed. In the beginning mostly tests without hold times and heating rates of 5.8 K/s with a minimum temperature of 200°C and later due to designing changes also with a minimum temperature of 100°C. In addition also hold time TMF experiments were necessary to study the creep-fatigue behaviour. The definition for the hold time experiments are: HTH, hold time at the higher temperature T_H , HTL, hold time at the lower temperature T_L and HTHL, hold time at both temperatures. Hold times of 100 and 1000 s had been realised.

After a peer selection process evaluated data of about 350 TMF-experiments, with and without hold times, performed in the last 15 years, have been transferred into the Mat-DB, the data bank system of the Joint Research Center, Petten:

The austenitic stainless steel:
AISI 316 L, as received, 33 tests without hold times, 22 tests with 100s hold times.

And the ferritic/martensitic steels:
MANET I, as received, 42 tests without hold times, 44 tests with 100s hold times, 4 tests with 1000s hold times.
MANET II, as received, 32 tests without hold times, 38 tests with 100s hold times, 5 tests with 1000s hold times.
OPTIFER IV, as received, 20 tests without hold times, 6 tests with 100s hold times.
F82H mod., as received, 23 tests without hold times, 18 tests with 100s hold times, 13 tests with 1000s hold times.
EUROFER 97, as received, 9 tests without hold times, 17 tests with 100s hold times, 23 tests with 1000s hold times.
EUROFER 97, heat treated, 7 tests without hold times, 18 tests with 1000s hold times.

Initially TMF experiments on the austenitic stainless steel AISI 316L have been performed because the in vessel structures of the first bigger nuclear fusion facilities were planned to be built from this material.

3.1 AISI 316L

Tests without hold times and heating rates of 5.8 K/s with a minimum temperature of 200°C and variable maximum temperatures from 550°C to 750°C had been conducted on hollow hour glass specimens. In Fig. 3-1 is plotted in double logarithmic scale the dependency of the total mechanical strain amplitude $\Delta\varepsilon_{t,m}$ from 0.4 % to 1.4 % versus the number of cycles to failure N_f.

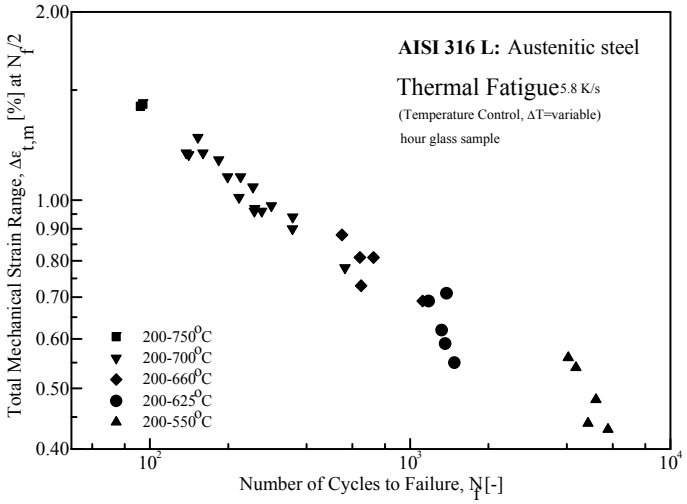

Fig. 3-1 TMF behaviour of AISI 316L without hold time in a temperature range between 200°C and 550 to 750°C in a $\Delta\varepsilon_{t,m}$ versus N_f plot

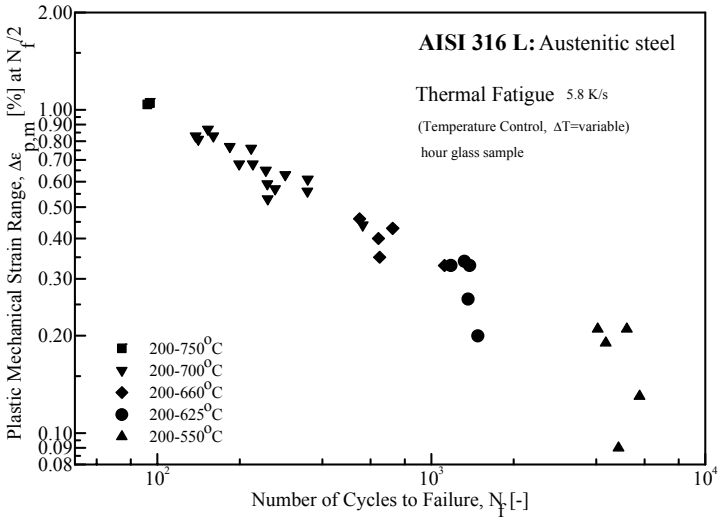

Fig. 3-2 TMF behaviour of AISI 316L without hold time in a temperature range between 200°C and 550 to 750°C in a $\Delta\varepsilon_{p,m}$ versus N_f plot

In Fig. 3-2 is plotted in double logarithmic scale the dependency of the total plastic mechanical strain amplitude $\Delta\varepsilon_{p,m}$ from 0.09 % to 1.2 % versus the number of cycles to failure N_f, with increasing scatter for lower $\Delta\varepsilon_{p,m}$.

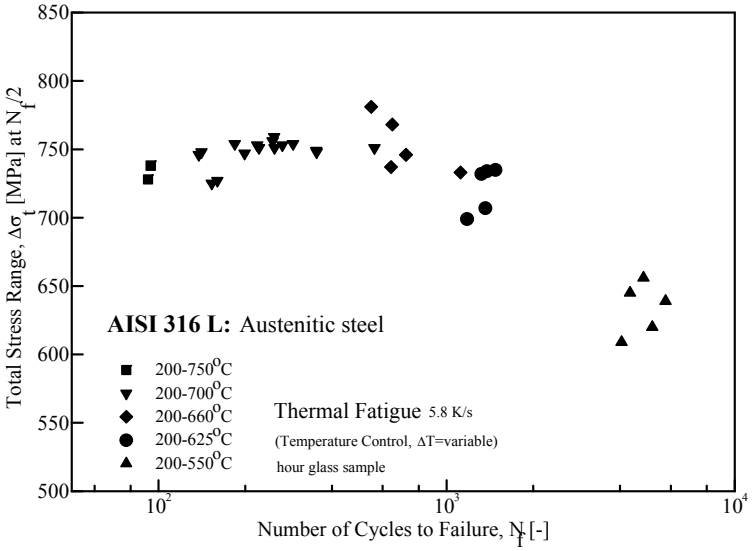

Fig. 3-3 TMF behaviour of AISI 316L without hold time in a temperature range between 200°C and 550 to 750°C in a $\Delta\sigma_t$ versus N_f plot

The total saturation stress $\Delta\sigma_t$ shown in Fig. 3-3 is at TMF testing nearly independent of the number of cycles to failure N_f and decreasing for the lowest temperature range of 200 – 550°C only.

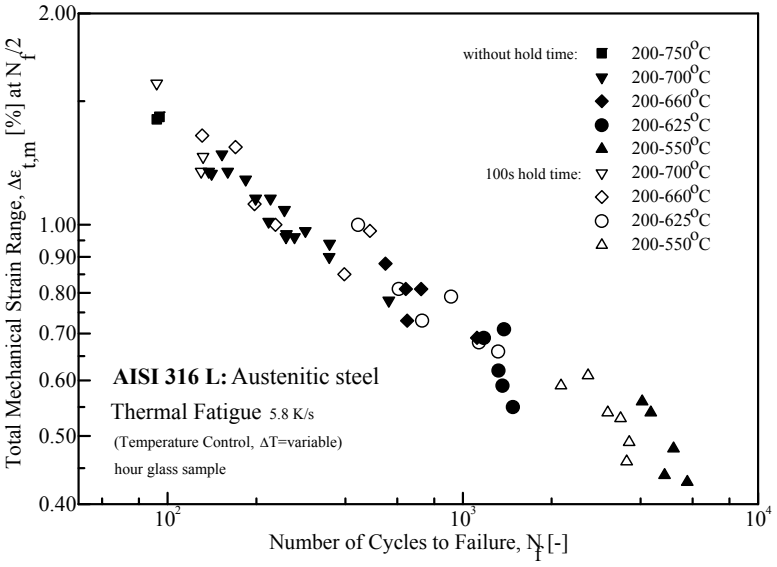

Fig. 3-4 TMF behaviour of AISI 316L with 100s and without hold time in a temperature range between 200°C and 550 to 750°C in a $\Delta\varepsilon_{t,m}$ versus N_f plot

Tests with 100 s hold times and heating rates of 5.8 K/s with a minimum temperature of 200°C and variable maximum temperatures from 550°C to 750°C had been conducted on hollow hour glass specimens. In Fig 3-4 are compared data of these tests with results of TMF tests without hold times in the same temperature range. In double logarithmic scale the de-

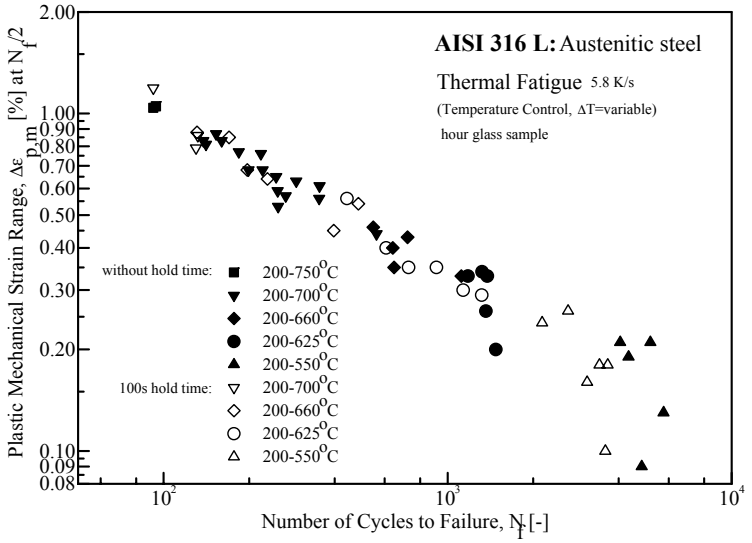

Fig. 3-5 TMF behaviour of AISI 316L with 100s and without hold time in a temperature range between 200°C and 550 to 750°C in a $\Delta\varepsilon_{p,m}$ versus N_f plot

pendency of the total mechanical strain amplitude $\Delta\varepsilon_{t,m}$ from 0.4 % to 1.4 % versus the num ber of cycles to failure N_f is decreasing with increasing scatter for lower temperature ranges. The influence of hold times in all three positions of the cycle, i.e. HTH, hold time at the higher temperature T_H, HTL, hold time at the lower temperature T_L and HTHL, hold time at both temperatures is nearly a factor of 2 in this austenitic steel.

In Fig. 3-5 is plotted in double logarithmic scale the dependency of the total plastic mechanical strain amplitude $\Delta\varepsilon_{p,m}$ from 0.1 % to 1.2 % versus the number of cycles to failure N_f, with increasing scatter for lower $\Delta\varepsilon_{p,m}$. Also for this quantity the influence of hold times in all three positions of the cycle, i.e. HTH, HTL and HTHL is nearly a factor of 2 in this austenitic steel.

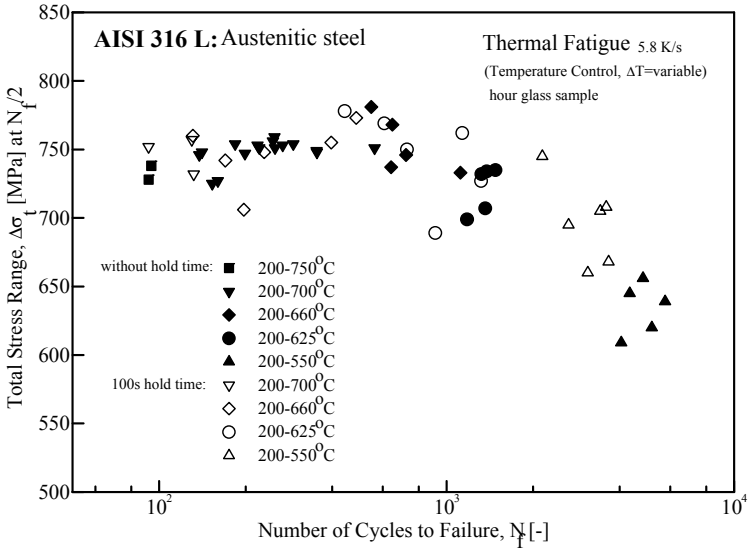

Fig. 3-6 TMF behaviour of AISI 316L with 100s and without hold time in a temperature range between 200°C and 550 to 750°C in a $\Delta\sigma_t$ versus N_f plot

In Fig. 3-6 is plotted in half logarithmic scale the dependency of the total saturation stress $\Delta\sigma_t$ from 600 MPa to 800 MPa versus the number of cycles to failure N_f, with a broad scatter over the whole range of N_f and with decreasing stresses for the lower temperature range of 200 – 550°C. Also for this quantity the influence of hold times in all three positions of the cycle, i.e. HTH, HTL and HTHL is nearly a factor of 2 in this austenitic steel.

Detailed results of every TMF test of AISI 316L will be found in chapter 7.3.1 of the Annex and in the enclosed CD.

3.2 MANET I and MANET II

Tests on MANET I without hold times and heating rates of 5.8 K/s with a minimum temperature of 200°C and variable maximum temperatures from 550°C to 700°C had been conducted on hollow hour glass specimens. In Fig. 3-7 is plotted in double logarithmic scale the dependency of the total mechanical strain amplitude $\Delta\varepsilon_{t,m}$ from 0.3 % to 0.7 % versus the number of cycles to failure N_f. With increasing maximum temperature $\Delta\varepsilon_{t,m}$ is increasing and reaches in the temperature range 200 – 700°C only numbers of cycles to failure in the range of hundreds. Due to the fact that the ferrite-martensite steels show cyclic softening, the values for total mechanical strain range, plastic mechanical strain range and total stress range had been taken at the half value of number of cycles to failure.

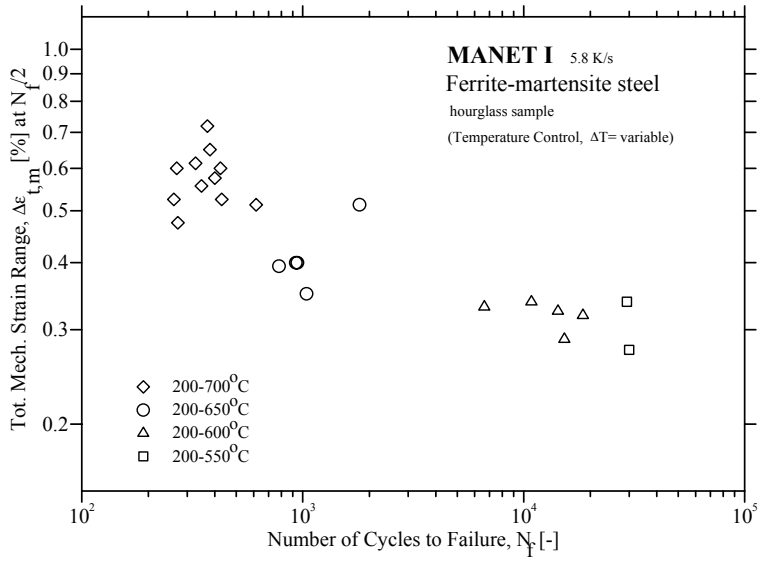

Fig. 3-7 TMF behaviour of MANET I without hold time and 200°C as the lower temperature in a $\Delta\varepsilon_{t,m}$ versus N_f plot

The thermal fatigue life is found to be in the range of two times (200 – 700°C) till 10 times (200 – 550°C) of that received on AISI 316L under comparable TMF testing conditions. The reason is the strong difference in thermal expansion of both materials.

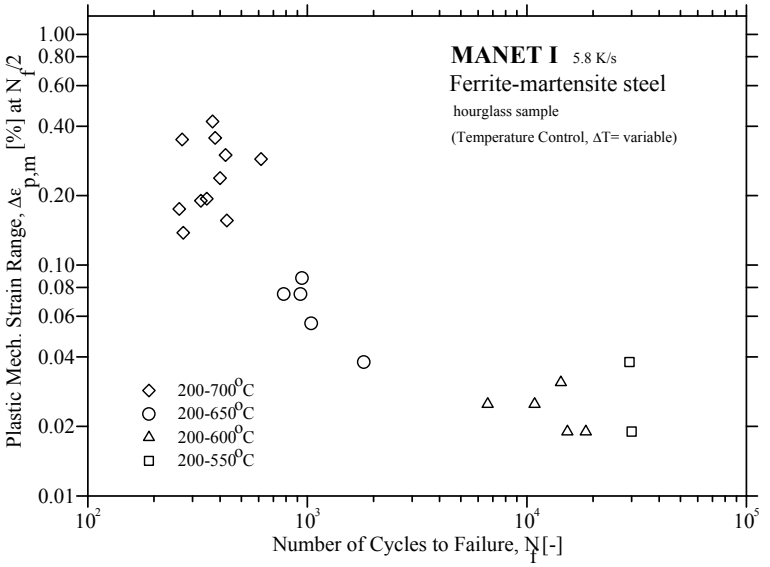

Fig. 3-8 TMF behaviour of MANET I without hold time and 200°C as the lower temperature in a $\Delta\varepsilon_{p,m}$ versus N_f plot

In Fig. 3-8 is plotted in double logarithmic scale the dependency of the plastic mechanical strain amplitude $\Delta\varepsilon_{p,m}$ from 0.02 % to 0.4 % versus the number of cycles to failure N_f. With

increasing maximum temperature $\Delta\varepsilon_{p,m}$ is increasing and reaches in the temperature range 200 – 700°C only numbers of cycles to failure in the range of hundreds.

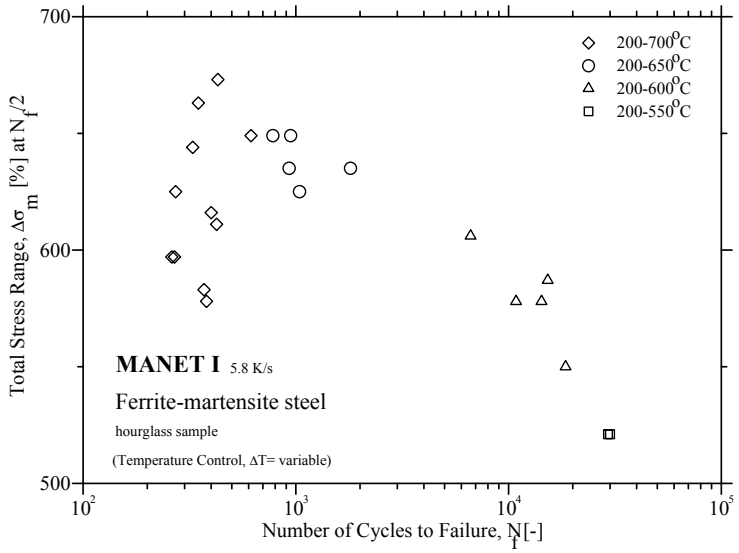

Fig. 3-9 TMF behaviour of MANET I without hold time and 200°C as the lower temperature in a $\Delta\sigma_t$ versus N_f plot

The total saturation stress $\Delta\sigma_t$ depicted in Fig. 3-9 shows at TMF testing a broad scatter versus number of cycles to failure N_f and is decreasing for the lowest temperature range of 200 – 550°C only.

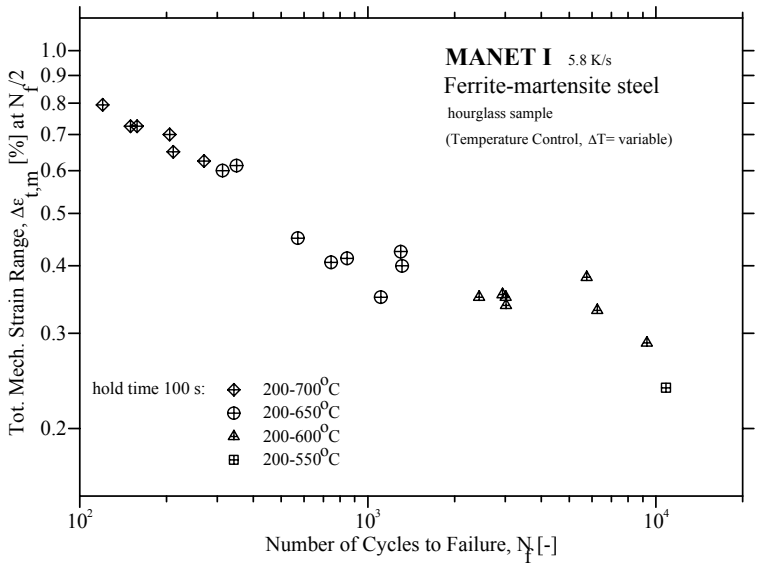

Fig. 3-10 TMF behaviour of MANET I with 100 s hold time and 200°C as the lower temperature in a $\Delta\varepsilon_{t,m}$ versus N_f plot

Also on MANET I tests with 100 s hold times and heating rates of 5.8 K/s with a minimum temperature of 200°C and variable maximum temperatures from 550°C to 700°C had been conducted on hollow hour glass specimens.
In Fig. 3-10 is plotted in double logarithmic scale the dependency of the total mechanical strain amplitude $\Delta\varepsilon_{t,m}$ from 0.25 % to 0.8 % versus the number of cycles to failure N_f. With increasing maximum temperature $\Delta\varepsilon_{t,m}$ is increasing and reaches in the temperature range 200 – 700°C only numbers of cycles to failure in the range of hundreds, but with lower scatter than at tests without hold times. Compared to results presented in Fig. 3-7, the material- reaches lower N_f -values, if a hold time of 100s is applied.

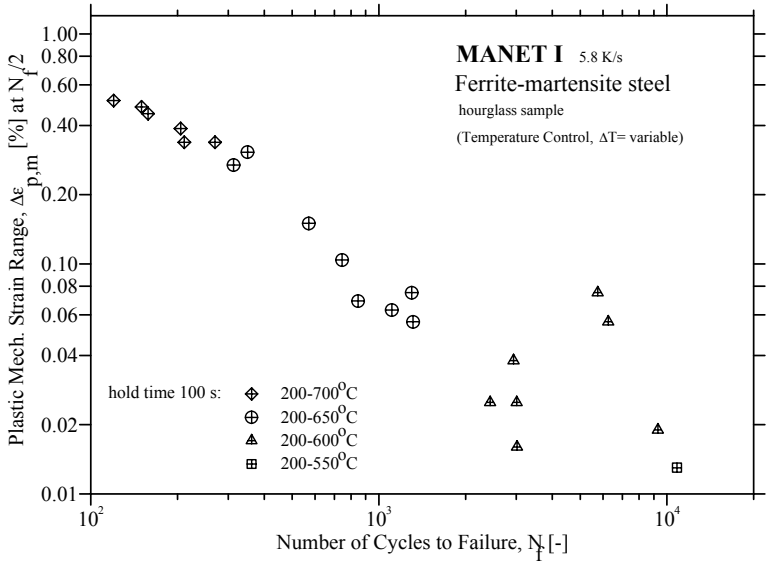

Fig. 3-11 TMF behaviour of MANET I with 100 s hold time and 200°C as the lower temperature in a $\Delta\varepsilon_{p,m}$ versus N_f plot

In Fig. 3-11 is plotted in double logarithmic scale the dependency of the plastic mechanical strain amplitude $\Delta\varepsilon_{p,m}$ from 0.013 % to 0.5 % versus the number of cycles to failure N_f. With increasing maximum temperature $\Delta\varepsilon_{p,m}$ is increasing and reaches in the temperature range 200 – 700°C only numbers of cycles to failure in the range of hundreds but at lower N_f – valued for higher plastic mechanical strain amplitudes $\Delta\varepsilon_{p,m}$ than at tests without hold times. Only in the lower temperature range of 200°C – 600°C the scatter in $\Delta\varepsilon_{p,m}$ was higher.

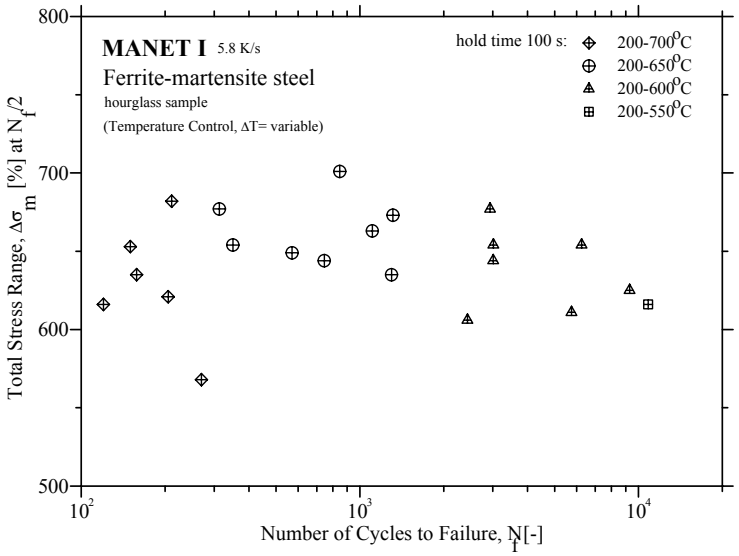

Fig. 3-12 TMF behaviour of MANET I with 100 s hold time and 200°C as the lower temperature in a $\Delta\sigma_t$ versus Nf plot

Whereas the total saturation stress $\Delta\sigma_t$ displayed in Fig. 3-12 shows at TMF testing with 100 s hold times a broad scatter versus number of cycles to failure N_f and except of the results at lower ΔT is nearly independent from temperature range.

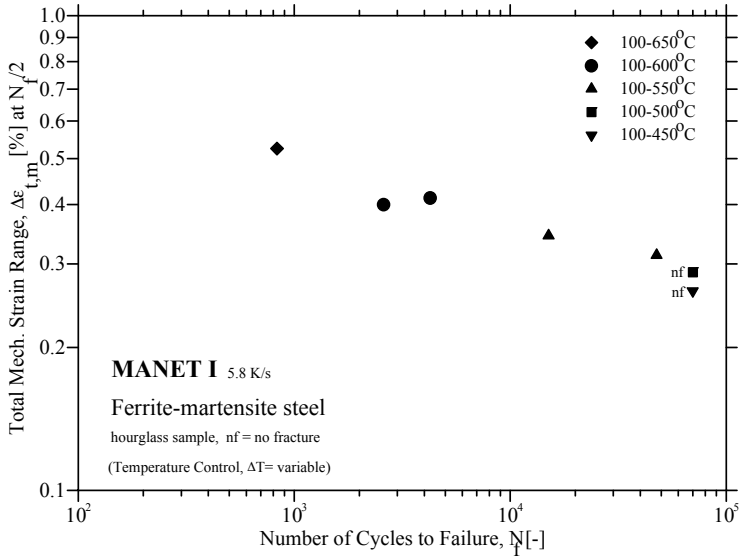

Fig. 3-13 TMF behaviour of MANET I without hold time and 100°C as the lower temperature in a $\Delta\varepsilon_{t,m}$ versus N_f plot

Tests on MANET I without hold times and heating rates of 5.8 K/s with a minimum temperature of 100°C and variable maximum temperatures from 450°C to 600°C had been con-

ducted on hollow hour glass specimens, too. In Fig. 3-13 is plotted in double logarithmic scale the dependency of the total mechanical strain amplitude $\Delta\varepsilon_{t,m}$ from 0.28 % to 0.5 % versus the number of cycles to failure N_f. With increasing maximum temperature $\Delta\varepsilon_{t,m}$ is increasing and reaches in the comparable temperature range 100 – 600°C numbers of cycles to failure of one order to magnitude higher, than between 200 – 700°C (Fig. 3-7). At temperature ranges below 100°C – 500°C no fracture occurred in the design window of 70000 cycles.

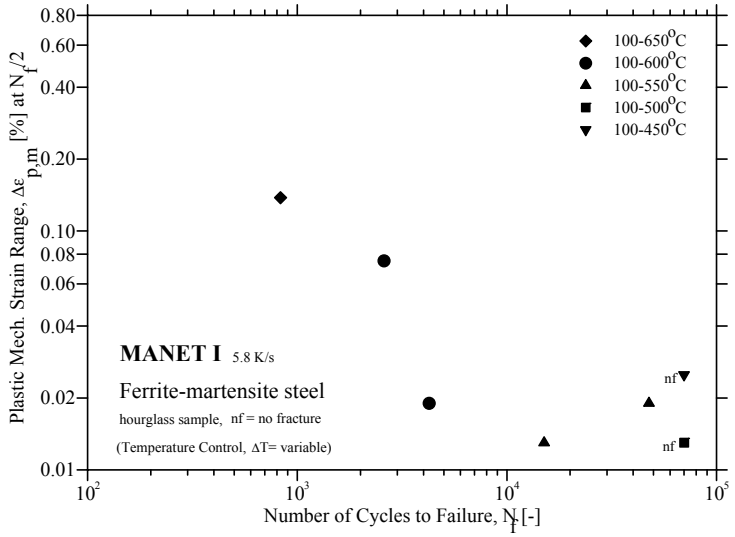

Fig. 3-14 TMF behaviour of MANET I without hold time and 100°C as the lower temperature in a $\Delta\varepsilon_{p,m}$ versus N_f plot

In Fig. 3-14 is plotted in double logarithmic scale the dependency of the plastic mechanical strain amplitude $\Delta\varepsilon_{p,m}$ from 0.013 % to 0.15 % of MANET I versus the number of cycles to failure N_f. With decreasing maximum temperature $\Delta\varepsilon_{p,m}$ is decreasing and reaches in the comparable temperature range 100 – 600°C numbers of cycles to failure of one order to magnitude higher, than between 200 – 700°C (Fig. 3-8).

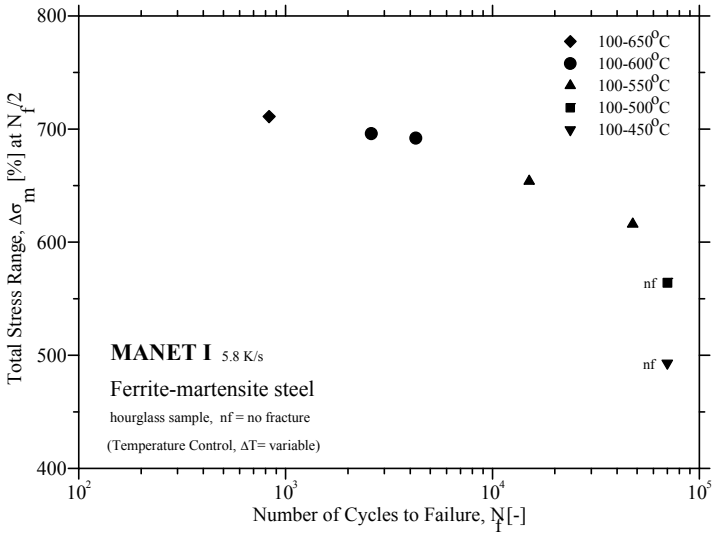

Fig. 3-15 TMF behaviour of MANET I without hold time and 100°C as the lower temperature in a $\Delta\sigma_t$ versus N_f plot

The total saturation stress $\Delta\sigma_t$ of MANET I in Fig. 3-15 shows at TMF testing a decreasing behaviour versus number of cycles to failure N_f with decreasing temperature range.

Detailed results of every TMF test of MANET I will be found in chapter 7.3.2 of the Annex and in the enclosed CD.

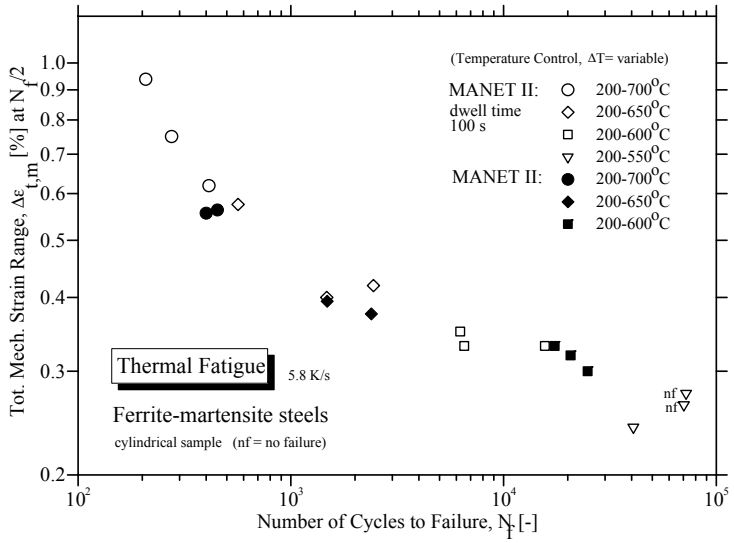

Fig. 3-16 TMF behaviour of MANET II without hold time and with 100 s hold time in a $\Delta\varepsilon_{t,m}$ versus N_f plot

The influence of hold time of 100 s on thermal fatigue behaviour of MANET II had been examined and the results are shown in Figs. 3-16 to 3-18. A comparison between both MANET materials show that $\Delta\varepsilon_{t,m}$ of MANET II is in the same ΔT-range (Fig. 3-7) of a factor of half of the values of MANET I (Fig. 3-16).

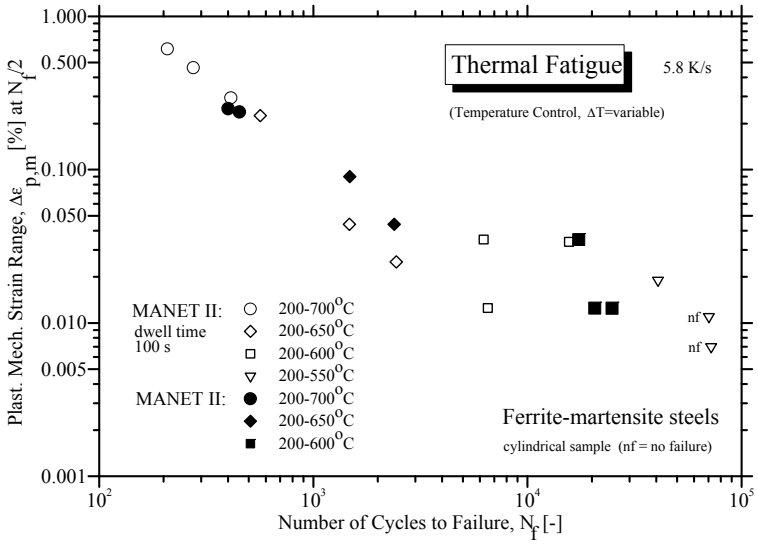

Fig. 3-17 TMF behaviour of MANET II without hold time and with 100 s hold time in a $\Delta\varepsilon_{p,m}$ versus N_f plot

The comparison between tests without and 100s hold time on thermal fatigue behaviour of MANET II is made in Fig. 3–16 in respect to total strain range $\Delta\varepsilon_{t,m}$ vs. number of cycles to

failure at comparable temperature changes. The hold time is at rapidly increasing total strain range much more damaging.

The comparison of thermally fatigued MANET II samples between tests without and 100s hold time in respect to plastic strain range $\Delta\varepsilon_{p,m}$ results for the hold time in much higher strain and shorter life values as for the condition without hold time. This is shown in Fig. 3-17. Also here the test condition 200°C to 550°C with 100s hold time leads into 70000 cycles not to a fracture of the specimen.

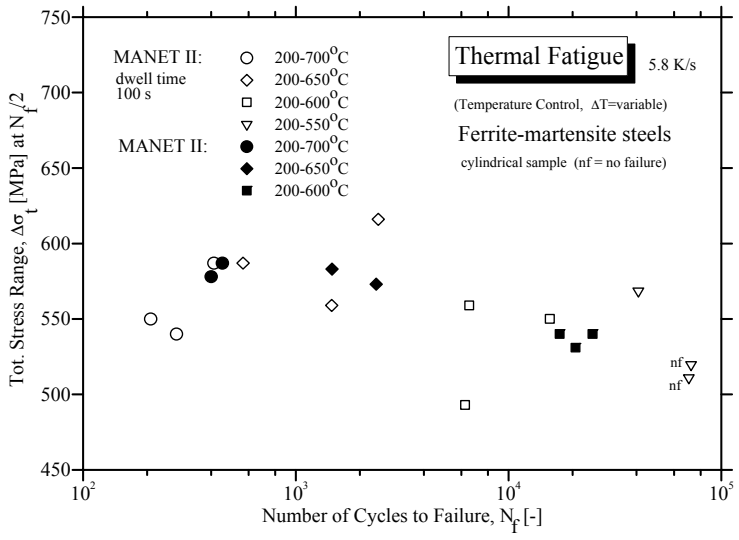

Fig. 3-18 TMF behaviour of MANET II without hold time and with 100 s hold time in a $\Delta\sigma_t$ versus N_f plot

The influence to stress range (Fig. 3-18) is nearly independent of testing parameters and disappears in a broad scatter band.

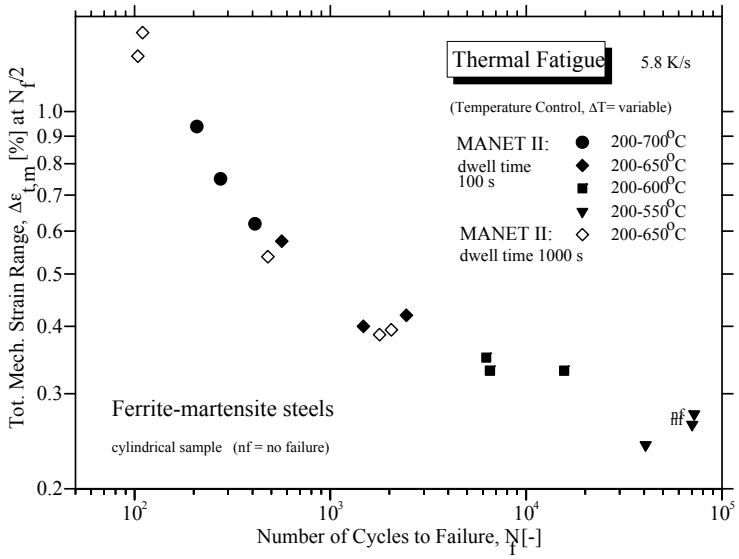

Fig. 3-19 TMF behaviour of MANET II with 100 s and 1000 s hold time in a $\Delta\varepsilon_{t,m}$ versus N_f plot

The influence of two different hold times (100 s and 1000 s) on thermal fatigue behaviour of this steel had been examined and the results are shown in Figs. 3-19 to 3–21.

The comparison between 100 s and 1000 s hold time on thermal fatigue behaviour of MANET II is made in Fig. 3–19 in respect to total strain range $\Delta\varepsilon_{t,m}$ vs. number of cycles to failure at comparable temperature changes. The longer hold time is much more damaging,

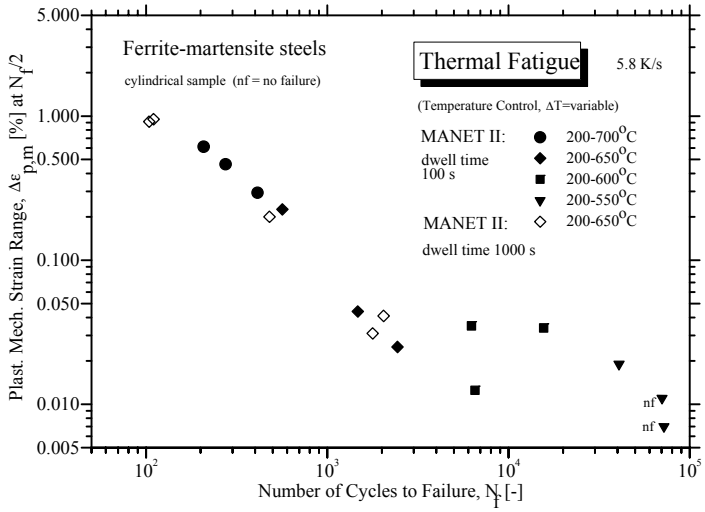

Fig. 3-20 TMF behaviour of MANET II with 100 s and 1000 s hold time in a $\Delta\varepsilon_{p,m}$ versus N_f plot

mainly if the hold time is applied at T_{min} and T_{max}, so called HTHL condition.

The comparison of thermally fatigued MANET II samples of both test conditions in respect to plastic strain range $\Delta\varepsilon_{p,m}$ results for the longer hold time in much higher strain and shorter life values as for the shorter hold time. This is shown in Fig. 3-20.

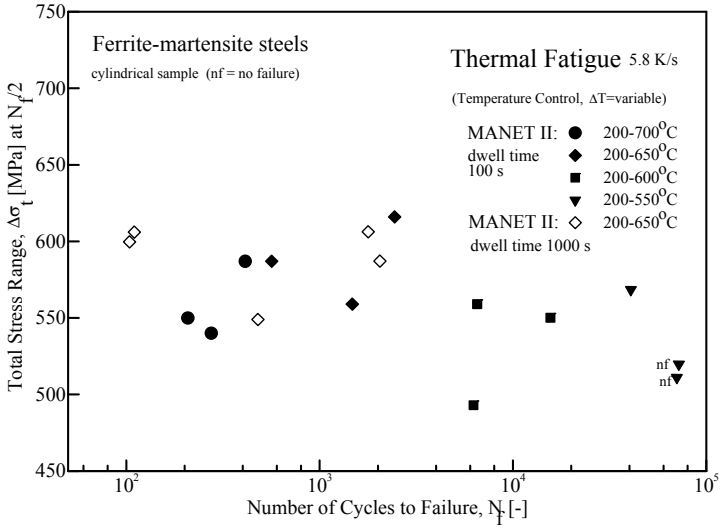

Fig. 3-21 TMF behaviour of MANET II with 100 s and 1000 s hold time in a $\Delta\sigma_t$ versus N_f plot

The influence to stress range (Fig. 3-21) disappears in a broad scatter band again.

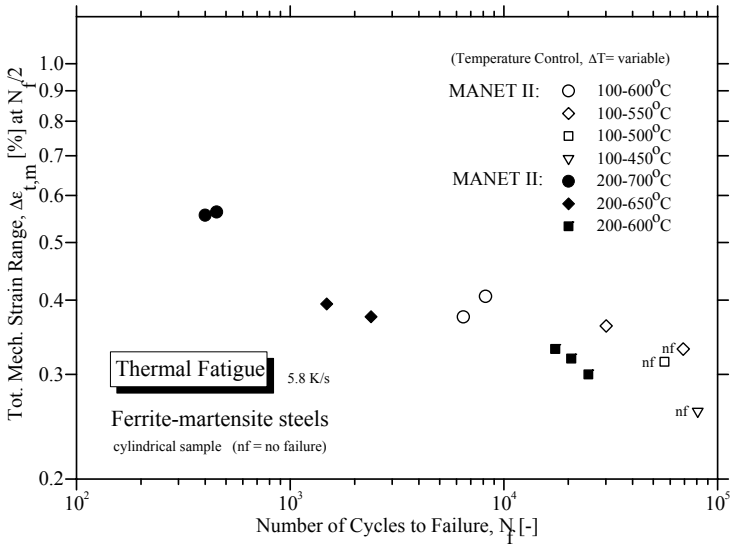

Fig. 3-22 TMF behaviour of MANET II for two different minimum temperatures and similar temperature ranges in a $\Delta\varepsilon_{t,m}$ versus N_f plot

Tests on MANET II without hold times and heating rates of 5.8 K/s with two different minimum temperatures of 100°C and 200°C and variable maximum temperatures from 450°C to 700°C had been conducted on cylindrical specimens. In Fig 3-22 is plotted in double logarithmic scale the dependency of the total mechanical strain amplitude $\Delta\varepsilon_{t,m}$ from 0.3 % to 0.6 % versus the number of cycles to failure N_f. With increasing maximum temperature $\Delta\varepsilon_{t,m}$ is increasing and reaches in the temperature range 200 – 700°C only numbers of cycles to failure in the range of hundreds. Whereas the test series with the lower minimum temperature of 100°C, but the same ΔT leads to a smaller total mechanical strain amplitude $\Delta\varepsilon_{t,m}$ of 0.4 % and reaches N_f-values of more than one magnitude higher.

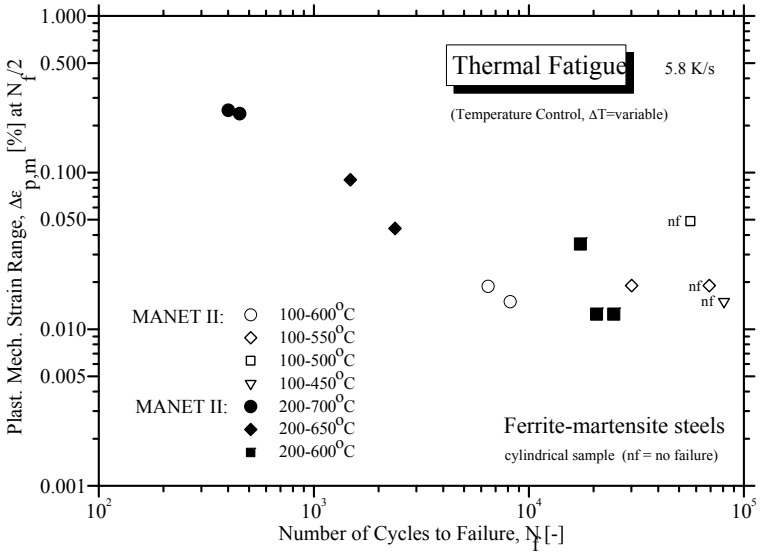

Fig. 3-23 TMF behaviour of MANET II for two different minimum temperatures and similar temperature ranges in a $\Delta\varepsilon_{p,m}$ versus N_f plot

In Fig. 3-23 is plotted in double logarithmic scale the dependency of the plastic mechanical strain amplitude $\Delta\varepsilon_{p,m}$ from 0.015 % to 0.3 % versus the number of cycles to failure N_f. With increasing maximum temperature $\Delta\varepsilon_{p,m}$ is increasing and reaches in the temperature range 200 – 700°C only numbers of cycles to failure in the range of hundreds. Whereas the test series with the lower minimum temperature of 100°C, but the same ΔT leads to a smaller total mechanical strain amplitude $\Delta\varepsilon_{p,m}$ of 0.018 % and reaches N_f-values of more than one magnitude higher.

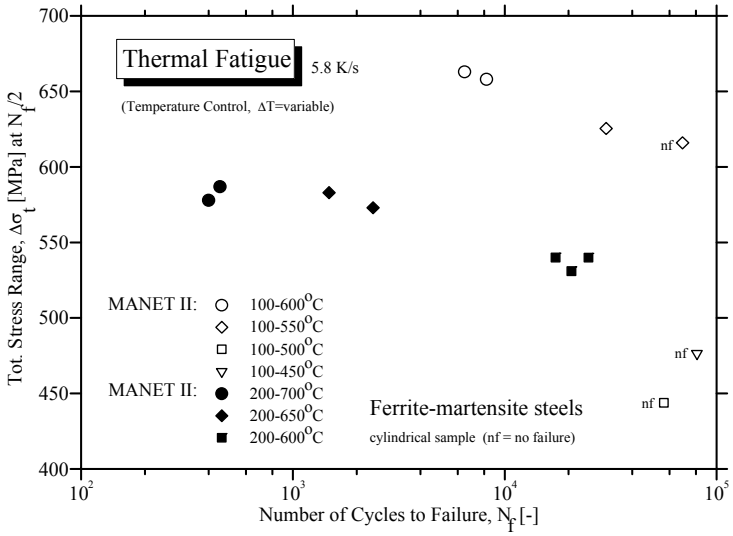

Fig. 3-24 TMF behaviour of MANET II for two different minimum temperatures and similar temperature ranges in a $\Delta\sigma_t$ versus N_f plot

The total saturation stress $\Delta\sigma_t$ shown in Fig. 3-24 shows at the tests with the higher minimum temperature of 200°C a stress level between 550 and 600 Mpa, whereas tests with the lower minimum temperature of 100°C, at the same ΔT lead to higher $\Delta\sigma_t$ of 650 MPa and reaches N_f-values of more than one magnitude higher.

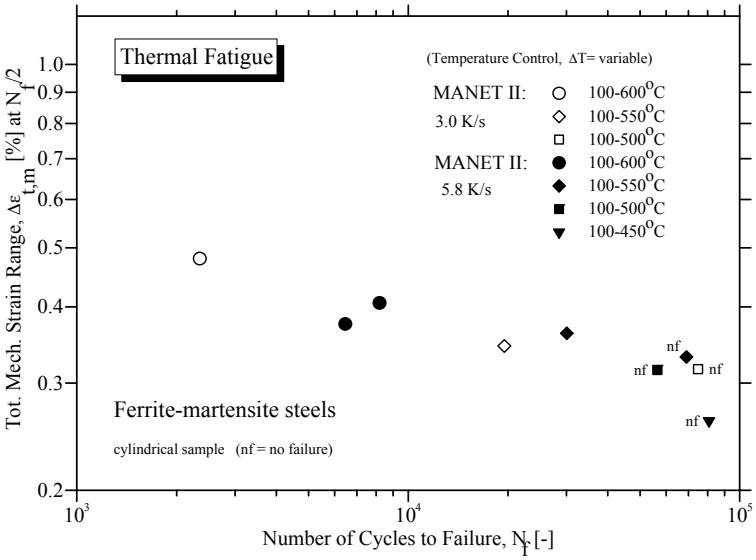

Fig. 3-25 Comparison of the TMF behaviour of MANET II without hold time for two heating and cooling rates with similar temperature range in a $\Delta\varepsilon_{t,m}$ versus N_f plot

In Fig. 3-25 is plotted in double logarithmic scale the dependency of the total mechanical strain amplitude $\Delta\varepsilon_{t,m}$ from 0.25 % to 0.5 % versus the number of cycles to failure N_f for two

heating and cooling rates in a similar temperature range. With increasing minimum temperature $\Delta\varepsilon_{t,m}$ is decreasing and reaches e.g. in the temperature range 100 – 600°C higher numbers of cycles to failure by a factor of 2.5.

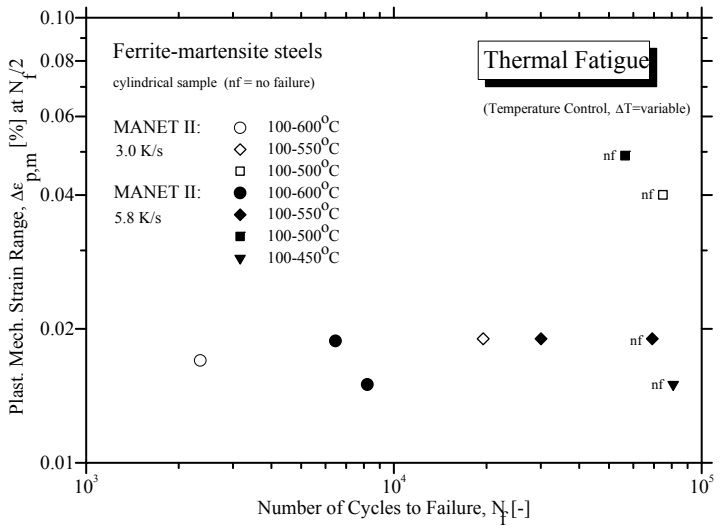

Fig. 3-26 Comparison of the TMF behaviour of MANET II without hold time for two heating and cooling rates with similar temperature range in a $\Delta\varepsilon_{p,m}$ versus N_f plot

In Fig. 3-26 is plotted in double logarithmic scale the dependency of the plastic mechanical strain amplitude $\Delta\varepsilon_{p,m}$ from 0.015 % to 0.04 % versus the number of cycles to failure N_f for

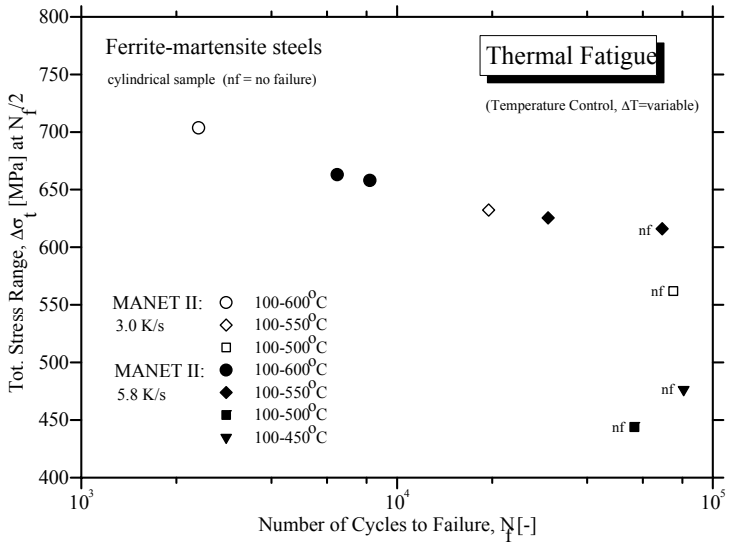

Fig. 3-27 Comparison of the TMF behaviour of MANET II without hold time for two heating and cooling rates with similar temperature range in a $\Delta\sigma_t$ versus N_f plot

two heating and cooling rates in a similar temperature range. The plastic mechanical strain amplitude $\Delta\varepsilon_{p,m}$ is independent of the temperature range. Only in the temperature range 100 – 500°C the plastic mechanical strain amplitude $\Delta\varepsilon_{p,m}$ is increasing, but specimens failure was not reached into 70.000 cycles.

The total saturation stress $\Delta\sigma_t$ shown in Fig. 3-27 for two heating and cooling rates with similar temperature ranges decreases at TMF testing with decreasing temperature range.

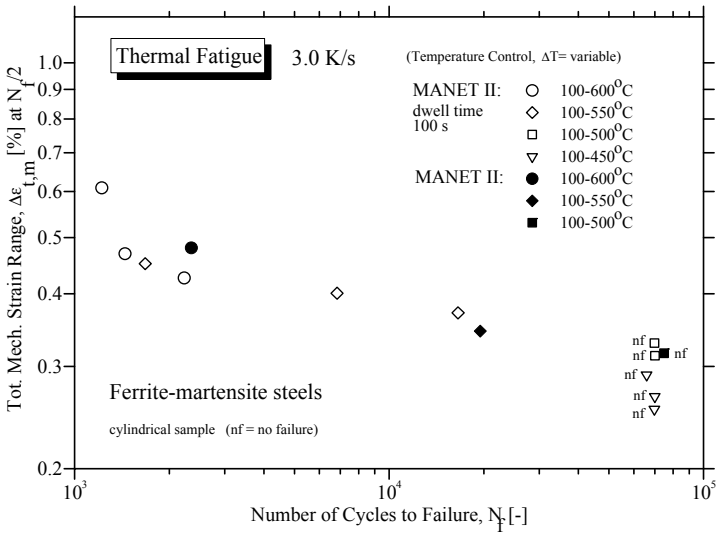

Fig. 3-28 TMF behaviour of MANET II without hold time and with 100 s hold time for a heating and cooling rate of 3 K/s in a $\Delta\varepsilon_{t,m}$ versus N_f plot

The comparison between tests without and 100s hold time on thermal fatigue behaviour of MANET II with a heating and cooling rate of 3 K/s and the start with the lower minimum temperature of 100°C is made in Fig. 3–28 in respect to total strain range $\Delta\varepsilon_{t,m}$ vs. number of cycles to failure at comparable temperature changes. The lower heating rate leads to an increase in total strain range $\Delta\varepsilon_{t,m}$ and also the hold time is at rapidly increasing total strain range much more damaging.

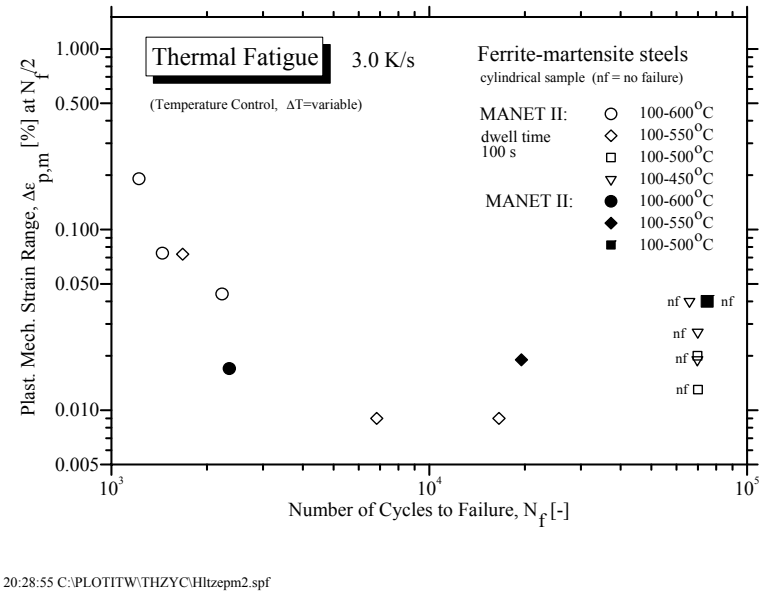

Fig. 3-29 TMF behaviour of MANET II without hold time and with 100 s hold time for a heating and cooling rate of 3 K/s in a $\Delta\varepsilon_{p,m}$ versus N_f plot

In Fig. 3-29 is plotted in double logarithmic scale the dependency of the plastic mechanical strain amplitude $\Delta\varepsilon_{p,m}$ from 0.01 % to 0.2 % versus the number of cycles to failure N_f with a heating and cooling rate of 3 K/s and the start with the lower minimum temperature of 100°C. Mainly in case of hold time with increasing maximum temperature $\Delta\varepsilon_{p,m}$ is increasing and reaches in the temperature range 100 – 600°C values of 0.2 % with higher scatter for higher plastic mechanical strain amplitudes $\Delta\varepsilon_{p,m}$ than at tests without hold times.

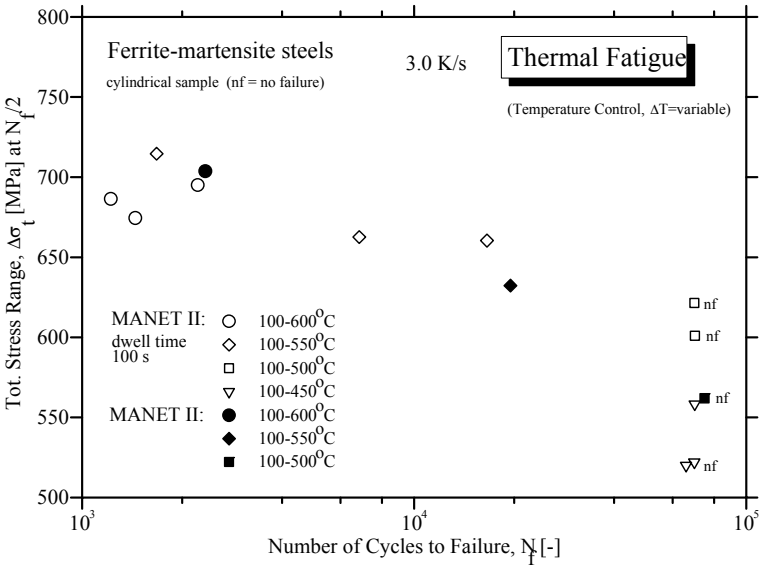

Fig. 3-30 TMF behaviour of MANET II without hold time and with 100 s hold time for a heating and cooling rate of 3 K/s in a $\Delta\sigma_t$ versus N_f plot

Whereas the total saturation stress $\Delta\sigma_t$ depicted in Fig. 3-30 shows at TMF testing with 100 s hold times an increasing tendency but the difference to tests without hold times und otherwise unchanged conditions is low.

Detailed results of every TMF test of MANET II will be found in chapter 7.3.3 of the Annex and in the enclosed CD.

3.3 OPTIFER IV

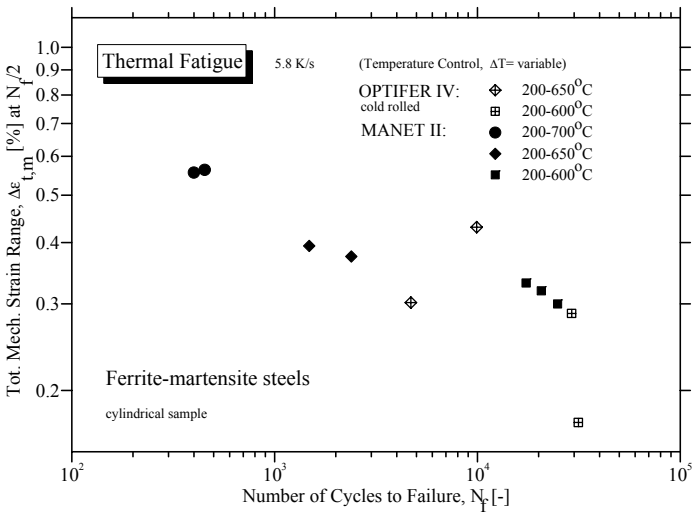

Fig. 3-31 Comparison of the TMF behaviour of OPTIFER IV (cold rolled) and MANET II without hold time in a $\Delta\varepsilon_{t,m}$ versus N_f plot

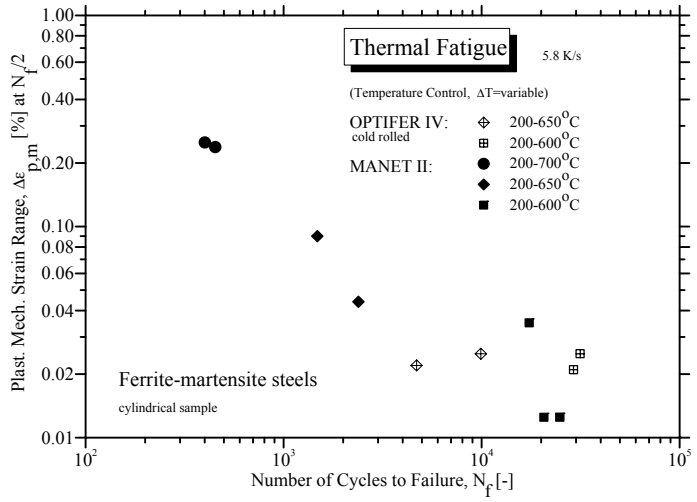

Fig. 3-32 Comparison of the TMF behaviour of OPTIFER IV (cold rolled) and MANET II without hold time in a $\Delta\varepsilon_{p,m}$ versus N_f plot

Tests on OPTIFER IV (cold rolled) and MANET II without hold times and heating rates of 5.8 K/s with a minimum temperature of 200°C and variable maximum temperatures from 600°C to 700°C had been conducted on cylindrical specimens. In Fig. 3-31 is compared in double logarithmic scale the dependency of the total mechanical strain amplitude $\Delta\varepsilon_{t,m}$ from 0.18 % to 0.6 % versus the number of cycles to failure N_f. With increasing maximum temperature $\Delta\varepsilon_{t,m}$ is increasing on both materials and reaches in the comparable temperature range 200 – 650°C higher numbers of cycles to failure for the cold rolled OPTIFER IV.

In Fig. 3-32 is compared in double logarithmic scale the dependency of the plastic mechanical strain amplitude $\Delta\varepsilon_{p,m}$ from 0.01 % to 0.3 % of OPTIFER IV (cold rolled) and MANET II versus the number of cycles to failure N_f. With decreasing maximum temperature $\Delta\varepsilon_{p,m}$ is decreasing.

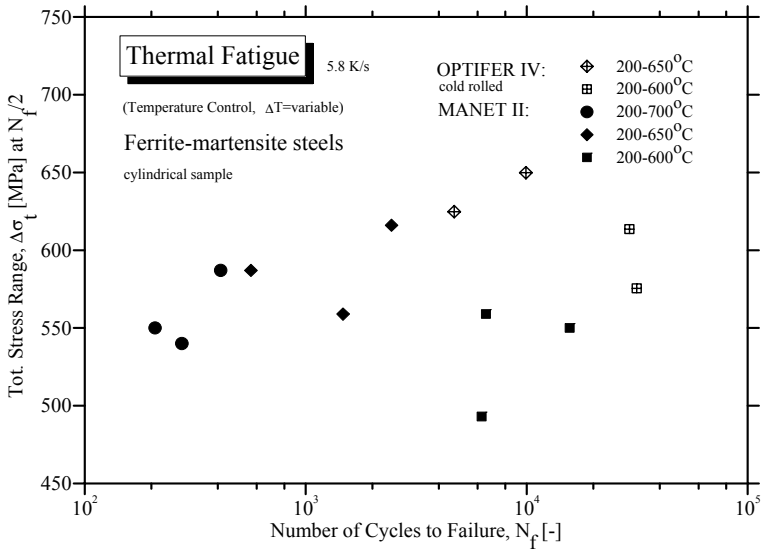

Fig. 3-33 Comparison of the TMF behaviour of OPTIFER IV (cold rolled) and MANET II without hold time in a $\Delta\sigma_t$ versus N_f plot

The total saturation stress $\Delta\sigma_t$ of OPTIFER IV (cold rolled) and MANET II in Fig. 3-33 shows at TMF testing for both materials a slightly increasing behaviour versus number of cycles to failure N_f, but with a broad scatter. OPTIFER IV reaches during TMF testing higher stresses than MANET II.

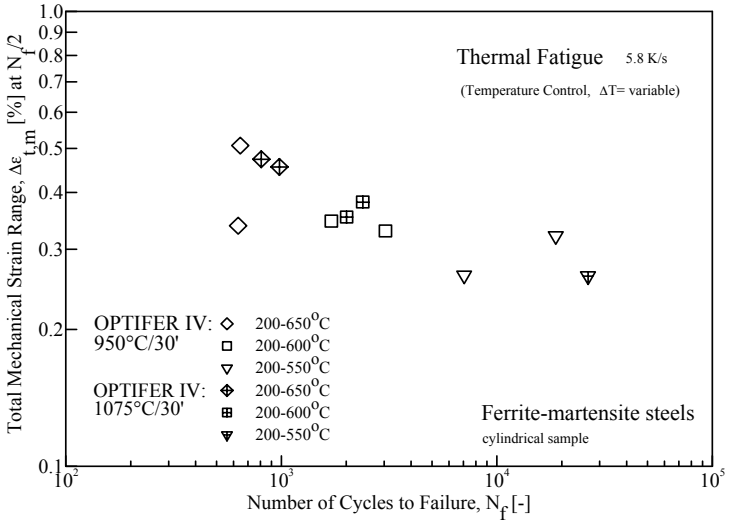

Fig. 3-34 Comparison of the TMF behaviour of OPTIFER IV in two annealing conditions without hold time in a $\Delta\varepsilon_{t,m}$ versus N_f plot

In Fig. 3-34 is plotted the TMF behaviour of OPTIFER IV in two annealing conditions without hold time in double logarithmic scale the dependency of the total mechanical strain amplitude $\Delta\varepsilon_{t,m}$ from 0.28 % to 0.5 % versus the number of cycles to failure N_f. With increasing maximum temperature $\Delta\varepsilon_{t,m}$ is increasing. The higher annealing temperature of 1050°C has nearly no influence on TMF behaviour of this material.

Detailed results of every TMF test of OPTIFER IV will be found in chapter 7.3.4 of the Annex and in the enclosed CD.

3.4 F82H mod.

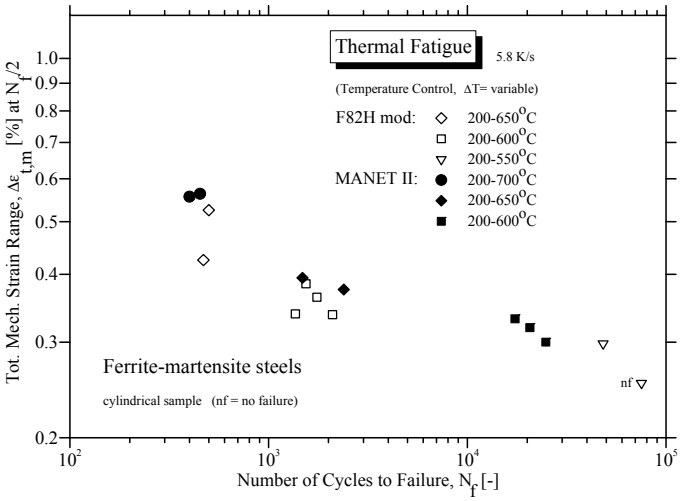

Fig. 3-35 Comparison of the TMF behaviour of F82H mod. and MANET II without hold time in a $\Delta\varepsilon_{t,m}$ versus N_f plot

Tests on F82H mod. without hold times and heating rates of 5.8 K/s with a minimum temperature of 200°C and variable maximum temperatures from 550°C to 650°C had been conducted on cylindrical specimens. In Fig. 3-35 is plotted in double logarithmic scale the de-

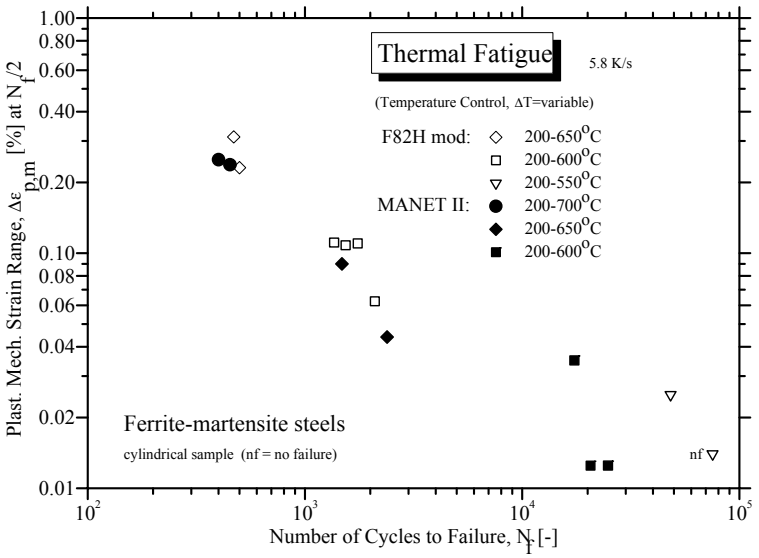

Fig. 3-36 Comparison of the TMF behaviour of F82H mod. and MANET II without hold time in a $\Delta\varepsilon_{p,m}$ versus N_f plot

pendency of the total mechanical strain amplitude $\Delta\varepsilon_{t,m}$ from 0.28 % to 0.55 % versus the number of cycles to failure N_f. With increasing maximum temperature $\Delta\varepsilon_{t,m}$ of both materials is increasing and reaches in the comparable temperature range, e.g. 200 – 650°C, for F82H mod. numbers of cycles to failure of one order of magnitude lower. At a temperature range below 200°C – 550°C on one F82H mod.-specimen no fracture occurred in the design window of 70000 cycles.

In Fig. 3-36 is compared in double logarithmic scale the dependency of the plastic mechanical strain amplitude $\Delta\varepsilon_{p,m}$ from 0.013 % to 0.15 % of F82H mod. and MANET II without hold time versus the number of cycles to failure N_f. Both materials show very similar dependency in $\Delta\varepsilon_{p,m}$.

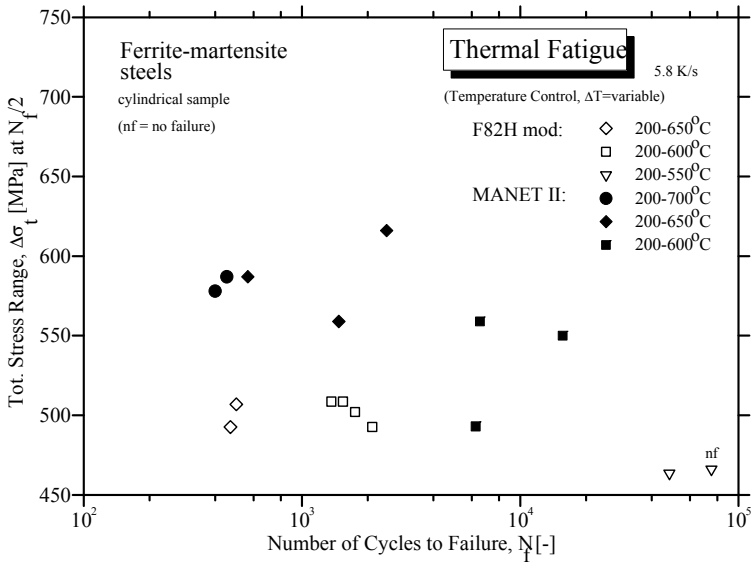

Fig. 3-37 Comparison of the TMF behaviour of F82H mod. and MANET II without hold time in a $\Delta\sigma_t$ versus N_f plot

The total saturation stress $\Delta\sigma_t$ of F82H mod. and MANET II in Fig. 3-37 shows in the comparable temperature range for F82H mod. lower mean values than for MANET II.

F82H mod. shows at a temperature change of 200 - 600°C e.g. at increasing total mechanical strain ranges (Fig. 3-38) a drastic reduction in number of cycles to failure of about one order of magnitude compared to MANET II. Whereas the hot forged OPTIFER IV under the same test conditions reacts at decreasing total mechanical strain ranges with a slight increase in number of cycles to failure. It should be mentioned that OPTIFER IV regularly will be applied in the tempered condition.

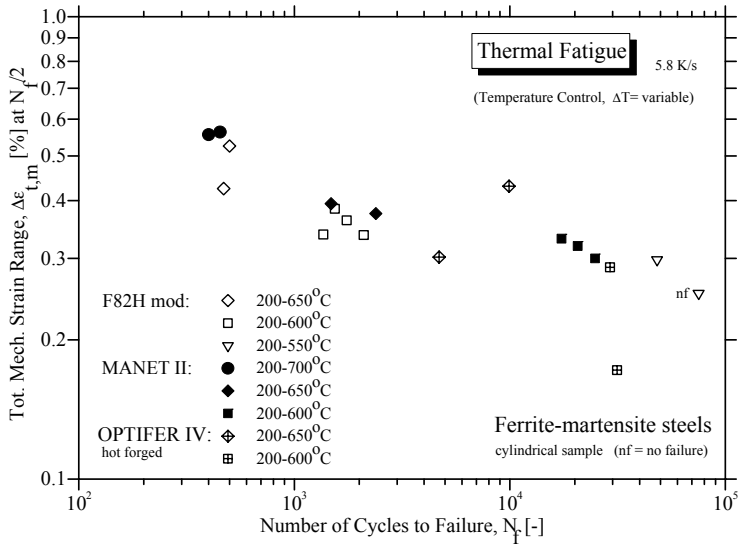

Fig. 3-38 Comparison of the TMF behaviour of F82H mod., MANET II and OPTIFER IV (hot forged) without hold time in a $\Delta\varepsilon_{t,m}$ versus N_f plot

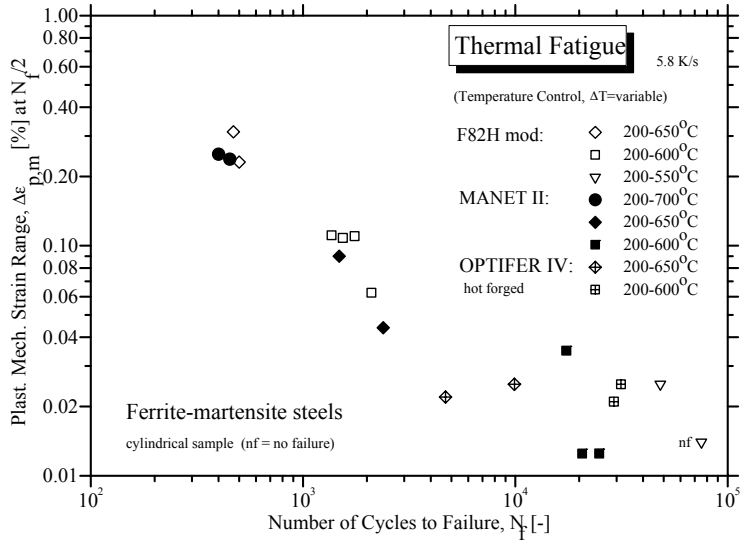

Fig. 3-39 Comparison of the TMF behaviour of F82H mod., MANET II and OPTIFER IV (hot forged) without hold time in a $\Delta\varepsilon_{p,m}$ versus N_f plot

Also at increasing total plastic strain ranges (Fig. 3-39) the reduction in number of cycles to failure of about one order of magnitude compared to MANET II takes place. Whereas the hot forged OPTIFER IV under the same test conditions reacts at similar plastic mechanical strain ranges with a slight increase in number of cycles to failure.

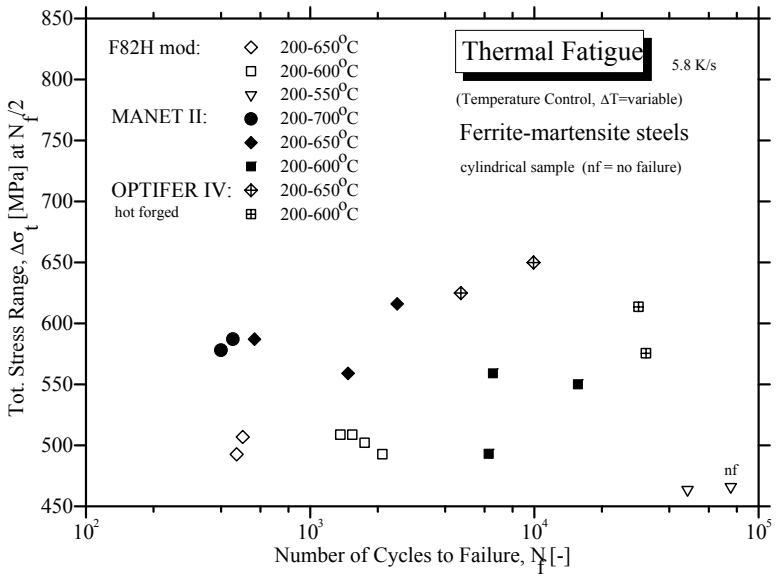

Fig. 3-40 Comparison of the TMF behaviour of F82H mod., MANET II and OPTIFER IV (hot forged) without hold time in a $\Delta\sigma_t$ versus N_f plot

The total saturation stress $\Delta\sigma_t$ of the three materials shown in Fig. 3-40 results at TMF testing in a broad scatter versus number of cycles to failure N_f and is decreasing for the lowest temperature range of 200 – 550°C only. The highest stress level reaches the hot forged OPTIFER IV at the highest N_f-values.

In thermal fatigue experiments of F82H mod. with hold times starting from 200 °C as the low temperature, the dramatic effect of the hold time of 1000 s at both temperatures, i.e. the HTHL - condition, on the shortening of the life time was found, as can be seen from Fig. 3-41. For 100 s the results of HTL - and HTH - tests of 200 to 550 °C are found in a smaller scatter of $\Delta\varepsilon_{t,m}$ around 0.3 % but in a broader scatter in respect to N_f . Here are found N_f - values for HTL of around 25000 cycles, for HTH of around 8000 cycles and for HTHL of around 2500 cycles only. For 1000 s the results of HTL - and HTH - tests of 200 to 550 °C are found in a smaller scatter of $\Delta\varepsilon_{t,m}$ around 0.3 % but in a broader scatter in respect to N_f . Here are found N_f - values for HTL of around 12000 cycles, for HTH of around 4000 cycles and for HTHL of around 300 cycles at a $\Delta\varepsilon_{t,m}$ of around 0.8 %. In the data set for the temperature range from 200 to 600 °C this tendency is similar.

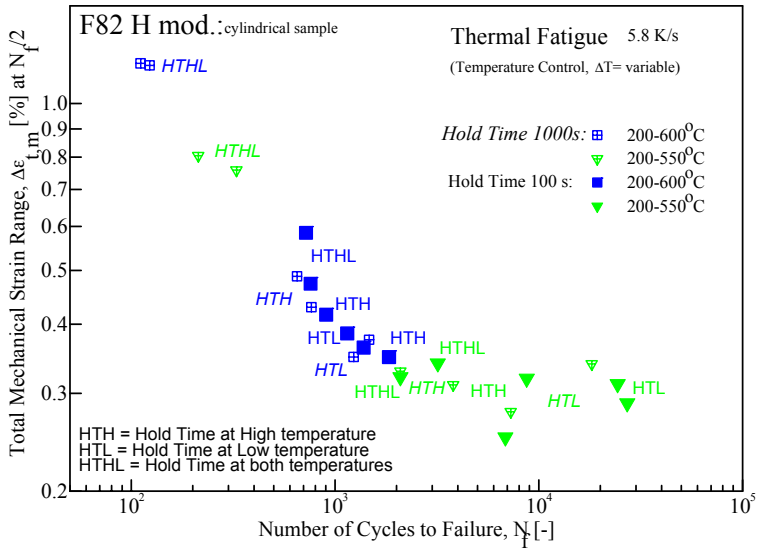

Fig. 3-41 Comparison of the TMF behaviour of F82H mod. at 200°C lower temperature with 100s and 1000 s hold times in a $\Delta\varepsilon_{t,m}$ versus N_f plot

For 100 s the results of HTL tests of 200 to 550 °C are found in a smaller scatter of $\Delta\varepsilon_{p,m}$ around 0.009 % but in a broader scatter in respect to N_f . Here are found N_f - values for HTL

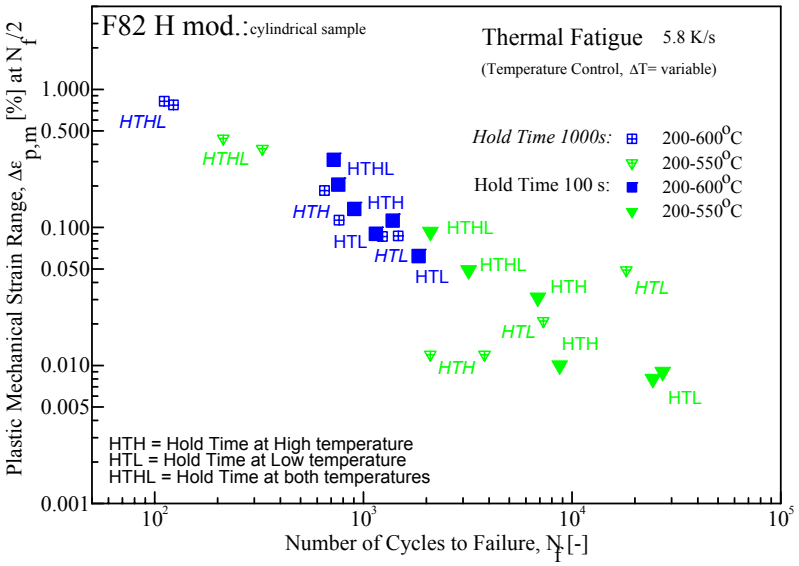

Fig. 3-42 Comparison of the TMF behaviour of F82H mod. at 200°C lower temperature with 100s and 1000 s hold times in a $\Delta\varepsilon_{p,m}$ versus N_f plot

of around 25000 cycles, for HTH of around 8000 cycles and for HTHL of around 2500 cycles only. For 1000 s the results of HTL - and HTH - tests of 200 to 550 °C are found in a smaller scatter of $\Delta\varepsilon_{p,m}$ between 0.01 and 0.05 % and a broader scatter in respect to N_f . Here are found N_f - values for HTL from 8000 to 18000 cycles, for HTH from 2000 to 5000 cycles and for HTHL of around 300 cycles at a $\Delta\varepsilon_{p,m}$ of around 0.4 %. In the data set for the temperature range from 200 to 600 °C this tendency is similar.

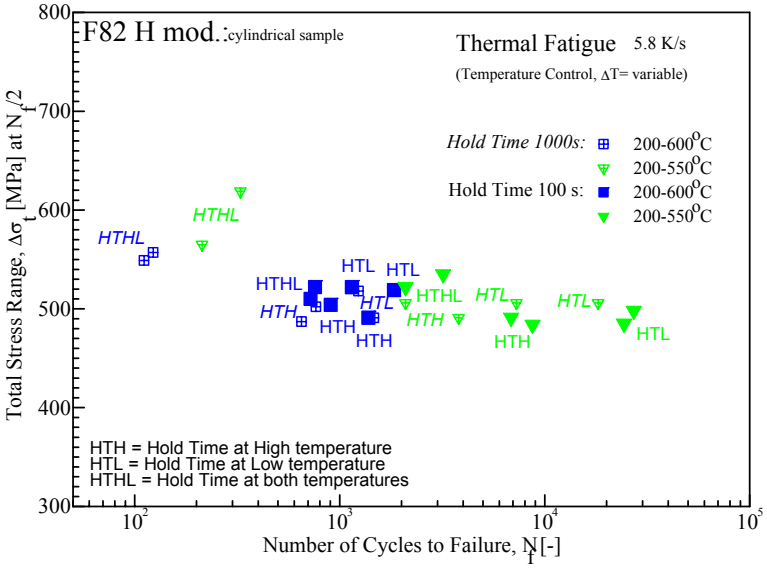

Fig. 3-43 Comparison of the TMF behaviour of F82H mod. at 200°C lower temperature with 100s and 1000 s hold times in a $\Delta\sigma_t$ versus N_f plot

HTHL applied at hold times of 1000 s (Fig. 3-43) increases the total stress range $\Delta\sigma_t$ of F82H mod. compared to 100 s hold times values.

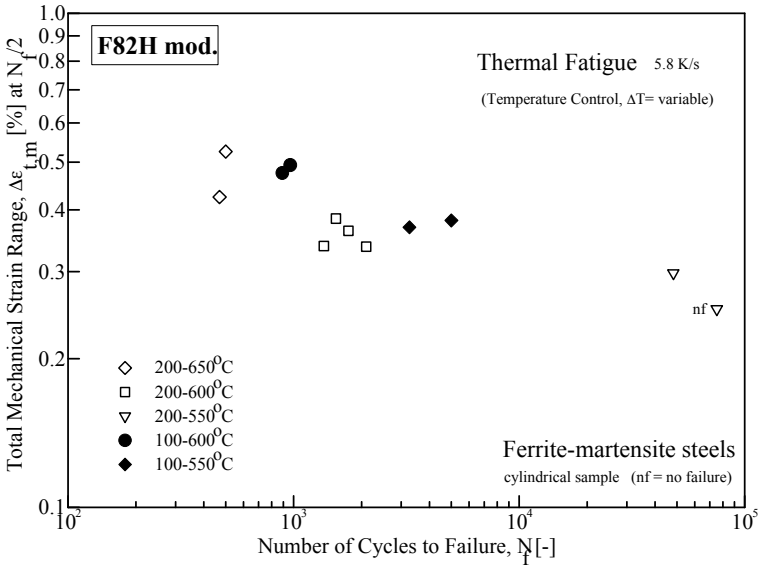

Fig. 3-44 Comparison of the TMF behaviour of F82H mod. with two different lower temperatures in a $\Delta\varepsilon_{t,m}$ versus N_f plot

Tests on F82H mod. without hold times and heating rates of 5.8 K/s with two different minimum temperatures of 100°C and 200°C and variable maximum temperatures from 550°C to 650°C had been conducted on cylindrical specimens. In Fig. 3-44 is plotted in double logarithmic scale the dependency of the total mechanical strain amplitude $\Delta\varepsilon_{t,m}$ from 0.25 % to 0.55 % versus the number of cycles to failure N_f. With increasing maximum temperature $\Delta\varepsilon_{t,m}$ is increasing and reaches in the temperature range 200 – 650°C only numbers of cycles to failure in the range of hundreds. Whereas the test series with the lower minimum temperature of 100°C, but the same ΔT leads to a smaller total mechanical strain amplitude $\Delta\varepsilon_{t,m}$ of 0.35 % and reaches N_f-values of more than one magnitude higher.

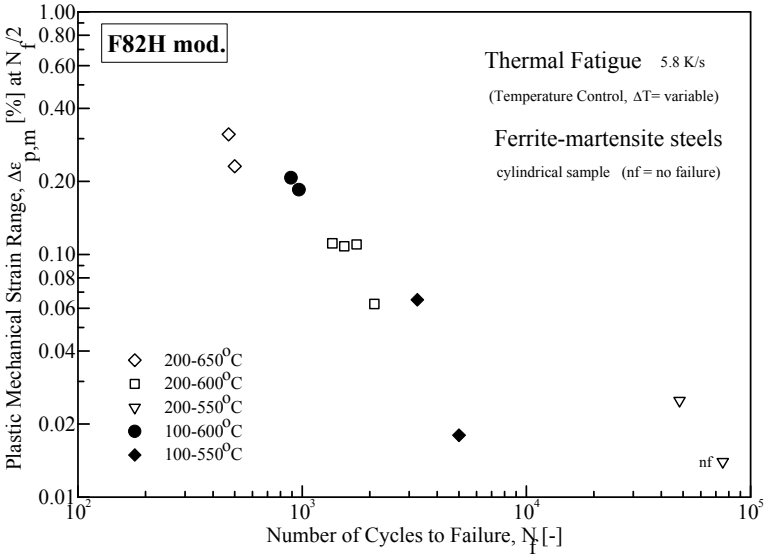

Fig. 3-45 Comparison of the TMF behaviour of F82H mod. with two different lower temperatures in a $\Delta\varepsilon_{p,m}$ versus N_f plot

In Fig. 3-45 is plotted in double logarithmic scale the dependency of the plastic mechanical strain amplitude $\Delta\varepsilon_{p,m}$ from 0.013 % to 0.3 % versus the number of cycles to failure N_f. With increasing maximum temperature $\Delta\varepsilon_{p,m}$ is increasing and reaches in the temperature range

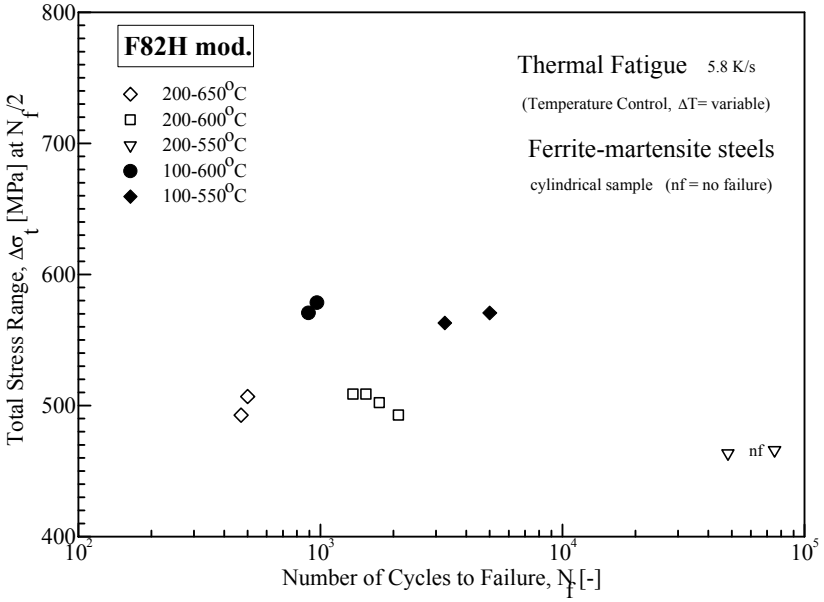

Fig. 3-46 Comparison of the TMF behaviour of F82H mod. with two different lower temperatures in a $\Delta\sigma_t$ versus N_f plot

200 – 650°C only numbers of cycles to failure in the range of hundreds. Whereas the test series with the lower minimum temperature of 100°C, but the same ΔT leads to a smaller plastic mechanical strain amplitude $\Delta\varepsilon_{p,m}$ of 0.018 % and reaches N_f-values of more than one magnitude higher.

The total saturation stress $\Delta\sigma_t$ of F82H mod., Fig. 3-46, shows at the tests with the higher minimum temperature of 200°C a stress level around 500 Mpa, but tests at the same ΔT leads to higher $\Delta\sigma_t$ of 600 MPa and reaches N_f-values of more than one magnitude higher.

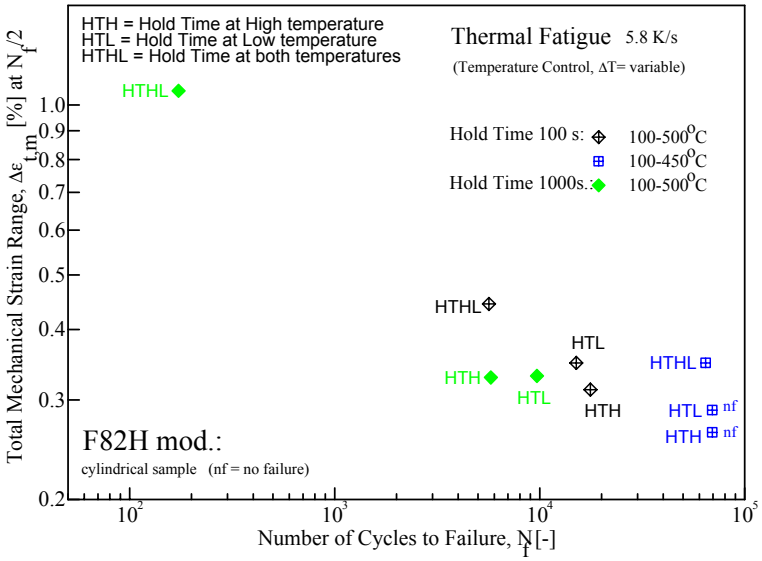

Fig. 3-47 Comparison of the TMF behaviour of F82H mod. at 100°C lower temperature with 100s and 1000 s hold times in a $\Delta\varepsilon_{t,m}$ versus N_f plot

From F82H mod. material are also available results of thermal fatigue tests at 100°C lower temperature with hold times of 100 s and 1000 s. This covers the temperature ranges of 100 to 450 °C (100s only) and 100 to 500 °C (100 and 1000 s). Normally for 100 s the results of HTL - and HTH - tests of 100 to 450 °C and 100 to 500 °C are found in a smaller scatter of $\Delta\varepsilon_{t,m}$ around 0.3 % and of N_f around 16.000 cycles. In case of a 100 to 500 °C temperature range the N_f - values without hold times are found around 10.000 cycles (Fig. 3-47). So the hold times at the low temperature or at the high temperature leads to a slight increase in life time. But at the HTHL condition was found for 100 s hold time with increasing $\Delta\varepsilon_{t,m}$ up to 0.45 % a reduction in life time down to 6000 cycles i.e. a factor of 1.6. At increasing hold time of 1000 s even the HTL -and HTH - values are found to be less than 10000 cycles, but the HTHL - condition shortens the N_f - values down to 200 cycles at a very high $\Delta\varepsilon_{t,m}$ - value of around 1.1 % strain. This is a reduction in life of rather 1.5 orders of magnitude.

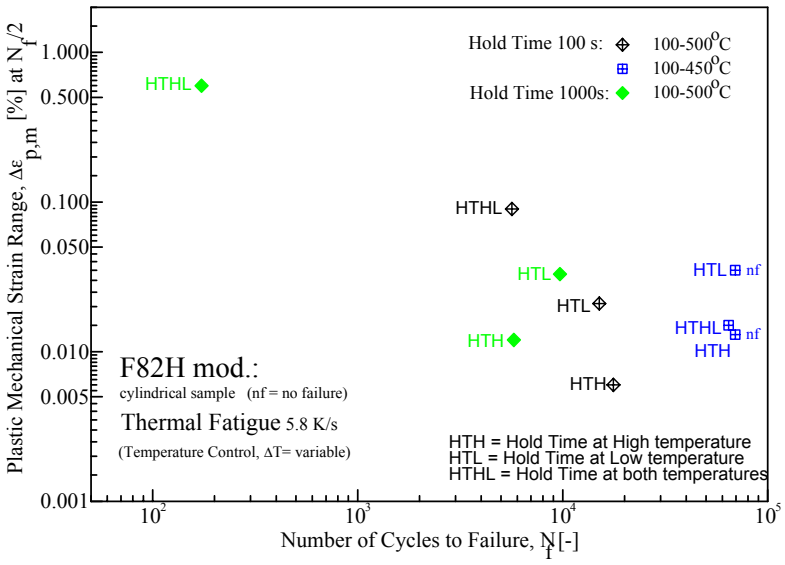

Fig. 3-48 Comparison of the TMF behaviour of F82H mod. at 100°C lower temperature with 100s and 1000 s hold times in a $\Delta\varepsilon_{p,m}$ versus N_f plot

The comparison of thermally fatigued F82H mod. samples of both test conditions in respect to plastic strain range $\Delta\varepsilon_{p,m}$ results for the longer hold time in much higher strain and shorter life values as for the shorter hold time. This is shown in Fig. 3-48.

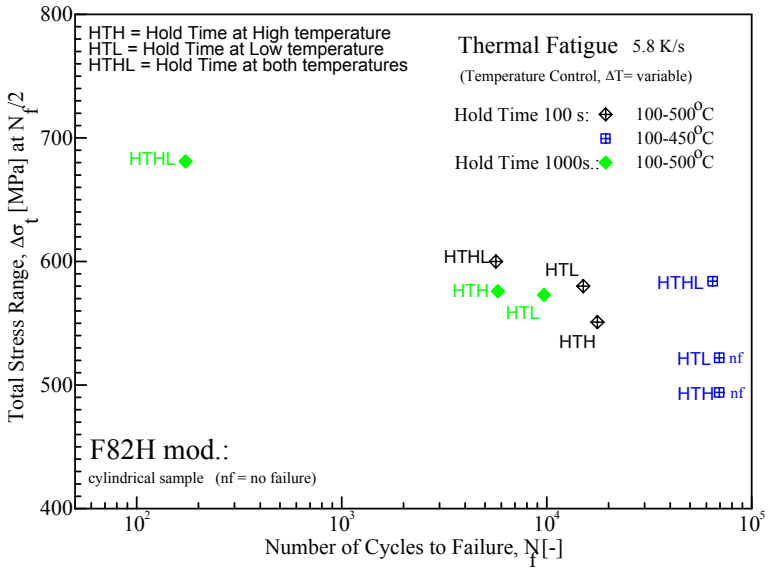

Fig. 3-49 Comparison of the TMF behaviour of F82H mod. at 100°C lower temperature with 100s and 1000 s hold times in a $\Delta\sigma_t$ versus N_f plot

The comparison of thermally fatigued F82H mod. samples of both test conditions in respect to total stress range $\Delta\sigma_t$ results for the longer hold time in much higher stress and shorter life values as for the shorter hold time (Fig. 3-49).

Detailed results of every TMF test of F82H mod. will be found in chapter 7.3.5 of the Annex and in the enclosed CD.

3.5 EUROFER 97

3.5.1 EUROFER 97, as received

In case of total mechanical strain range $\Delta\varepsilon_{t,m}$ vs. number of cycles to failure N_f (Fig. 3-50), F82H mod. and OPTIFER IV show in the temperature range of 100 and 550°C at a $\Delta\varepsilon_{t,m}$ of about 0.4 %, N_f-values between 3000 and 5000 cycles whereas EUROFER 97 at a similar $\Delta\varepsilon_{t,m}$ remains at around 1400 to 1800 that is a factor of 2.5 lower in life time. In the temperature range of 100 and 600°C at a $\Delta\varepsilon_{t,m}$ of about 0.5 %, F82H mod. and OPTIFER IV show N_f-values around 1000 cycles whereas EUROFER 97 at a slightly higher $\Delta\varepsilon_{t,m}$ of 0.55 % remains at around 600 that is still a factor of 1.6 lower in life time.
The small difference in $\Delta\varepsilon_{t,m}$ for the different materials is a sign for a certain insensitivity of the temperature cycles on the specimens reaction.

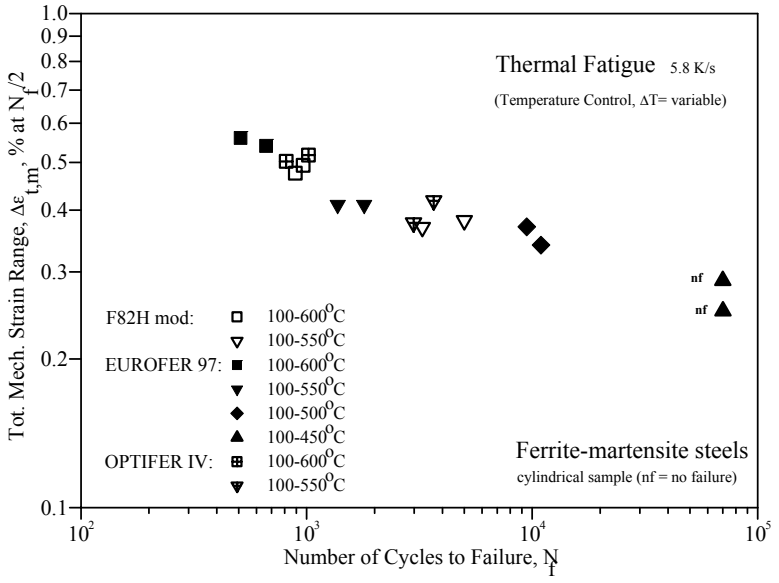

Fig. 3-50 Comparison of the TMF behaviour of F82H mod., EUROFER 97 and OPTIFER IV without hold time in a $\Delta\varepsilon_{t,m}$ versus N_f plot

A slightly different picture can be taken from the behaviour of plastic mechanical strain range $\Delta\varepsilon_{p,m}$ (Fig. 3-51) for the different materials under different temperature ranges. In case F82H

mod. and OPTIFER IV the plastic mechanical strain range $\Delta\varepsilon_{p,m}$ vs. number of cycles to failure N_f , show in the temperature range of 100 and 550°C a broad scatter mainly for F82H mod. with $\Delta\varepsilon_{p,m}$ - values between 0.02 and 0.06 %. The N_f-values remain the same (between 3000 and 5000 cycles) whereas OPTIFER IV and EUROFER 97 at different $\Delta\varepsilon_{p,m}$ – values of 0.035 and 0.15 %, respectively, give a smaller scatter in strain. The N_f-values remain at around 1400 to 1800 for EUROFER 97. In the temperature range of 100 and 600°C at a $\Delta\varepsilon_{p,m}$ of about 0.21 %, F82H mod. and OPTIFER IV show N_f-values around 1000 cycles whereas EUROFER 97 at similar $\Delta\varepsilon_{p,m}$ of 0.21 % remains at around 600 that is still a factor of 1.6 lower in life time.

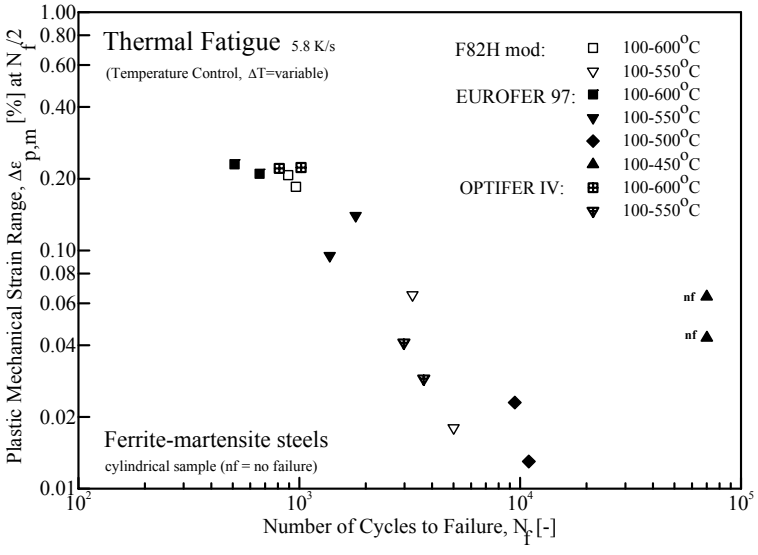

Fig. 3-51 Comparison of the TMF behaviour of F82H mod., EUROFER 97 and OPTIFER IV without hold time in a $\Delta\varepsilon_{p,m}$ versus N_f plot

The total stress range $\Delta\sigma_t$ (Fig. 3-52) of all tree materials and temperature ranges of 100 and 600°C as well as 100 and 550°C is nearly independent from material and temperature range.

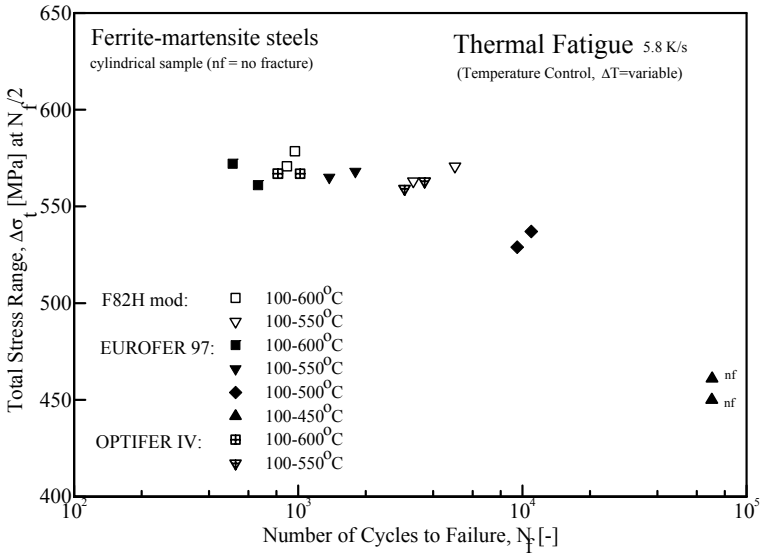

Fig. 3-52 Comparison of the TMF behaviour of F82H mod., EUROFER 97 and OPTIFER IV without hold time in a $\Delta\sigma_t$ versus N_f plot

Only EUROFER 97 results in temperature ranges of 100 and 500°C as well as 100 and 450°C reveal in lower $\Delta\sigma_t$ values at increasing N_f.

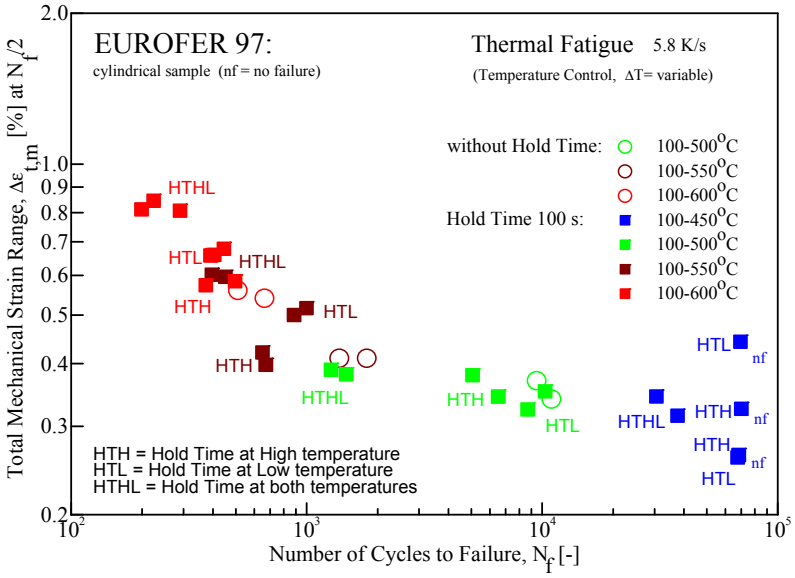

Fig. 3-53 Comparison of the TMF behaviour of EUROFER 97 without hold time and with 100 s hold time in a $\Delta\varepsilon_{t,m}$ versus N_f plot

TMF test results with 100 s hold times and heating rates of 5.8 K/s with a minimum temperature of 100°C and variable maximum temperatures from 450°C to 600°C conducted on cylindrical specimens of EUROFER 97 are plotted in Fig 3-53 in double logarithmic scale the dependency of the total mechanical strain amplitude $\Delta\varepsilon_{t,m}$ from 0.25 % to 0.85 % versus the number of cycles to failure N_f. With increasing maximum temperature $\Delta\varepsilon_{t,m}$ is increasing and reaches in the temperature range 100 – 600°C only numbers of cycles to failure in the range of hundreds, but with lower scatter than at tests without hold times. The 100s hold time at minimum and maximum temperature (HTHL) is the most damaging condition in all examined temperature ranges and reduces N_f -values additionally.

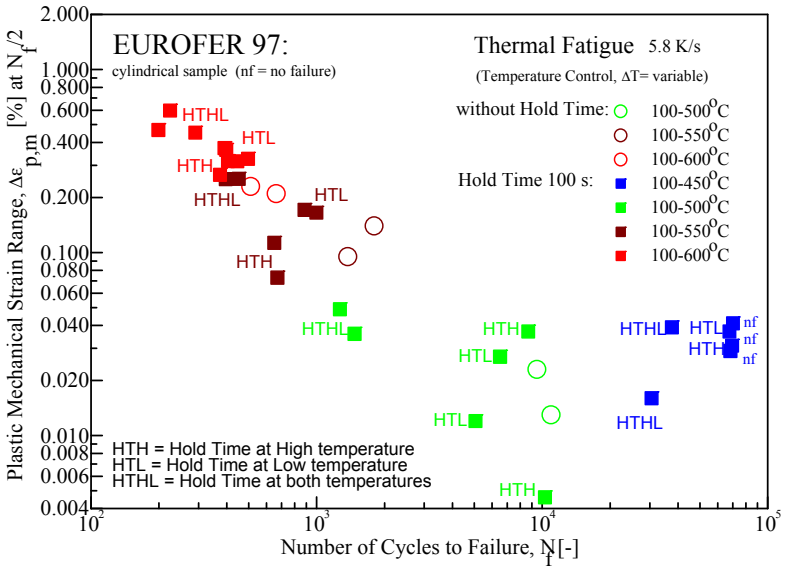

Fig. 3-54 Comparison of the TMF behaviour of EUROFER 97 without hold time and with 100 s hold time in a $\Delta\varepsilon_{p,m}$ versus N_f plot

In Fig. 3-54 is plotted in double logarithmic scale the dependency of the plastic mechanical strain amplitude $\Delta\varepsilon_{p,m}$ from 0.004 % to 0.6 % versus the number of cycles to failure N_f. With increasing maximum temperature $\Delta\varepsilon_{p,m}$ is increasing and reaches in the temperature range 100 – 600°C only numbers of cycles to failure in the range of hundreds. Only in the lower temperature range of 100°C – 500°C the scatter in $\Delta\varepsilon_{p,m}$ was higher.

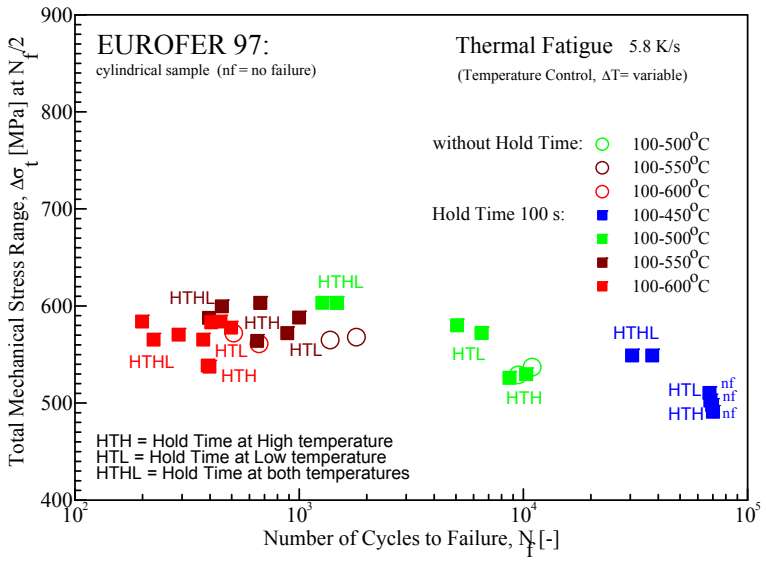

Fig. 3-55 Comparison of the TMF behaviour of EUROFER 97 without hold time and with 100 s hold time in a $\Delta\sigma_t$ versus N_f plot

Whereas the total saturation stress $\Delta\sigma_t$ depicted in Fig. 3-55 shows at TMF testing with 100 s hold times a broad scatter versus number of cycles to failure N_f and is above a maximum temperature of 500°C nearly independent from temperature range.

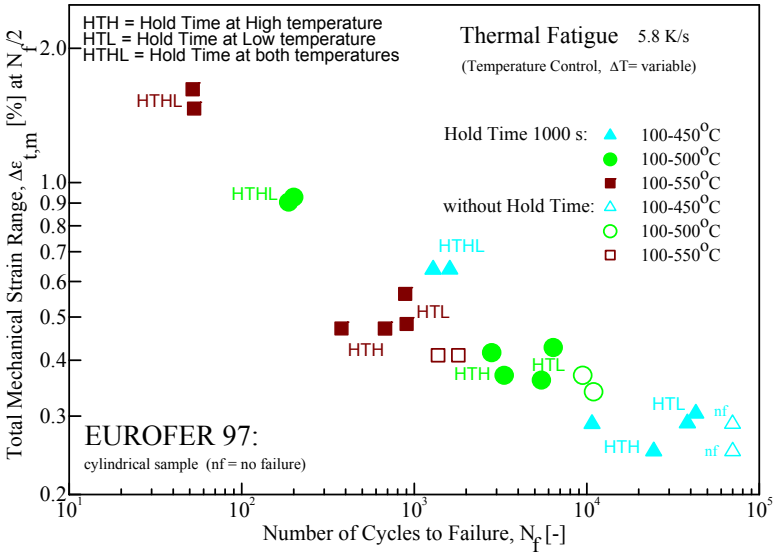

Fig. 3-56 Comparison of the TMF behaviour of EUROFER 97 without hold time and with 1000 s hold time in a $\Delta\varepsilon_{t,m}$ versus N_f plot

TMF test results with 1000 s hold times conducted on EUROFER 97 under otherwise unchanged conditions are plotted in Fig 3-56 in double logarithmic scale as the dependency of the total mechanical strain amplitude $\Delta\varepsilon_{t,m}$ from 0.25 % to 1.6 % versus the number of cycles to failure N_f. With increasing maximum temperature $\Delta\varepsilon_{t,m}$ is increasing and reaches in the temperature range 100 – 550°C only numbers of cycles to failure in the range of tens. The 1000 s hold time at minimum and maximum temperature (HTHL) is the most damaging condition in all examined temperature ranges. Whereas at TMF of 100 -450°C without hold times no failure in the design window of 70000 cycles was found, the implication of 1000 s holdtimes led to damages below 70000 cycles.

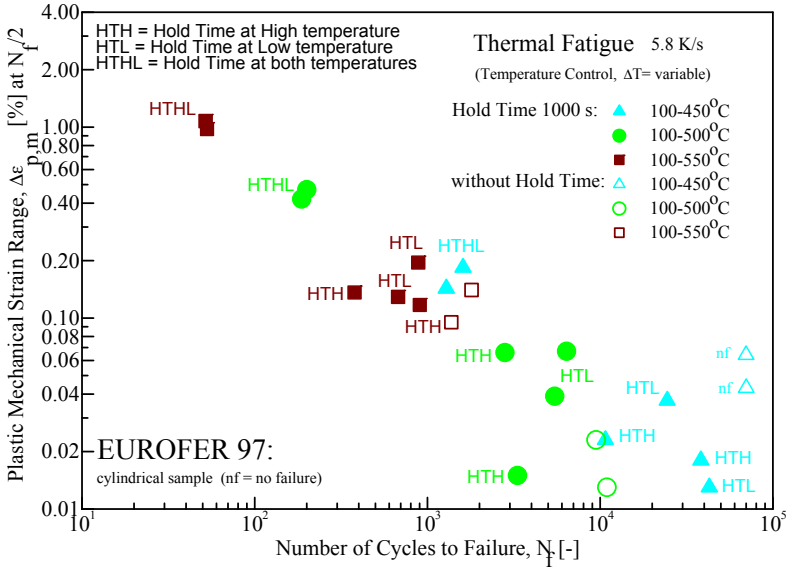

Fig. 3-57 Comparison of the TMF behaviour of EUROFER 97 without hold time and with 1000 s hold time in a $\Delta\varepsilon_{p,m}$ versus N_f plot

In Fig. 3-57 is plotted in double logarithmic scale the dependency of the plastic mechanical strain amplitude $\Delta\varepsilon_{p,m}$ from 0.015 % to 1.1 % versus the number of cycles to failure N_f. With increasing maximum temperature $\Delta\varepsilon_{p,m}$ is increasing and reaches in the temperature range 100 – 550°C only numbers of cycles to failure in the range of tens. Only in the lower temperature range of 100°C – 450°C the scatter in $\Delta\varepsilon_{p,m}$ was higher.

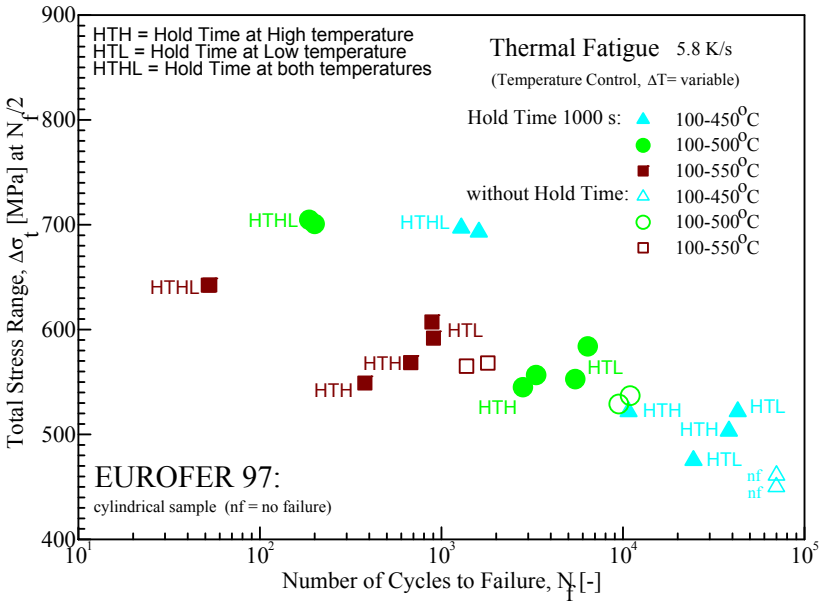

Fig. 3-58 Comparison of the TMF behaviour of EUROFER 97 without hold time and with 1000 s hold time in a $\Delta\sigma_t$ versus N_f plot

Whereas the total saturation stress $\Delta\sigma_t$ displayed in Fig. 3-58 shows at TMF testing with 1000 s hold times a slight decrease with increasing number of cycles to failure N_f and the highest stress levels are reached under all temperature ranges for the HTHL conditions.

Detailed results of every TMF test of EUROFER 97, as received, will be found in chapter 7.3.6.1 of the Annex and in the enclosed CD.

3.5.2 EUROFER 97, heat treated

TMF test results with 1000 s hold times conducted on as received and annealed EUROFER 97 under otherwise unchanged conditions are plotted in Fig. 3-59 in double logarithmic scale as the dependency of the total mechanical strain amplitude $\Delta\varepsilon_{t,m}$ from 0.14 % to 1.5 % versus the number of cycles to failure N_f. As for the as received material also for the annealed EUROFER 97 with increasing maximum temperature $\Delta\varepsilon_{t,m}$ is increasing and reaches in the temperature range 100 – 550°C only numbers of cycles to failure in the range of tens. The 1000 s hold time at minimum and maximum temperature (HTHL) is the most damaging condition in all examined temperature ranges, but the as received material results in longer lives for the lowest temperature conditions whereas the as received material behaves vice versa.

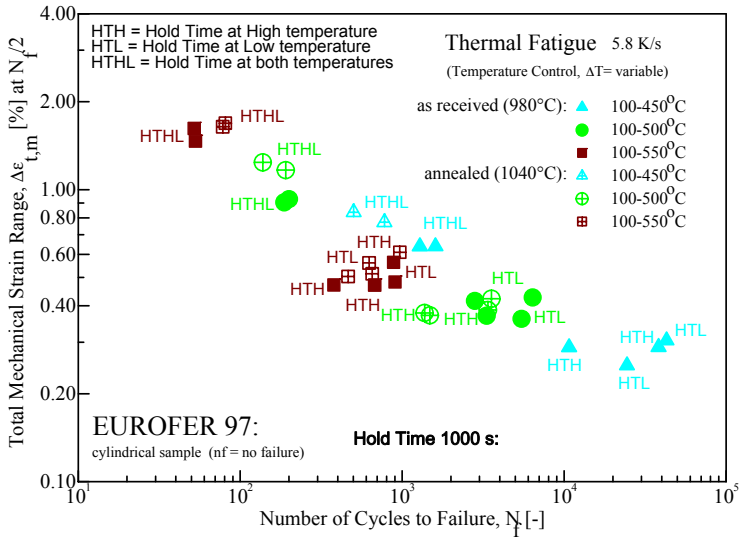

Fig. 3-59 Comparison of the TMF behaviour of as received and annealed EUROFER 97 with 1000 s hold time in a $\Delta\varepsilon_{t,m}$ versus N_f plot

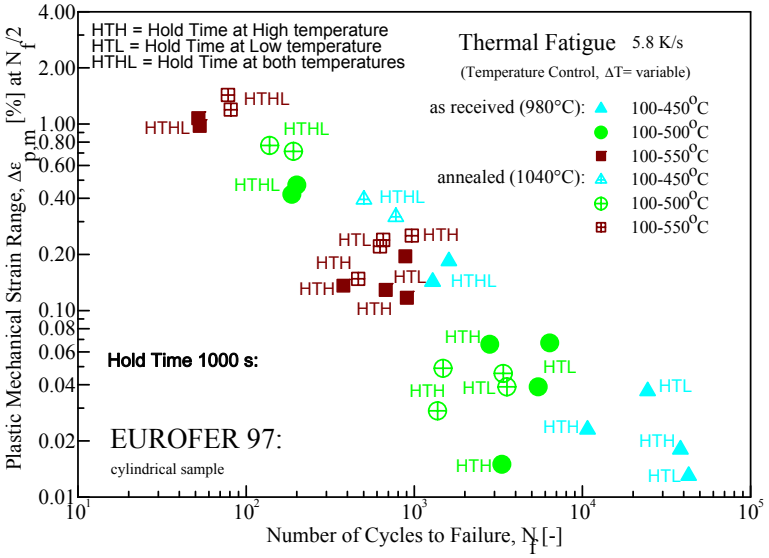

Fig. 3-60 Comparison of the TMF behaviour of as received and annealed EUROFER 97 with 1000 s hold time in a $\Delta\varepsilon_{p,m}$ versus N_f plot

In Fig. 3-60 is plotted in double logarithmic scale the dependency of the plastic mechanical strain amplitude $\Delta\varepsilon_{p,m}$ from 0.013 % to 0.5 % versus the number of cycles to failure N_f of as received and annealed EUROFER 97. With increasing maximum temperature $\Delta\varepsilon_{p,m}$ is increasing and reaches in the temperature range 100 – 550°C only numbers of cycles to failure

in the range of hundreds but with lower scatter for higher plastic mechanical strain amplitudes $\Delta\varepsilon_{p,m}$ than at tests without hold times. Only in the lower temperature range of 100°C – 500°C the scatter in $\Delta\varepsilon_{p,m}$ was higher.

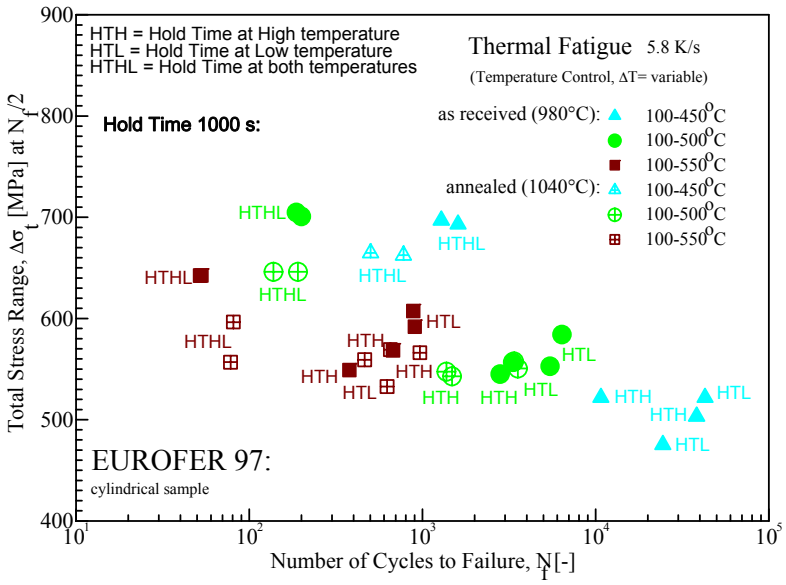

Fig. 3-61 Comparison of the TMF behaviour of as received and annealed EUROFER 97 with 1000 s hold time in a $\Delta\sigma_t$ versus N_f plot

Whereas the total saturation stress $\Delta\sigma_t$ shown in Fig. 3-61 results for as received and annealed EUROFER 97 at TMF testing with 1000 s hold times in a broad scatter versus number of cycles to failure N_f and is for the HTH and HTL conditions nearly independent from temperature range. Only the HTHL conditions reaches for the as received conditions the highest stress values.

Detailed results of every TMF test of EUROFER 97, annealed, will be found in chapter 7.3.6.2 of the Annex and in the enclosed CD.

4 Discussion

4.1 Austenitic steels

Tests without hold times and with 100 s hold times and heating rates of 5.8 K/s with a minimum temperature of 200°C and variable maximum temperatures from 550°C to 750°C had been conducted on hollow hour glass specimens. In Fig. 4-1 are plotted in double logarithmic scale the dependency of the total mechanical strain amplitude $\Delta\varepsilon_{t,m}$ from 0.4 % to 1.4 % versus the number of cycles to failure N_f and compared with isothermal LCF data from literature in the temperature range from RT to 430°C from references [14] and [15] and in the temperature range from 527°C to 600°C from references [16] and [17].

The thermal fatigue life is found to be shorter than isothermal strain controlled fatigue life at a temperature equal to the mean temperature of thermal cycling and in some cases even shorter than at the maximum temperature [2]. The influence of hold times in all three positions of the cycle, i.e. HTH, hold time at the higher temperature T_H, HTL, hold time at the lower temperature T_L and HTHL, hold time at both temperatures is negligible in respect to $\Delta\varepsilon_{t,m}$ in this austenitic steel, but reduces the N_f -values.

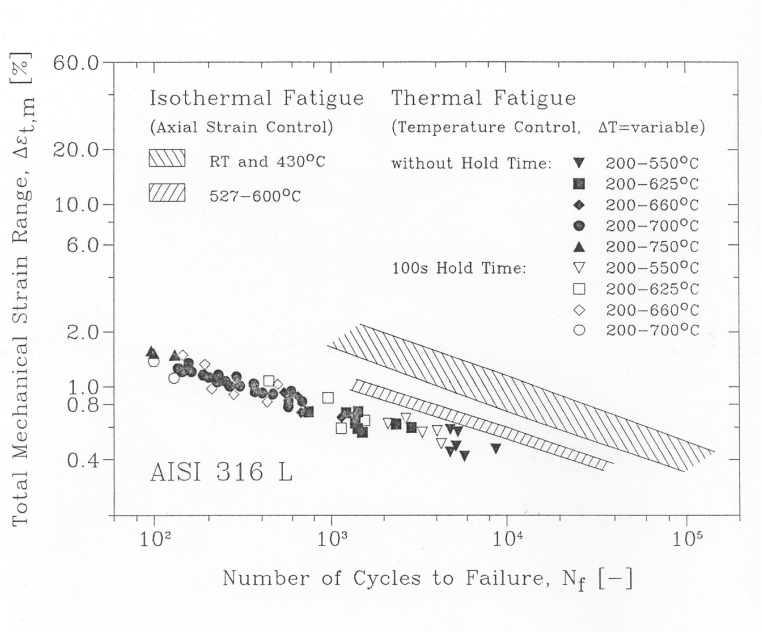

Fig. 4-1 Comparison of the TMF behaviour of AISI 316L without hold time and with 100s hold time to isothermal strain controlled low cycle fatigue data in a similar temperature range in a $\Delta\varepsilon_{t,m}$ versus N_f plot

In Fig. 4-2 is plotted in double logarithmic scale the dependency of the total plastic mechanical strain amplitude $\Delta\varepsilon_{p,m}$ from 0.1 % to 1.2 % versus the number of cycles to failure N_f, with increasing scatter for lower $\Delta\varepsilon_{p,m}$. Also for this quantity the influence of hold times in all three positions of the cycle, i.e. HTH, HTL and HTHL is negligible in this austenitic steel, but reduces the N_f -values.

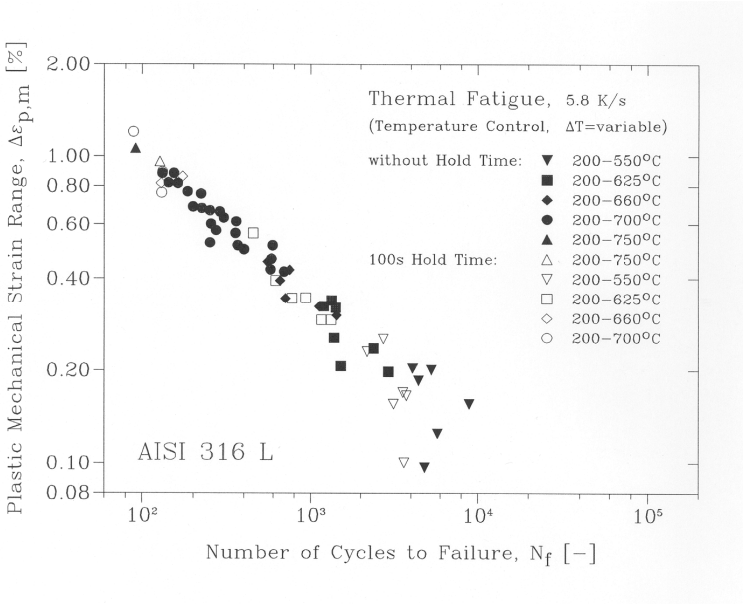

Fig. 4-2 TMF behaviour of AISI 316L without hold time and with 100s hold times in a $\Delta\varepsilon_{p,m}$ versus N_f plot

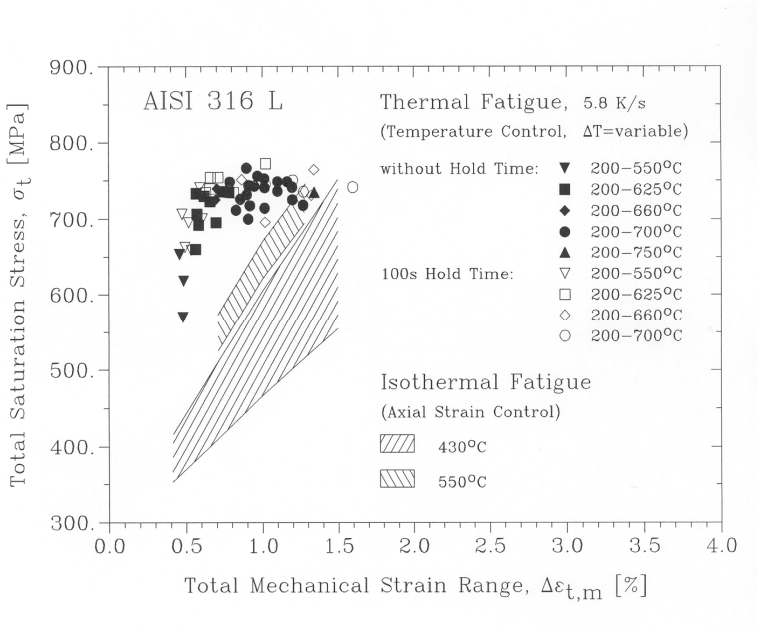

Fig. 4-3 Comparison of the TMF behaviour of AISI 316L without hold time and with 100s hold time to isothermal strain controlled low cycle fatigue data in a similar temperature range in a σ_t versus $\Delta\varepsilon_{t,m}$ plot

The total saturation stress σ_t shown in Fig. 4-3 is at TMF testing independent of the total mechanical strain range $\Delta\varepsilon_{t,m}$, apart from the lower $\Delta\varepsilon_{t,m}$ level. The isothermal strain controlled LCF σ_t data however are strongly dependent of $\Delta\varepsilon_{t,m}$ [15] [17].

In order to design components operating under combined thermal and mechanical cycling, it is necessary to supply reasonable calculations of fatigue life. Two different approaches to life calculations had been considered: (a) development of relationships directly from thermal-mechanical fatigue experiments and (b) development of methods for correlating thermal-

mechanical with isothermal fatigue resistance. Although the first approach was more straightforward than the second, it required the conduction of costly experiments over long periods of time when long-life fatigue (> 10^4 cycles) were of interest. This limitation made it desirable to use the second approach and develop methods of relating the results of thermal-mechanical cycling experiments to isothermal experiments. Such methods had been developed and reported in [18] to provide a rational basis for extrapolating the results of relatively short-lived, thermal-mechanical experiments of AISI 316 L.

Corresponding to a - by tend - similar mechanical behaviour of TMF and LCF loading (Fig. 4-1) the dislocation structures of AISI 316L formed under thermal fatigue are similar to that obtained in LCF tests. The typical dislocation structures for LCF testing of austenitic steels are veins and walls, labyrinth and persistent slip bands. Layers and cells, were all observed also during TMF. Fig. 4-4 shows the well developed veins and walls structure observed on samples thermally cycled between 200 and 550°C. Only planar arrangements of dislocations generated under low strain LCF amplitudes [19] or low temperatures [20] were never observed under TMF loading.

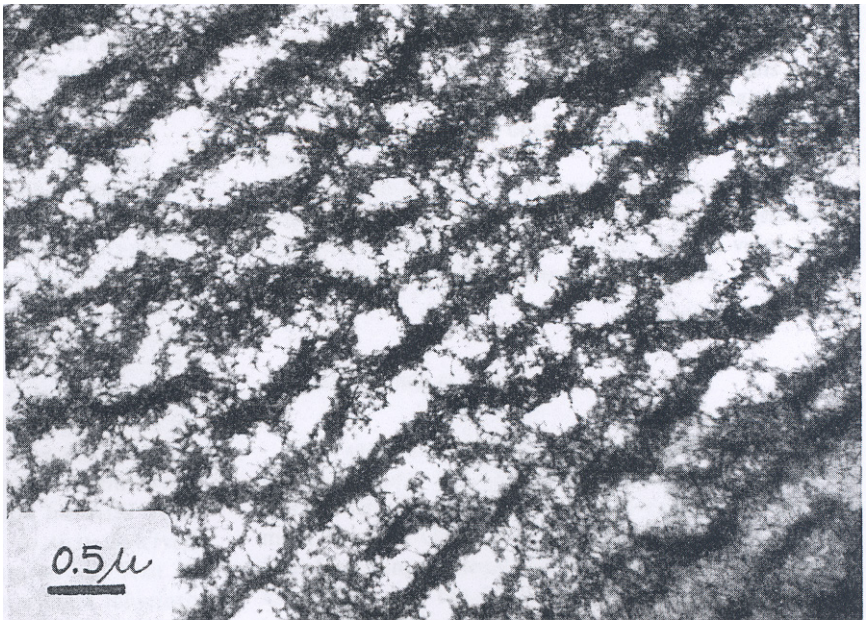

Fig. 4-4 Veins and walls structure on thermally cycled AISI 316L between 200 and 550°C

Depending on the temperature range different types of dislocation structures have been obtained. Samples thermally cycled between 200 and 660°C are showing in Fig. 4-5 the transformation from a wall structure into equiaxed cells. More details are found in [21].

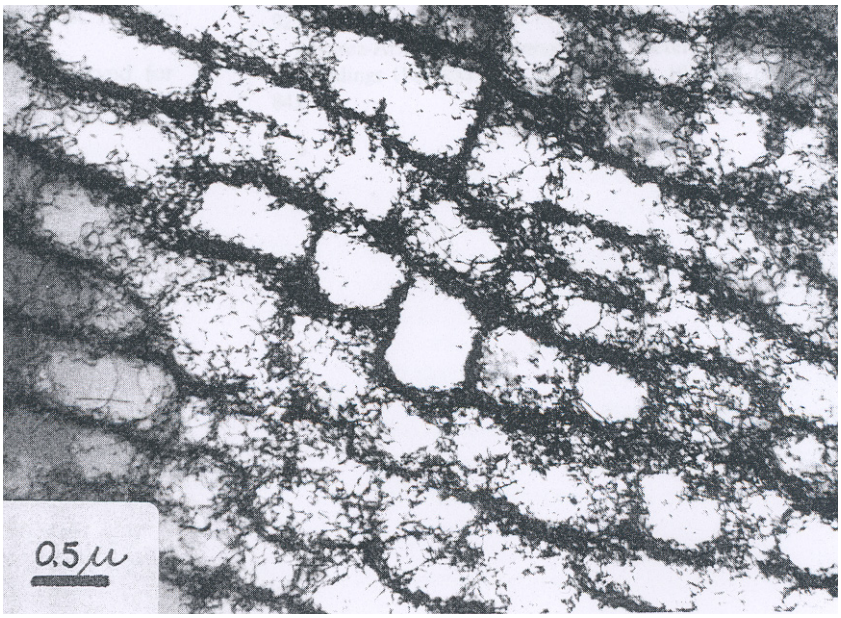

Fig. 4-5 Transformation from wall structure into equiaxed cells of a AISI 316L sample thermally cycled between 200 and 660°C

4.2 Ferritic martensitic steels

Tests on both materials, MANET I and MANET II, without hold times and heating rates of 5.8 K/s with a minimum temperature of 200°C and variable maximum temperatures from 550°C to 700°C had been conducted on hollow hour glass specimens.

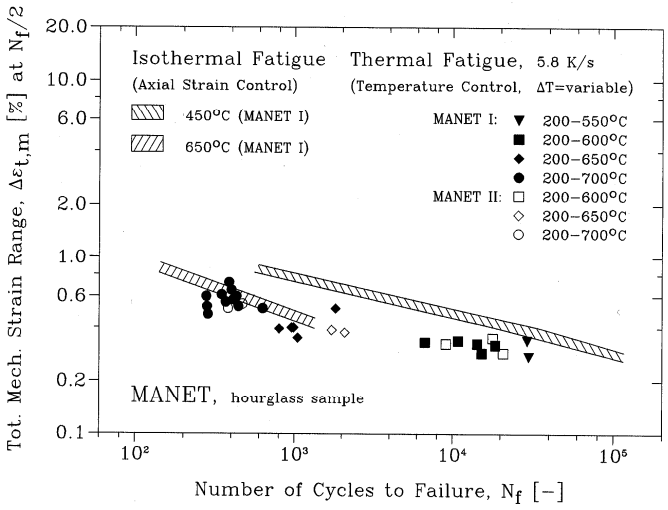

Fig. 4-6 Comparison of the TMF behaviour of MANET I and MANET II without hold time to isothermal LCF data in a similar temperature range in a $\Delta\varepsilon_{t,m}$ versus N_f plot

In Fig. 4-6 are plotted in double logarithmic scale the dependency of the total mechanical strain amplitude $\Delta\varepsilon_{t,m}$ from 0.3 % to 0.8 % versus the number of cycles to failure N_f and compared with isothermal LCF data of MANET I at the temperature of 450°C and of 650°C from [22].

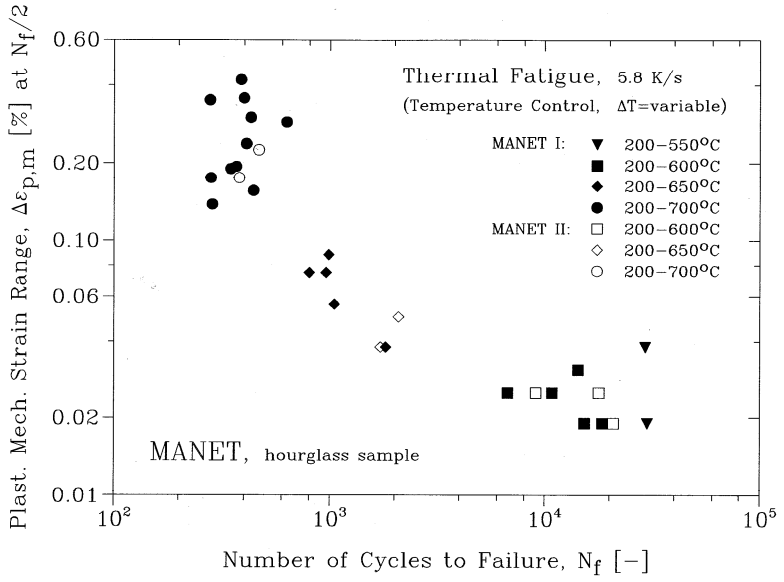

Fig. 4-7 TMF behaviour of MANET I and MANET II without hold time in a $\Delta\varepsilon_{p,m}$ versus N_f plot

In Fig. 4-7 are plotted in double logarithmic scale the dependency of the total mechanical strain amplitude $\Delta\varepsilon_{p,m}$ from 0.024 % to 0.4 % versus the number of cycles to failure N_f, but due to the fact that plastic mechanical strain was not analysed in the isothermal LCF data set of MANET I at the temperature of 450°C and of 650°C no comparison is possible.

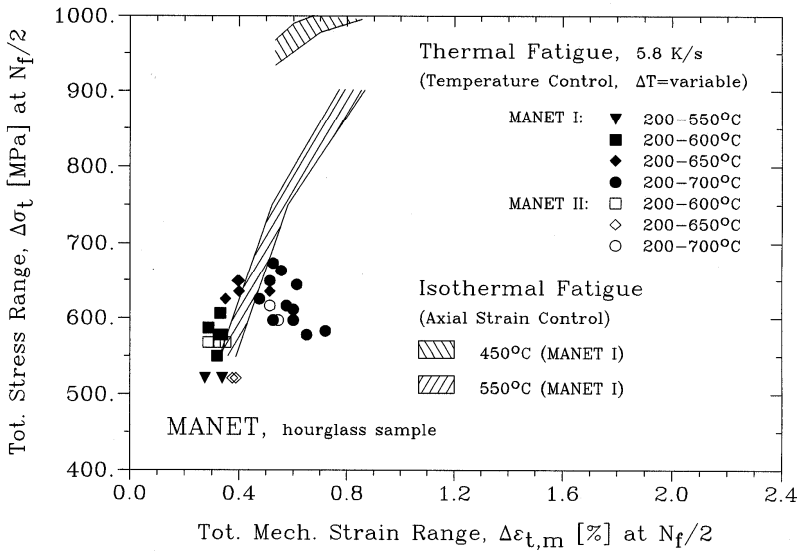

Fig. 4-8 Comparison of the TMF behaviour of MANET I and MANET II without hold time to isothermal strain controlled low cycle fatigue data in a similar temperature range in a $\Delta\sigma_t$ versus $\Delta\varepsilon_{t,m}$ plot

The total saturation stress $\Delta\sigma_t$ shown in Fig. 4-8 goes at TMF testing through a maximum with total mechanical strain range $\Delta\varepsilon_{t,m}$,. Whereas the isothermal strain controlled LCF $\Delta\sigma_t$ data are strongly dependent of $\Delta\varepsilon_{t,m}$.

4.2.1 Modelling of MANET data

The shape of the hourglass specimens was chosen in order to slightly induce the concentration of the strain in the central part of the specimen and, therefore, to initiate and propagate the fatigue cracks there. In case of LCF the average strain in between the ridges of the specimen was controlled and the load was recorded. This results in a inhomogeneous redistribution of the strain along the gauge length of the specimen, which is even amplified by the softening behaviour at various strain amplitudes. Therefore, a detailed analysis was performed [23] to obtain a relation between the applied average strain range and the local strain range in the half-life of the specimen, which is a decisive factor for the life evaluation. This analysis, incorporated the following steps :

1. Complementary LCF tests were performed on cylindrical specimens at six different temperatures in the range 20 to 550°C. During these tests, all the hysteresis stress-strain loops were recorded.

2. A relation, which contains for the plastic strain an expression derived from the Ramberg-Osgood relation

$$\varepsilon_t\ [\%] = (100\ \sigma/E) + 10^{(a + b \log \sigma)} \qquad (1)$$

was fitted to the second tensile hysteresis half-loop plotted in relative coordinates, and the parameters E, a and b were evaluated from the experimental data at each temperature and strain range. Since the form of the hysteresis loop in cyclic straining changes slowly, we can assume that relation (1) remains valid during cycling, keeping the Young´s modulus constant, and optimizing the parameters a and b to obtain the load measured experimentally. This procedure was performed cycle by cycle for the tests on all temperatures.

3. The hourglass specimen was separated into thin discs in which stress and strain are constant. The stress-strain relation found in step "2" was applied to the deformation of each disc, imposing the condition of equal load and the condition of applied average strain, derived from the displacement of the ridges of the specimen. The result of this procedure was compared to results of a numerical simulation of the strain redistribution, using the finite element method (ABAQUS) with the identical stress-strain law. Both methods yield fairly similar results which shows that the thin disc approximation describes the redistribution of the strain very well [23].

4. The evolution of the hysteresis loops during cycling, obtained in step "2" for cylindrical specimens, was then inserted into the evaluation procedure for hourglass specimen described in step "3". It results in an iterative numerical procedure which adjusts cycle by cycle the parameters of the hysteresis loops to the load measured in the experiments. In the first approximation, using the same evolution of the stress-strain law in all discs, the total and the plastic strain ranges in the central part of the specimen can be found, for each average strain range and each temperature.

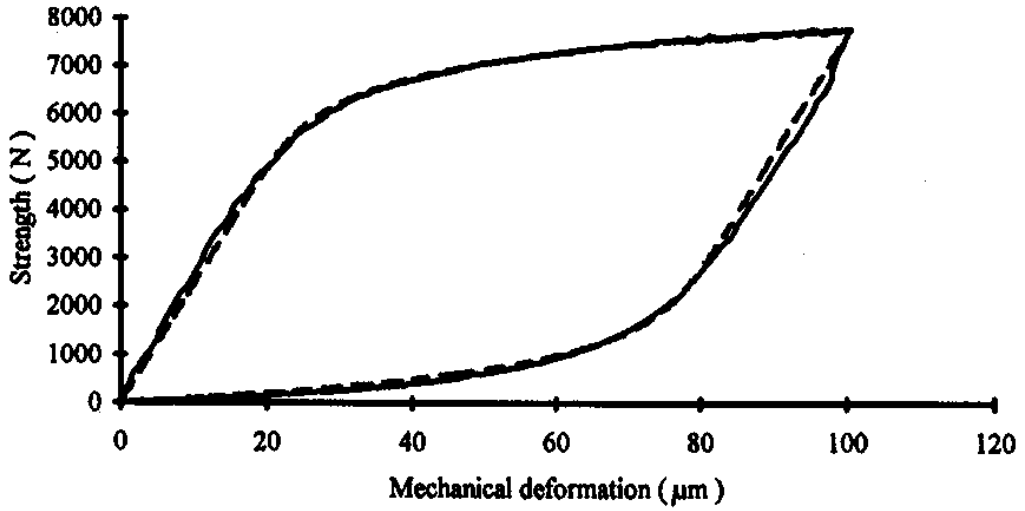

Fig. 4-9 Comparison between measured (full curve) and calculated (dotted curve) hysteresis loops of an LCF experiment at 550°C with a total strain of 1.33 %

Fig. 4-9 shows for a typical LCF hysteresis a good agreement between the measured and the calculated loop using this procedure.

For calculating the TMF hysteresis loops of hollow hourglass samples this stepwise analysis had to be modified in steps "2" and "3" in that way, to introduce a temperature dependance of the parameters E, a and b. These new parameters E(T), a(T) and b(T) were evaluated from the experimental TMF-data.

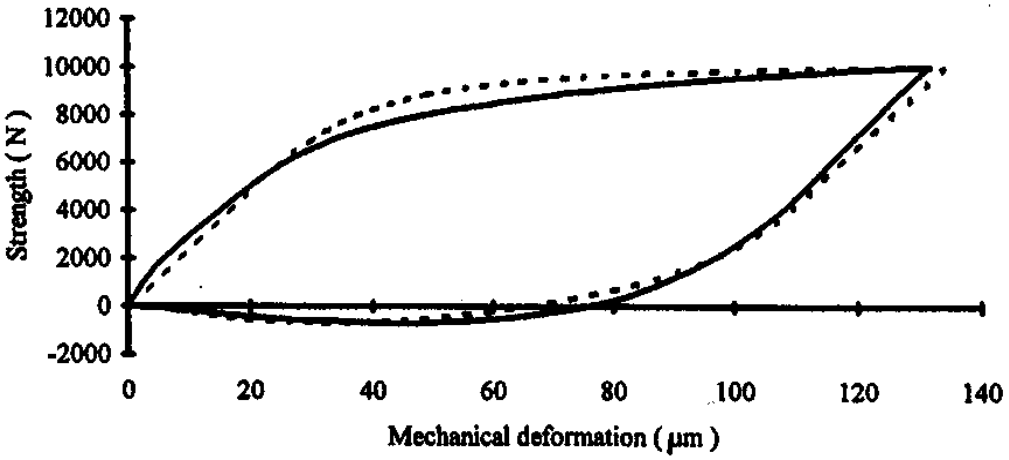

Fig. 4-10 Comparison between measured (full curve) and calculated (dotted curve) hysteresis loops of a TMF experiment cycling between 200 and 550°C with a total strain of 1.33 %

In Fig. 4-10 is shown a typical TMF hysteresis with a good agreement between the measured and the calculated loop using this procedure. G. Degallaix et al. demonstrated in previous studies [24][25] that the complete high temperature LCF behaviour, in a wide temperature

range, can be described by considering that the damage process is controlled simultaneously by two kinds of mechanisms, depending upon the plastic strain range, athermally or thermally-activated. We obtained the following relationship from the Coffin approach [26] (frequency modified fatigue life), which explicitly bring out a strain rate effect and can be written as :

$$\frac{1}{N_R} = \left(\frac{1}{\overset{o}{\varepsilon}_t}\right)^{\alpha} \left(\frac{\Delta\varepsilon_p}{C_p}\right)^{\frac{1}{c}} \left[1 + \left(\frac{1}{\overset{o}{\varepsilon}_t}\right)^{\alpha} A\left(\Delta\varepsilon_p\right)^{b} e^{\frac{-Q}{RT}}\right] \qquad (2)$$

where C_p=165 and c=0.753 are the well-known constants of the Manson-Coffin law and A=4203, b= - 0.64 and the apparent activation energy Q=12.2 Kcal/mol, are material constants, independent of $\Delta\varepsilon_p$ and T, in the whole domain of strains and temperatures. In case of LCF loading it was sufficient to use room temperature data, to determine, by a least-squares method, the values of the coefficients of α=0.055. Finally, an iterative computer code, using a non-linear least-squares method, was used to obtain the values of A and Q. Coefficient b was taken equal to zero, expressing that the Manson-Coffin curves are roughly

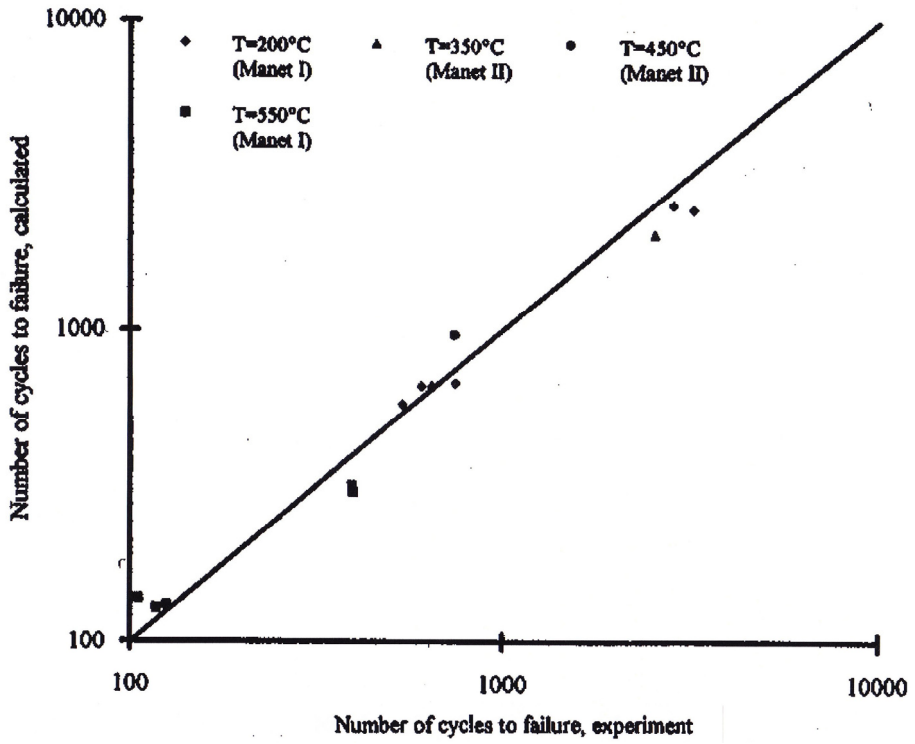

Fig. 4-11 Data correlation of MANET I and MANET II for LCF loading using model (2)

parallel to each other for the various temperatures. It can be noted that the relative small value of the apparent activation energy Q indicates that the contribution from thermally-activated mechanisms to the damage per cycle remains relatively weak, even at the highest temperatures, and thus, that the temperature dependence of LCF behaviour of the MANET steels is moderate.

Fig. 4-11 shows the very good correlation between the experimental and calculated LCF-values. All points fall within a scatter band with a factor of 1.39 (with a mean value of 1.2).

Based on the Taira equivalence concept [27], the calculation of damage for TMF loading will be done on the stabilized hysteresis loop, using a linear damage rule. The damage will be calculated from the elementary contributions of plastic strain, temperature and strain rate during the entire hysteresis loop with the following equation:

$$d(\delta\varphi) = \left(\frac{1}{\dot{\varepsilon}_t}\right)^{\alpha}\left(\frac{\Delta\varepsilon_p}{C_p}\right)^{\frac{1}{c}}\frac{1}{\Delta\varepsilon_p}\left[\frac{1}{c}+\left(\frac{1}{c}+b\right)A\left(\Delta\varepsilon_p\right)^{b}e^{\frac{-Q}{RT}}\right]d\left(\delta\varepsilon_p\right)$$

$$+\left(\frac{1}{\dot{\varepsilon}_t}\right)^{\alpha}\left(\frac{\Delta\varepsilon_p}{C_p}\right)^{\frac{1}{c}}\left[A\left(\Delta\varepsilon_p\right)^{b}\frac{Q}{RT^2}e^{\frac{-Q}{RT}}\right]dT$$

$$-\alpha\frac{1}{\dot{\varepsilon}_t}\left(\frac{1}{\dot{\varepsilon}_t}\right)^{\alpha}\left(\frac{\Delta\varepsilon_p}{C_p}\right)^{\frac{1}{c}}\left[1+A\left(\Delta\varepsilon_p\right)^{b}e^{\frac{-Q}{RT}}\right]d\dot{\varepsilon}_t$$

The integration over every half cycle of the hysteresis gives the damage per cycle:

$$\frac{1}{N_R} = \int_{T_1}^{T_2} d(\delta\varphi) + \int_{T_2}^{T_1} d(\delta\varphi) \qquad (3)$$

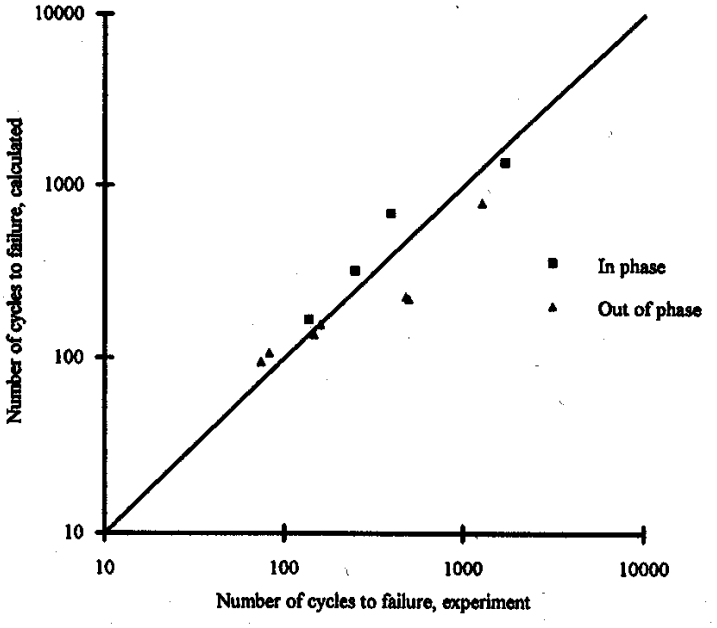

Fig. 4-12 Data correlation of MANET I for in phase and out of phase TMF loading between 200 and 550°C using model (3)

The integration of the elementary increment of damage (assumed to be isothermal, and connected at each time with the increments of plastic strain and temperature) on the TMF cycle will give an estimation of the fatigue life.

Fig. 4-12 shows the good correlation between the experimental and calculated TMF-values. Both damage models express the detrimental effect of higher temperatures on fatigue life. Moreover, the models present notable advantages for the designer. As they correspond to singles and continuous "fatigue strength surfaces", they enable a reliable interpolation to be made throughout the studied domain of strains and temperatures, and allow for reasonable extrapolation out of this domain, provided that no different metallurgical phenomena occur.

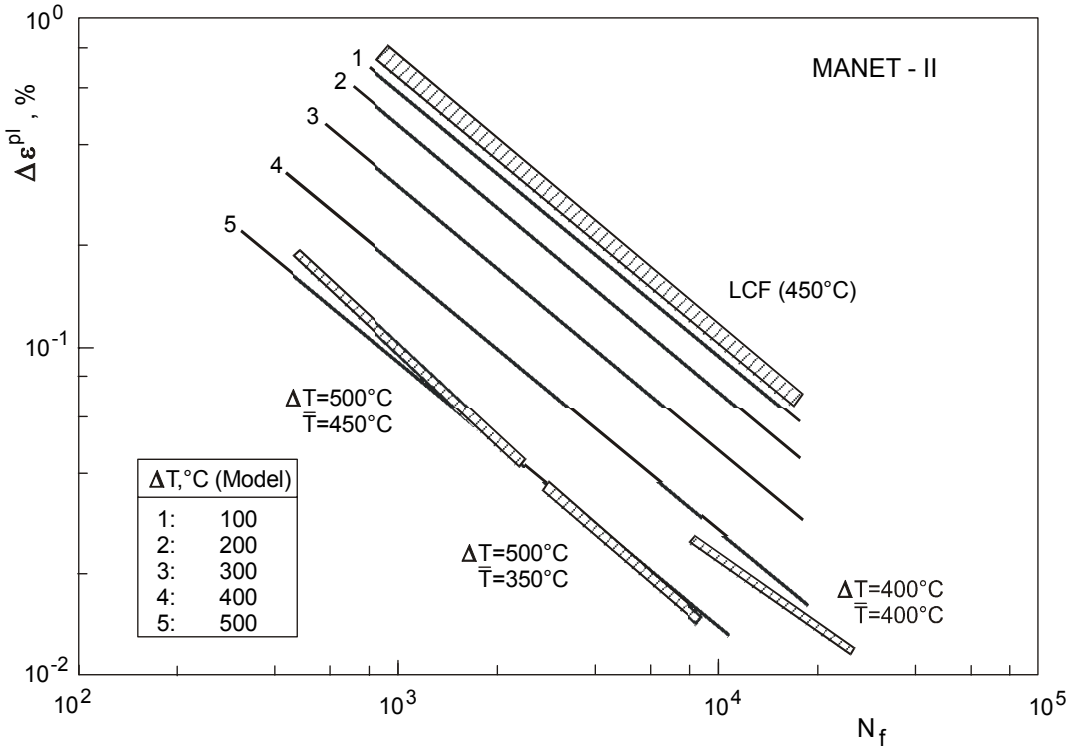

Fig. 4-13 Comparison of TMF and LCFdata for MANET-II in plastic strain range, $\Delta\varepsilon^{pl}$ at $N_f/2$ versus number of cycles to failure, N_f

A "straightforward" way of interpolation by due averaging the material response at LCF conditions over the temperature range in cycle appears to be non-conservative. Appearance of LCF- and TMF-data of MANET-II steel, when represented in logarithmic axes in plastic strain range in cycle versus lifetime, allows, to employ a simple multiplicative model for TMF degradation (Fig. 4-13). According to this model, the strain-related LCF degradation at the mean temperature of the cycle is multiplied by a factor reflecting the effect of temperature oscillation. On this basis an interpolation has been carried out between available LCF- and TMF-data, thus predicting TMF lifetime of this steel within ranges of plastic strain and temperature just expected under ITER conditions. The latter ranges still are not covered by the thermal fatigue experiments performed on rigidly constrained specimens [28].

Recent simulations of thermo-mechanical fatigue tests on selected EUROFER 97 specimens using the finite element method in combination with an advanced coupled deformation damage model result in a local mechanical strain range greater than that assumed experimentally on the base of strain gauge measurements. However, the lifetime due to the calculated local fatigue load is still higher than the lifetime observed experimentally with the corresponding high fatigue load derived from isothermal fatigue experiments. On the basis of strain localization observed in the finite element simulations, geometric nonlinear deformation instabilities are expected, which would yield even higher local fatigue load and thus explain the very low fatigue lifetime observed experimentally. To verify this assumption, geometrically nonlinear simulations, which require development of additional tools, as well as thermo-mechanical fatigue tests with specimens of different geometries are recommended [29].

5 Conclusion

Blanket Modules of a future nuclear fusion reactor are subjected during service to alternating thermal and mechanical stresses as a consequence of the pulsed reactor operation. Therefore the Thermo Mechanical Fatigue (TMF) behaviour of reduced activation ferrite/martensite stainless steels, as its structural material, is examined. After the development of the testing method and the setup of the facilities for TMF testing a series of different materials had been examined.

Since ITER is planned to be constructed with austenitic steels TMF experiments on AISI 316L were performed. There is a remarkable reduction in life time after TMF loading, compared to data of isothermal LCF tests in the same temperature range.

For a DEMO blanket austenitic steels are not any more applicable, due to the high irradiation damage during operation of such a facility. Therefore the ferrite/martensite stainless steels MANET I and MANET II as a modification of a W.Nr. 1.4914 steel had been the first material with better irradiation resistance tested with TMF loading. As reduced activation ferrite/martensite stainless steels, the German heat OPTIFER IV as well as the Japanese F82H mod. and finally the European EUROFER 97 were tested by the TMF method.

All TMF results of examined steels show a remarkable reduction in life time compared to isothermal low cycle fatigue (LCF) tests. The application of hold times up to 1000 s in TMF-experiments leads to a different damage reactions than during LCF loading. Micro structural evaluation during both cyclic loading procedures is very similar and gives no indication of the different damage behaviour.

6 Acknowledgement

The author thanks H. Schneider and G.H. Rubiolo, UNR, for the support during the development of the 7 TMF facilities and D. Rodrian for keeping the TMF facilities as well as the digi-

tal data acquisition over 15 years on the technical state of the art and for performing the TMF experiments during this time.

Many thanks are also given to H. Bergmann and W. Dietz from MECS to put evaluated TMF data into the Mat-DB of JRC, Petten, and to reprocess the data in a hand able form for the enclosed CD.

7 References

[1] ITER web-page: www.iter.org

[2] C. Petersen and G.H. Rubiolo: “High Temperature Thermal Fatigue of AISI 316L“, Journal of Nuclear Materials, Vols. 179 – 181, (1991), pp. 488 – 491.

[3] A. F. Armas, M. Avalos, I. Alvarez-Armas, C. Petersen and R. Schmitt: "Dynamic Strain Aging Evidences during Low Cycle Fatigue Deformation in Ferritic-Martensitic Stainless Steels“, Journal of Nuclear Materials. Vols. 258 – 263, (1998), pp. 1204 – 1208.

[4] C. Petersen: “Thermal Fatigue Behavior of Low Activation Ferritic-Martensitic Steels“, Journal of Nuclear Materials, Vols. 258 – 263, (1998), pp. 1285 – 1290.

[5] A. F. Armas, M. Avalos, I. Alvarez-Armas, C. Petersen and R. Schmitt: “Dynamic Strain Aging Evidences during Low Cycle Fatigue Deformation in Ferritic-Martensitic Stainless Steels“,Fourth International Conference on Low Cycle Fatigue and Elasto-Plastic Behaviour of Materials, LCF 4, Garmisch-Partenkirchen, September 1998, Proc. of LCF 4, eds.: K.-T. Rie and P. D. Portella, (1999) pp. 63 – 68.

[6] C. Petersen: „Thermal Fatigue Behavior of Reduced Activation Ferritic-Martensite Steels“, 20th Symposium on Fusion Technology, 7. – 11. September 1998, Marseille, Frankreich, Proc. of 20th SOFT, eds.: B. Beaumont, P. Libeyre, B. de Gentile and G. Tonon, Vol. 2, pp. 1317 – 1320.

[7] L. Belyaeva, A. Orychtchenko, C. Petersen and V. Rybin: “Postirradiation Thermocyclic Loading of Ferritic-Martensitic Stuctural Materials“, Journal of Nuclear Materials, Vol. 271&272, (1999), pp. 151 – 154.

[8] E. Diegele, C. Petersen, J. Aktaa, and R. Schmitt: “Cyclic Behaviour of Structural Materials for the First Wall of Fusion Reactor“, FZK-Nachrichten, Vol. 31, Issue 1/99, (1999) pp. 55 – 66 (in German)

[9] C. Petersen, D. Rodrian and H. Schneider: „Thermal Fatigue on Steels for the NET-Blanket“, Proceedings of 16th MPA-Seminar, 4. – 5. October 1990, Stuttgart, FRG, pp. 19.1 – 19.15

[10] M. Schirra, S. Heger and A. Falkenstein: “Das Zeitstandfestigkeits- und Kriechverhalten des martensitischen Stahles MANET-II“, FZKA-report 5722, October 1996, Forschungszentrum Karlsruhe (in German)

[11] M. Schirra et al.: “Untersuchungen an 4 Chargen der W-haltigen Legierung OPTIFER-IVc”, Internal report: 31.02.02, June 2000, Forschungszentrum Karlsruhe (in German)

[12] M. Schirra et. al.: “Ergebnisse von Charakterisierungsuntersuchungen zu physikalischen und mechanischen Eigenschaften des martensitischen 9% Cr-Stahles EUROFER 97“, FZKA-report 6707, April 2002, Forschungszentrum Karlsruhe (in German)

[13] M. Schirra, S. Heger and A. Falkenstein: “Das Zeitstandfestigkeits- und Kriechverhalten des niedrigaktivierenden Stahles F82H-mod. (Abschlußbericht)”, FZKA-report 6265, May 1999, Forschungszentrum Karlsruhe (in German)

[14] J. Neumann: “Untersuchungen zur thermozyklischen Ermuedung von Rohren aus dem austenitischen Stahl 1.4436.“ KfK-Report 4669, December 1989, Phd-thesis, Universitaet Karlsruhe 1989 (in German)

[15] W. Vandermeulen et al.: “Influence of neutron irradiation at 430°C on the fatigue properties of SA 316L steel”, Journal of Nuclear Materials, Vol. 155 - 157, (1988), pp. 953 – 956.

[16] B. van der Schaaf: “The effect of neutron irradiation on the fatigue and fatigue-creep behaviour of structural material”, Journal of Nuclear Materials, Vol. 155 - 157, (1988), pp. 156 - 163

[17] W. Scheibe et al.: MAT 1.9 in: Nuclear Fusion Project Semi-annual report of the Association KfK/EURATOM, KfK Report Nr. 4488 (1988)

[18] C. Petersen and G.H. Rubiolo: “High Temperature Thermal Fatigue of Stainless Steels“, Proceedings of “FATIGUE 90”, Vol. III, ISBN 1 872 136 06 0, (1990), pp. 1559 – 1564.

[19] A.F. Armas, O.R. Bettin, I Alvarez-Armas and G.H. Rubiolo: “Strain aging effects on the cyclic behavior of austenitic stainless steels”, J. Nucl. Mater. 155 – 157 (1988) 644 - 649

[20] M. Gerland, J. Mendez, P. Violan and A. Saadi: “Evolution of dislocation structures and cyclic behaviour of a 316L-type austenitic stainless steel cycled *in vacuo* at room temperature”, Mater. Sci. Eng. A 118 (1989) 83-95

[21] a A. F. Armas, I. Alvarez-Armas and C. Petersen: "Thermal fatigue behaviour and dislocation substructures of 316-type austenitic stainless steels“, Journal of Nuclear Materials. Vols. 191 – 194, (1992), pp. 672 – 675

[22] C. Petersen, R. Schmitt and D. Garnier: “Thermal and isothermal low cycle fatigue of MANET I and II”, Journal of Nuclear Materials, 233-237, 1996, Pages 285-288

[23] G. Degallaix, J. Rech, Y. Desplanques, C. Petersen and F. Wolter, Proc. of *Int. Symp. Fatigue under Thermal and Mechanical Loading*, Petten (N.H.), The Netherlands, May 22-24 1995.

[24] G. Degallaix, S. Degallaix and J. Foct: “A damage law for predicting the elevated temperature low cycle fatigue life of a martensitic stainless steel”, Mat. Sci. Engng. 58 (1983), 55-62.

[25] G. Degallaix and P.M. Lesne, Proc. *ECF 6, Fracture Control of Engineering Structures*, Amsterdam (The Netherlands), Ed. T.U. Delft, (1986), p. 44.

[26] L.F. Jr Coffin, *Creep-Fatigue Interaction* ASME-MPC-3 Symp., New York (USA), (1976), 349.

[27] S. Taira, ASTM STP 520 (1973), 80.

[28] A. Zisman, V. Rybin, C. Petersen and R. Schmitt: “Multiplicative Model for Out-of-phase Thermal Fatigue Degradation of Ferritic-Martensitic Steel MANET II“, Journal of Nuclear Materials, Vol. 264, (1999), pp. 234 – 237.

[29] J. Aktaa, M. Klotz and C. Petersen: „“Deformation damage of RAFM steels under thermo-mechanical loading: a challenge for constitutive equations“, Journal of Nuclear Materials, Vol. 367-370, (2007), pp. 550 – 555.

8 Appendix

8.1 Chemical Composition of Steels

Steel Type	C	Cr	Ni	Mo	V	Nb	Si	Mn	Ta	B	W	N
AISI 316L	0.022	17.4	12.34	2.30	-	-	0.46	1.82	-	-	-	0.060-
MANET I	0.14	10.8	0.92	0.77	0.2	0.16	0.37	0.76	-	0.0085	-	0.02
MANET II	0.10	10.3	0.65	0.57	0.19	0.14	0.14	0.75	-	-	-	0.03
OPTIFER IV*)	0.12	9.35	0.007	<0.002	0.26	<0.0006	0.022	0.54	0.07	<0.004	1.03	0.05
F82H mod. *)	0.089	8.16	0.019	0.0018	0.16	0.0001	0.11	0.161	0.02	<0.0002	2.17	0.0065
EUROFER 97*)	0.12	8.93	0.022	0.0015	0.2	0.0022	0.06	0.47	0.14	<0.001	1.07	0.018

Tab. 8-1: Chemical composition of tested materials in wt % (base metal: Fe)

*) In the RAF/M steels also other elements, e.g. Co, Bi, Cd, Ag, etc., so called tramp impurities must be restricted to extremely low levels to reach the reduced activation criteria.

8.2 Heat Treatments of Ferritic/Martensitic Steels

Type	Austenitisation	Tempering
AISI 316L Heat 12247	Not relevant	Not relevant
MANET I Heat 53645	Normalization: 2 h at 980°C, 30 min at 1075°C, air cooled	2 h at 750°C, air cooled
MANET II Heat 50805	Normalization: 2 h at 965°C, 30 min at 1075°C, air cooled	2 h at 750°C, air cooled
OPTIFER IV, Heat 986779	30 min at 1075°C, air cooled	2 h at 750°C, air cooled
F82H mod., Heat 9753	38 min at 1040°C, air cooled	2 h at 750°C, air cooled
EUROFER 97, as received, Heat E83697	31 min at 980°C, air cooled	90 min at 760°C, air cooled
EUROFER 97, heat treated, Heat E83697	31 min at 1040°C, air cooled	90 min at 760°C, air cooled

Tab. 8-2: Thermal treatment of the examined Ferritic/Martensitic materials

8.3 TMF-Results

8.3.1 AISI 316L

Material identifier	Shape identifier	Specimen/Test identifier	Specimen identifier	Test identifier	Condition identifier	heating rate identifier	Hold time identifier	Interrupted identifier	N_{Break}-identifier	Remark identifier
AISI 316L	hourglass	FZK/26,P13/A1	26,P13	A1	200-700 °C	5,8 K/s	-	no	269	OK
AISI 316L	hourglass	FZK/36,P13/A2	36,P13	A2	200-625 °C	5,8 K/s	-	no	1479	OK
AISI 316L	hourglass	FZK/44,P13/A3	44,P13	A3	200-660 °C	5,8 K/s	-	no	641	OK
AISI 316L	hourglass	FZK/25,P13/A4	25,P13	A4	200-660 °C	5,8 K/s	-	no	684	OK
AISI 316L	hourglass	FZK/1,P16/A5	1,P16	A5	200-660 °C	5,8 K/s	-	no	723	OK
AISI 316L	hourglass	FZK/5,P16/A6	5,P16	A6	200-550 °C	5,8 K/s	-	no	5755	irregularities
AISI 316L	hourglass	FZK/7,P16/A7	7,P16	A7	200-750 °C	5,8 K/s	-	no	94	irregularities
AISI 316L	hourglass	FZK/51,P13/A8	51,P13	A8	200-750 °C	5,8 K/s	-	no	92	irregularities
AISI 316L	hourglass	FZK/6,P16/A9	6,P16	A9	200-550 °C	5,8 K/s	100 s (u)	no	3661	OK
AISI 316L	hourglass	FZK/56,P16/A10	56,P16	A10	200-700 °C	5,8 K/s	100 s (o)	no	132	OK
AISI 316L	hourglass	FZK/58,P16/A11	58,P16	A11	200-550 °C	5,8 K/s	100 s (o+u)	no	2656	irregularities
AISI 316L	hourglass	FZK/60,P16/A12	60,P16	A12	200-625 °C	5,8 K/s	100 s (o+u)	no	607	OK
AISI 316L	hourglass	FZK/8,P14/A12	8,P14	A13	200-625 °C	5,8 K/s	100 s (o)	no	913	OK
AISI 316L	hourglass	FZK/28,P13/B1	28,P13	B1	200-700 °C	5,8 K/s	-	no	249	OK
AISI 316L	hourglass	FZK/37,P13/B2	37,P13	B2	200-625 °C	5,8 K/s	-	no	1379	OK
AISI 316L	hourglass	FZK/45,P13/B3	45,P13	B3	200-550 °C	5,8 K/s	-	no	4051	OK
AISI 316L	hourglass	FZK/27,P13/B4	27,P13	B4	200-660 °C	5,8 K/s	-	no	547	OK
AISI 316L	hourglass	FZK/2,P16/B5	2,P16	B5	200-550 °C	5,8 K/s	-	no	4333	OK
AISI 316L	hourglass	FZK/53,P16/B6	53,P16	B6	200-550 °C	5,8 K/s	100 s (o)	no	3425	OK
AISI 316L	hourglass	FZK/30,P16/B7	30,P16	B7	200-700 °C	5,8 K/s	100 s (o+u)	no	92	OK
AISI 316L	hourglass	FZK/59,P16/B8	59,P16	B8	200-660 °C	5,8 K/s	100 s (u)	no	485	OK
AISI 316L	hourglass	FZK/10,P14/B9	10,P14	B9	200-625 °C	5,8 K/s	100 s (o+u)	no	442	OK
AISI 316L	hourglass	FZK/55,P16/C23	55,P16	C23	200-550 °C	5,8 K/s	100 s (o+u)	no	2152	OK

Material identifier	Shape identifier	Specimen/Test identifier	Specimen identifier	Test identifier	Condition identifier	heating rate identifier	Hold time identifier	Interrupted identifier	N_{Break}-identifier	Remark identifier
AISI 316L	hourglass	FZK/63,P16/C24	63,P16	C24	200-660 °C	5,8 K/s	100 s (o+u)	no	131	OK
AISI 316L	hourglass	FZK/14,P14/C31	14,P14	C31	200-450 °C	5,8 K/s	100 s (o+u)	no	101	irregularities
AISI 316L	hourglass	FZK/29,P13/C8	29,P13	C8	200-700 °C	5,8 K/s	-	no	141	OK
AISI 316L	hourglass	FZK/34,P13/C9	34,P13	C9	200-700 °C	5,8 K/s	-	no	160	OK
AISI 316L	hourglass	FZK/35,P13/C10	35,P13	C10	200-700 °C	5,8 K/s	-	no	184	OK
AISI 316L	hourglass	FZK/41,P13/C11	41,P13	C11	200-700 °C	5,8 K/s	-	no	138	OK
AISI 316L	hourglass	FZK/42,P13/C12	42,P13	C12	200-700 °C	5,8 K/s	-	no	153	OK
AISI 316L	hourglass	FZK/43,P13/C13	43,P13	C13	200-700 °C	5,8 K/s	-	no	223	OK
AISI 316L	hourglass	FZK/47,P13/C14-15	47,P13	C14-15	200-550 °C	5,8 K/s	-	yes	5172	OK
AISI 316L	hourglass	FZK/15,P13/C1	15,P13	C1	200-700 °C	5,8 K/s	-	no	353	OK
AISI 316L	hourglass	FZK/16,P13/C2-3	16,P13	C2-3	200-700 °C	5,8 K/s	-	yes	562	OK
AISI 316L	hourglass	FZK/17,P13/C4	17,P13	C4	200-700 °C	5,8 K/s	-	no	220	OK
AISI 316L	hourglass	FZK/18,P13/C5	18,P13	C5	200-700 °C	5,8 K/s	-	no	293	OK
AISI 316L	hourglass	FZK/19,P13/C6	19,P13	C6	200-700 °C	5,8 K/s	-	no	354	OK
AISI 316L	hourglass	FZK/20,P13/C7	20,P13	C7	200-660 °C	5,8 K/s	-	no	1117	OK
AISI 316L	hourglass	FZK/30,P13/D1	30,P13	D1	200-700 °C	5,8 K/s	-	no	252	OK
AISI 316L	hourglass	FZK/33,P13/D2	33,P13	D2	200-625 °C	5,8 K/s	-	no	1362	OK
AISI 316L	hourglass	FZK/38,P13/D3	38,P13	D3	200-625 °C	5,8 K/s	100 s (u)	no	1318	OK
AISI 316L	hourglass	FZK/48,P13/D4	48,P13	D4	200-625 °C	5,8 K/s	100 s (o)	no	728	OK
AISI 316L	hourglass	FZK/64,P16/D8	64,P16	D8	200-660 °C	5,8 K/s	100 s (o)	no	232	OK
AISI 316L	hourglass	FZK/66,P16/D9	66,P16	D9	200-625 °C	5,8 K/s	100 s (u)	no	1134	OK
AISI 316L	hourglass	FZK/11,P14/D10	11,P14	D10	200-600 °C	5,8 K/s	100 s (u)	no	397	OK
AISI 316L	hourglass	FZK/12,P14/D11	12,P14	D11	200-600 °C	5,8 K/s	100 s (o)	no	197	OK
AISI 316L	hourglass	FZK/13,P14/D12	13,P14	D12	200-600 °C	5,8 K/s	100 s (o+u)	no	170	OK
AISI 316L	hourglass	FZK/61,P16/E22	61,P16	E22	200-700 °C	5,8 K/s	100 s (u)	no	130	irregularities
AISI 316L	hourglass	FZK/65,P16/E23	65,P16	E23	200-550 °C	5,8 K/s	100 s (o)	no	3591	OK

Material identifier	Shape identifier	Specimen/Test identifier	Specimen identifier	Test identifier	Condition identifier	heating rate identifier	Hold time identifier	Interrupted identifier	N_{Break}-identifier	Remark identifier
AISI 316L	hourglass	FZK/4,P14/E24	4,P14	E24	200-550 °C	5,8 K/s	100 s (u)	no	3098	OK
AISI 316L	hourglass	FZK/31,P13/E1	31,P13	E1	200-700 °C	5,8 K/s	-	no	253	OK
AISI 316L	hourglass	FZK/32,P13/E2	32,P13	E2	200-625 °C	5,8 K/s	-	no	1321	OK
AISI 316L	hourglass	FZK/39,P13/E3	39,P13	E3	200-625 °C	5,8 K/s	-	no	1178	OK
AISI 316L	hourglass	FZK/40,P13/E4	40,P13	E4	200-700 °C	5,8 K/s	-	no	199	OK
AISI 316L	hourglass	FZK/49,P13/E6	49,P13	E6	200-550 °C	5,8 K/s	-	no	4823	irregularities

no storage

Tab. 8-3: TMF data of AISI 316L

AISI 316L	hourglass	5.8 K/s	without HT				
Nf Krit. [-]	d Sigma t [MPa]	d Eps t,m [%]	d Eps p,m [%]	Nf Krit. [-]	d Sigma t [MPa]	d Eps t,m [%]	d Eps p,m [%]
200-750 °C				**200-660 °C**			
94	738	1.425	1.05	641	737	0.81	0.4
92	728	1.413	1.04	648	768	0.73	0.35
200-700 °C				723	746	0.81	0.43
269	753	0.96	0.57	547	781	0.88	0.46
249	756	1.05	0.65	1117	733	0.69	0.33
353	749	0.9	0.56	**200-625 °C**			
562	751	0.78	0.44	1479	735	0.55	0.2
220	753	1.01	0.76	1379	734	0.71	0.33
293	754	0.98	0.63	1362	707	0.59	0.26
354	748	0.94	0.61	1321	732	0.62	0.34
141	748	1.182	0.81	1178	699	0.69	0.33
160	727	1.19	0.83	**200-550 °C**			
184	754	1.16	0.77	5755	639	0.43	0.13
138	746	1.19	0.83	4051	609	0.56	0.21
153	725	1.26	0.87	4333	645	0.54	0.19
223	751	1.09	0.68	5172	620	0.48	0.21
252	759	0.96	0.59	4823	656	0.44	0.09
253	751	0.97	0.53				
199	747	1.09	0.68				

Tab. 8-4: Specific TMF values of AISI 316L at 200°C lower temperature without hold times

AISI 316L hourglass 5.8 K/s with 100 s HT

Nf Krit. [-]	d Sigma t [MPa]	d Eps t,m [%]	d Eps p,m [%]	Mode	Nf Krit. [-]	d Sigma t [MPa]	d Eps t,m [%]	d Eps p,m [%]	Mode
200-700 °C					**200-625 C**				
132	732	1.25	0.86	HTH	913	689	0.79	0.35	HTH
130	757	1.19	0.79	HTL	728	750	0.73	0.35	HTH
92	752	1.59	1.19	HTHL	1318	727	0.66	0.29	HTL
200-660 °C					1134	762	0.68	0.3	HTL
232	748	1	0.64	HTH	442	778	1	0.56	HTHL
197	706	1.07	0.68	HTH	607	769	0.81	0.4	HTHL
485	773	0.98	0.54	HTL	**200-550 C**				
397	755	0.45	0.45	HTL	3425	705	0.53	0.18	HTH
170	742	1.29	0.85	HTHL	3591	708	0.46	0.1	HTH
131	760	1.34	0.88	HTHL	3661	668	0.49	0.18	HTL
					3098	660	0.54	0.16	HTL
					2656	695	0.61	0.26	HTHL
					2152	745	0.59	0.24	HTHL

HTH = Hold Time at High temperature
HTL = Hold Time at Low temperature
HTHL = Hold Time at both temperatures

Tab. 8-5: Specific TMF values of AISI 316L at 200°C lower temperature with 100s hold times

8.3.2 MANET I

Material identifier	Shape identifier	Specimen/Test identifier	Specimen identifier	Test identifier	Condition identifier	heating rate identifier	Hold time identifier	Interrupted identifier	N_{Break}-identifier	Remark identifier
MANET I	hourglass	FZK/Fe 104T/A14	Fe 104T	A14	100-600 °C	5,8 K/s	-	no	4220	OK
MANET I	hourglass	FZK/Fe 111T/A15-17	Fe 111T	A15-17	100-500 °C	5,8 K/s	-	yes	70110	no fracture
MANET I	hourglass	FZK/Fe 109T/B10	Fe 109T	B10	100-550 °C	5,8 K/s	-	no	15043	OK
MANET I	hourglass	FZK/Fe 119T/B11	Fe 119T	B11	100-600 °C	5,8 K/s	-	no	1000	irregularities
MANET I	hourglass	FZK/Fe 121T/B12	Fe 121T	B12	100-600 °C	5,8 K/s	100 s (o+u)	no	1073	OK
MANET I	hourglass	FZK/Fe 133T/B13	Fe 133T	B13	100-550 °C	5,8 K/s	100 s (o+u)	no	2733	OK
MANET I	hourglass	FZK/Fe 149T/B14	Fe 149T	B14	100-600 °C	5,8 K/s	-	no	2593	OK
MANET I	hourglass	FZK/Fe 61T/C22	Fe 61T	C22	200-550 °C	5,8 K/s	-	no	29995	no fracture
MANET I	hourglass	FZK/Fe 103T/C25	Fe 103T	C25	200-700 °C	5,8 K/s	-	no	400	OK
MANET I	hourglass	FZK/Fe 125T/C26	Fe 125T	C26	200-700 °C	5,8 K/s	-	no	387	OK
MANET I	hourglass	FZK/Fe 94T/C27	Fe 94T	C27	200-650 °C	5,8 K/s	-	no	350	OK
MANET I	hourglass	FZK/Fe 96T/C28	Fe 96T	C28	200-650 °C	5,8 K/s	100 s (o)	no	350	OK
MANET I	hourglass	FZK/Fe 114T/C29	Fe 114T	C29	200-700 °C	5,8 K/s	-	no	430	OK
MANET I	hourglass	FZK/Fe 134T/C30	Fe 134T	C30	200-700 °C	5,8 K/s	-	no	410	OK
MANET I	hourglass	FZK/Fe 115T/C32-34	Fe 115T	C32-34	100-450 °C	5,8 K/s	-	yes	70000	no fracture
MANET I	hourglass	FZK/Fe 45T/C16	Fe 45T	C16	200-700 °C	5,8 K/s	-	no	281	OK
MANET I	hourglass	FZK/Fe 47T/C17	Fe 47T	C17	200-700 °C	5,8 K/s	-	no	285	OK
MANET I	hourglass	FZK/Fe 48T/C18	Fe 48T	C18	200-700 °C	5,8 K/s	-	no	278	OK
MANET I	hourglass	FZK/Fe 53T/C19	Fe 53T	C19	200-650 °C	5,8 K/s	-	no	986	OK
MANET I	hourglass	FZK/Fe 57T/C20	Fe 57T	C20	200-650 °C	5,8 K/s	-	no	958	OK
MANET I	hourglass	FZK/Fe 58T/C21	Fe 58T	C21	200-600 °C	5,8 K/s	-	no	6693	irregularities
MANET I	hourglass	FZK/Fe 43T/D5	Fe 43T	D5	200-700 °C	5,8 K/s	-	no	105	irregularities

Material identifier	Shape identi-fier	Specimen/Test iden-tifier	Specimen identifier	Test iden-tifier	Condition identifier	heating rate identifier	Hold time identifier	Interrupted identifier	N_{Break}-identifier	Remark identifier
MANET I	hourglass	FZK/Fe 81T/D6	Fe 81T	D6	200-700 °C	5,8 K/s	100 s (u)	no	274	OK
MANET I	hourglass	FZK/Fe 85T/D7	Fe 85T	D7	200-650 °C	5,8 K/s	100 s (o)	no	1325	irregularities
MANET I	hourglass	FZK/Fe 120T/D13	Fe 120T	D13	100-600 °C	5,8 K/s	-	no	200	no fracture
MANET I	hourglass	FZK/Fe 122T/D14	Fe 122T	D14	100-600 °C	5,8 K/s	100 s (o)	no	1809	OK
MANET I	hourglass	FZK/Fe 123T/D15	Fe 123T	D15	100-600 °C	5,8 K/s	100 s (u)	no	2373	OK
MANET I	hourglass	FZK/Fe 156T/D16	Fe 156T	D16	200-650 °C	5,8 K/s	100 s (o+u)	no	100	no fracture
MANET I	hourglass	FZK/Fe 157T/D17	Fe 157T	D17	200-650 °C	5,8 K/s	100 s (o+u)	no	20	no fracture
MANET I	hourglass	FZK/Fe 161T/D18	Fe 161T	D18	200-650 °C	5,8 K/s	100 s (o+u)	no	4	no fracture
MANET I	hourglass	FZK/Fe 184T/D19	Fe 184T	D19	200-650 °C	5,8 K/s	100 s (o+u)	no	260	no fracture
MANET I	hourglass	FZK/Fe 191T/D20	Fe 191T	D20	200-650 °C	5,8 K/s	100 s (o+u)	no	396	no fracture
MANET I	hourglass	FZK/Fe 136T/D21	Fe 136T	D21	200-650 °C	5,8 K/s	1000 s (o)	no	429	OK
MANET I	hourglass	FZK/Fe 64T/E18-19	Fe 64T	E18-19	200-600 °C	5,8 K/s	100 s (u)	yes	9337	irregularities
MANET I	hourglass	FZK/Fe 75T/E20	Fe 75T	E20	200-600 °C	5,8 K/s	-	no	31	irregularities
MANET I	hourglass	FZK/Fe 76T/E21	Fe 76T	E21	200-600 °C	5,8 K/s	-	no	15282	irregularities
MANET I	hourglass	FZK/Fe 164T/E25	Fe 164T	E25	200-600 °C	5,8 K/s	-	no	18541	irregularities
MANET I	hourglass	FZK/Fe 124T/E26	Fe 124T	E26	100-650 °C	5,8 K/s	-	no	832	OK
MANET I	hourglass	FZK/Fe 132T/E27-28	Fe 132T	E27-28	100-550 °C	5,8 K/s	-	yes	47583	irregularities
MANET I	hourglass	FZK/Fe 181T/E29-30	Fe 181T	E29-30	100-550 °C	5,8 K/s	100 s (u)	yes	7405	irregularities
MANET I	hourglass	FZK/Fe 193T/E31	Fe 193T	E31	200-650 °C	5,8 K/s	1000 s (o+u)	no	115	OK
MANET I	hourglass	FZK/Fe 138T/E32	Fe 138T	E32	200-650 °C	5,8 K/s	1000 s (u)	no	1602	OK
MANET I	hourglass	FZK/Fe 34T/E7	Fe 34T	E7	200-700 °C	5,8 K/s	-	no	442	OK
MANET I	hourglass	FZK/Fe 35T/E8	Fe 35T	E8	200-700 °C	5,8 K/s	-	no	368	OK
MANET I	hourglass	FZK/Fe 36T/E9	Fe 36T	E9	200-700 °C	5,8 K/s	-	no	629	irregularities
MANET I	hourglass	FZK/Fe 46T/E10	Fe 46T	E10	200-650 °C	5,8 K/s	-	no	2216	irregularities
MANET I	hourglass	FZK/Fe 52T/E11	Fe 52T	E11	200-700 °C	5,8 K/s	-	no	347	irregularities
MANET I	hourglass	FZK/Fe 55T/E12	Fe 55T	E12	200-650 °C	5,8 K/s	-	no	1047	OK

Material identifier	Shape identifier	Specimen/Test identifier	Specimen identifier	Test identifier	Condition identifier	heating rate identifier	Hold time identifier	Interrupted identifier	N_{Break}-identifier	Remark identifier
MANET I	hourglass	FZK/Fe 56T/E13-14	Fe 56T	E13-14	200-600 °C	5,8 K/s	-	yes	10841	irregularities
MANET I	hourglass	FZK/Fe 60T/E15-16	Fe 60T	E15-16	200-600 °C	5,8 K/s	-	yes	14296	irregularities
MANET I	hourglass	FZK/Fe 62T/E17	Fe 62T	E17	200-550 °C	5,8 K/s	-	no	29342	irregularities
MANET I	hourglass	FZK/Fe 113T/G14	Fe 113T	G14	100-550 °C	3,0 K/s	100 s (o+u)	no	1873	irregularities
MANET I	hourglass	FZK/Fe 154T/G22-24	Fe 154T	G2	200-550 °C	5,8 K/s	-	yes	86057	no fracture
MANET I	hourglass	FZK/Fe 65T/G1	Fe 65T	G1	200-650 °C	5,8 K/s	100 s (u)	no	1137	OK
MANET I	hourglass	FZK/Fe 100T/G2	Fe 100T	G22-24	200-650 °C	5,8 K/s	100 s (o)	no	593	OK
MANET I	hourglass	FZK/Fe 77T/G3	Fe 77T	G3	200-650 °C	5,8 K/s	100 s (u)	no	1327	irregularities
MANET I	hourglass	FZK/Fe 95T/G4	Fe 95T	G4	200-700 °C	5,8 K/s	-	no	2	irregularities
MANET I	hourglass	FZK/Fe 135T/G5	Fe 135T	G5	100-600 °C	3,0 K/s	-	no	2724	OK
MANET I	hourglass	FZK/Fe 144T/G6	Fe 144T	G6	100-600 °C	3,0 K/s	100 s (u)	no	1870	OK
MANET I	hourglass	FZK/Fe 147T/G7	Fe 147T	G7	100-600 °C	3,0 K/s	100 s (o)	no	1132	OK
MANET I	hourglass	FZK/Fe 148T/G8	Fe 148T	G8	100-600 °C	3,0 K/s	100 s (o+u)	no	815	OK
MANET I	hourglass	FZK/Fe 166T/G9	Fe 166T	G9	100-600 °C	3,0 K/s	-	no	1111	irregularities
MANET I	hourglass	FZK/Fe 170T/G10	Fe 170T	G10	100-600 °C	3,0 K/s	-	no	2106	OK
MANET I	hourglass	FZK/Fe 179T/G11	Fe 179T	G11	100-600 °C	3,0 K/s	100 s (u)	no	1765	OK
MANET I	hourglass	FZK/Fe 187T/G12	Fe 187T	G12	100-600 °C	3,0 K/s	100 s (o)	no	1166	OK
MANET I	hourglass	FZK/Fe 185T/G13	Fe 185T	G13	100-600 °C	3,0 K/s	100 s (o+u)	no	898	OK
MANET I	hourglass	FZK/Fe 172T/H14	Fe 172T	H14	100-550 °C	3,0 K/s	-	no	7982	OK
MANET I	hourglass	FZK/Fe 190T/H15	Fe 190T	H15	100-550 °C	3,0 K/s	100 s (o)	no	4978	OK
MANET I	hourglass	FZK/Fe 142T/H16-17	Fe 142T	H16-17	200-550 °C	5,8 K/s	1000 s (o+u)	yes	1403	irregularities
MANET I	hourglass	FZK/Fe 66T/H1	Fe 66T	H1	200-600 °C	5,8 K/s	100 s (o+u)	no	3033	OK
MANET I	hourglass	FZK/Fe 68T/H2	Fe 68T	H2	200-650 °C	5,8 K/s	100 s (o)	no	755	OK
MANET I	hourglass	FZK/Fe 70T/H3	Fe 70T	H3	200-700 °C	5,8 K/s	100 s (o+u)	no	16	irregularities
MANET I	hourglass	FZK/Fe 72T/H4	Fe 72T	H4	200-700 °C	5,8 K/s	100 s (o+u)	no	158	OK
MANET I	hourglass	FZK/Fe 79T/H5	Fe 79T	H5	200-650 °C	5,8 K/s	-	no	1817	OK

Material identifier	Shape identifier	Specimen/Test identifier	Specimen identifier	Test identifier	Condition identifier	heating rate identifier	Hold time identifier	Interrupted identifier	N_{Break}-identifier	Remark identifier
MANET I	hourglass	FZK/Fe 83T/H6	Fe 83T	H6	200-650 °C	5,8 K/s	-	no	1489	irregularities
MANET I	hourglass	FZK/Fe 88T/H7	Fe 88T	H7	200-600 °C	5,8 K/s	100 s (o+u)	no	2952	OK
MANET I	hourglass	FZK/Fe 80T/H8	Fe 80T	H8	200-700 °C	5,8 K/s	100 s (o+u)	no	172	OK
MANET I	hourglass	FZK/Fe 90T/H9	Fe 90T	H9	200-700 °C	5,8 K/s	100 s (o)	no	217	OK
MANET I	hourglass	FZK/Fe 93T/H10	Fe 93T	H10	200-650 °C	5,8 K/s	100 s (u)	no	350	irregularities
MANET I	hourglass	FZK/Fe 99T/H11	Fe 99T	H11	200-600 °C	5,8 K/s	100 s (o)	no	5762	OK
MANET I	hourglass	FZK/Fe 98T/H12	Fe 98T	H12	200-650 °C	5,8 K/s	100 s (o)	no	350	irregularities
MANET I	hourglass	FZK/Fe 169T/H13	Fe 169T	H13	100-550 °C	3,0 K/s	-	no	1004	irregularities
MANET I	hourglass	FZK/Fe 67T/I1	Fe 67T	I1	200-600 °C	5,8 K/s	100 s (o)	no	3028	OK
MANET I	hourglass	FZK/Fe 69T/I2	Fe 69T	I2	200-650 °C	5,8 K/s	100 s (o+u)	no	344	OK
MANET I	hourglass	FZK/Fe 71T/I3	Fe 71T	I3	200-700 °C	5,8 K/s	100 s (o)	no	159	OK
MANET I	hourglass	FZK/Fe 73T/I4	Fe 73T	I4	200-700 °C	5,8 K/s	100 s (u)	no	222	OK
MANET I	hourglass	FZK/Fe 78T/I5	Fe 78T	I5	200-600 °C	5,8 K/s	100 s (u)	no	6250	OK
MANET I	hourglass	FZK/Fe 84T/I6	Fe 84T	I6	200-650 °C	5,8 K/s	100 s (o+u)	no	399	OK
MANET I	hourglass	FZK/Fe 86T/I7	Fe 86T	I7	200-650 °C	5,8 K/s	100 s (u)	no	861	OK
MANET I	hourglass	FZK/Fe 89T/I8	Fe 89T	I8	200-650 °C	5,8 K/s	-	no	800	OK
MANET I	hourglass	FZK/Fe 91T/I9	Fe 91T	I9	200-600 °C	5,8 K/s	100 s (o)	no	2433	OK
MANET I	hourglass	FZK/Fe 92T/I10	Fe 92T	I10	200-550 °C	5,8 K/s	100 s (o+u)	no	10830	irregularities

no storage

Tab. 8-6: TMF data of MANET I

MANET I	hourglass	5.8 K/s	without HT				
Nf Krit. [-]	d Sigma t [MPa]	d Eps t,m [%]	d Eps p,m [%]	Nf Krit. [-]	d Sigma t [MPa]	d Eps t,m [%]	d Eps p,m [%]
100-650 °C				**100-550 °C**			
832	711	0.525	0.138	15043	654	0.344	0.013
100-600 °C				47583	616	0.313	0.019
4255	692	0.413	0.019	**100-500 °C**			
2593	696	0.4	0.075	70110	564	0.288	0.013
				100-450 °C			
				70000	493	0.263	0.025

Tab. 8-7: Specific TMF values of MANET I at 100°C lower temperature without hold times

MANET I	hourglass	5.8 K/s	without HT				
Nf Krit. [-]	d Sigma t [MPa]	d Eps t,m [%]	d Eps p,m [%]	Nf Krit. [-]	d Sigma t [MPa]	d Eps t,m [%]	d Eps p,m [%]
200-700 °C				**200-650 °C**			
261	597	0.525	0.175	945	649	0.4	0.088
272	625	0.475	0.138	930	635	0.4	0.075
269	597	0.6	0.35	1040	625	0.35	0.056
380	578	0.65	0.356	1805	635	0.513	0.038
370	583	0.719	0.419	780	649	0.394	0.075
424	611	0.6	0.3	**200-600 °C**			
400	616	0.575	0.238	6630	606	0.331	0.025
430	673	0.525	0.156	15278	587	0.288	0.019
348	663	0.556	0.194	18540	550	0.319	0.019
615	649	0.513	0.288	10840	578	0.338	0.025
327	644	0.613	0.19	14280	578	0.325	0.031
				200-550 °C			
				29342	521	0.338	0.038
				29995	521	0.275	0.019

Tab. 8-8: Specific TMF values of MANET I at 200°C lower temperature without hold times

MANET I hourglass 5.8 K/s with 100 s HT

Nf Krit. [-]	d Sigma t [MPa]	d Eps t,m [%]	d Eps p,m [%]	Mode	Nf Krit. [-]	d Sigma t [MPa]	d Eps t,m [%]	d Eps p,m [%]	Mode
200-700 °C					**200-600 °C**				
270	568	0.625	0.338	HTL	9300	625	0.288	0.019	HTL
150	653	0.725	0.481	HTHL	3015	654	0.338	0.016	HTHL
158	635	0.725	0.45	HTHL	2935	677	0.354	0.038	HTHL
205	621	0.7	0.388	HTH	5750	611	0.381	0.075	HTH
120	616	0.794	0.513	HTH	3008	644	0.35	0.025	HTH
211	682	0.65	0.338	HTL	6250	654	0.331	0.056	HTL
200-650 °C					2433	606	0.35	0.025	HTH
1300	635	0.425	0.075	HTH	**200-550 °C**				
1109	663	0.35	0.063	HTL	10830	616	0.238	0.013	HTHL
571	649	0.45	0.15	HTH					
1314	673	0.4	0.056	HTL					
745	644	0.406	0.104	HTH					
313	677	0.6	0.269	HTHL					
350	654	0.613	0.306	HTHL					
847	701	0.413	0.069	HTL					

HTH = Hold Time at High temperature
HTL = Hold Time at Low temperature
HTHL = Hold Time at both temperatures

Tab. 8-9: Specific TMF values of MANET I at 200°C lower temperature with 100s hold times

8.3.3 MANET II

Material identifier	Shape identifier	Specimen/Test identifier	Specimen identifier	Test identifier	Condition identifier	heating rate identifier	Hold time identifier	Interrupted identifier	N_{Break}-identifier	Remark identifier
MANET II	hourglass	FZK/II 9T/B24	II 9T	B24	100-600 °C	5,8 K/s	-	no	2672	OK
MANET II	hourglass	FZK/II 2T/D22	II 2T	D22	200-650 °C	5,8 K/s	-	no	2082	OK
MANET II	hourglass	FZK/II 3T/D23	II 3T	D23	200-650 °C	5,8 K/s	-	no	1721	OK
MANET II	hourglass	FZK/II 4T/D24-25	II 4T	D24-25	200-600 °C	5,8 K/s	-	yes	9094	irregularities
MANET II	hourglass	FZK/II 5T/D26-28	II 5T	D26-28	200-600 °C	5,8 K/s	-	yes	17854	irregularities
MANET II	hourglass	FZK/II 3T/D30	II 3T	D30	100-600 °C	5,8 K/s	-	no	2945	irregularities
MANET II	hourglass	FZK/II 1T/E33-34	II 1T	E33-34	200-600 °C	5,8 K/s	-	yes	20801	irregularities
MANET II	hourglass	FZK/II 6T/G20	II 6T	G20	200-700 °C	5,8 K/s	-	no	380	OK
MANET II	hourglass	FZK/II 7T/H19	II 7T	H19	200-700 °C	5,8 K/s	-	no	380	OK
MANET II	cyldr.	FZK/II 77TZ/A29-32	II 77TZ	A29-32	100-500 °C	5,8 K/s	100 s (u)	yes	71190	no fracture
MANET II	cyldr.	FZK/II 127TZ/A33	II 127TZ	A33	100-550 °C	3,0 K/s	-	no	19960	OK
MANET II	cyldr.	FZK/II 143TZ/A34-35	II 143TZ	A34-35	100-450 °C	3,0 K/s	100 s (u)	yes	65892	irregularities
MANET II	cyldr.	FZK/II 3TZ/A18-19	II 3TZ	A18-19	200-600 °C	5,8 K/s	-	yes	17420	irregularities
MANET II	cyldr.	FZK/II 35TZ/A20-21	II 35TZ	A20-21	100-600 °C	5,8 K/s	-	yes	8232	irregularities
MANET II	cyldr.	FZK/II 14TZ/A22	II 14TZ	A22	100-600 °C	5,8 K/s	-	no	6494	OK
MANET II	cyldr.	FZK/II 44TZ/A23	II 44TZ	A23	100-550 °C	5,8 K/s	100 s (o+u)	no	9127	OK
MANET II	cyldr.	FZK/II 16TZ/A24-25	II 16TZ	A24-25	100-550 °C	5,8 K/s	100 s (u)	yes	17864	irregularities
MANET II	cyldr.	FZK/II 22TZ/A26-28	II 22TZ	A26-28	200-550 °C	5,8 K/s	100 s (o+u)	yes	41170	irregularities
MANET II	cyldr.	FZK/II 106TZ/B29-32	II 106TZ	B29-32	100-450 °C	5,8 K/s	100 s (u)	yes	70454	no fracture
MANET II	cyldr.	FZK/II 116TZ/B33	II 116TZ	B33	100-550 °C	3,0 K/s	100 s (u)	no	16856	OK
MANET II	cyldr.	FZK/II 150TZ/B34-36	II 150TZ	B34-36	100-450 °C	3,0 K/s	100 s (o+u)	yes	69973	no fracture
MANET II	cyldr.	FZK/II 4TZ/B15	II 4TZ	B15	200-650 °C	5,8 K/s	-	no	1512	OK

Material identifier	Shape identifier	Specimen/Test identifier	Specimen identifier	Test identifier	Condition identifier	heating rate identifier	Hold time identifier	Interrupted identifier	N_{Break}-identifier	Remark identifier
MANET II	cyldr.	FZK/II 5TZ/B16	II 5TZ	B16	200-650 °C	5,8 K/s	-	no	2409	OK
MANET II	cyldr.	FZK/II 6TZ/B17	II 6TZ	B17	200-600 °C	5,8 K/s	-	no	20697	OK
MANET II	cyldr.	FZK/II 51TZ/B18	II 51TZ	B18	200-700 °C	5,8 K/s	-	no	464	OK
MANET II	cyldr.	FZK/II 48TZ/B19	II 48TZ	B19	200-700 °C	5,8 K/s	-	no	429	OK
MANET II	cyldr.	FZK/II 46TZ/B20	II 46TZ	B20	100-600 °C	5,8 K/s	100 s (o+u)	no	1311	OK
MANET II	cyldr.	FZK/II 62TZ/B21	II 62TZ	B21	100-600 °C	5,8 K/s	100 s (o)	no	2207	OK
MANET II	cyldr.	FZK/II 38TZ/B22	II 38TZ	B22	100-600 °C	5,8 K/s	100 s (u)	no	2951	OK
MANET II	cyldr.	FZK/II 29TZ/B23	II 29TZ	B23	200-600 °C	5,8 K/s	-	no	24987	OK
MANET II	cyldr.	FZK/II 75TZ/B25-28	II 75TZ	B25-28	200-550 °C	5,8 K/s	100 s (o)	yes	70441	no fracture
MANET II	cyldr.	FZK/II 141TZ/C48	II 141TZ	C48	250-600 °C	5,8 K/s	-	no	50508	OK
MANET II	cyldr.	FZK/II 147TZ/C49	II 147TZ	C49	300-600 °C	5,8 K/s	-	no	72349	no fracture
MANET II	cyldr.	FZK/II 18TZ/C35-40	II 18TZ	C35-40	200-550 °C	5,8 K/s	100 s (u)	yes	72143	no fracture
MANET II	cyldr.	FZK/II 104TZ/C41	II 104TZ	C41	100-600 °C	3,0 K/s	100 s (o+u)	no	1285	OK
MANET II	cyldr.	FZK/II 129TZ/C42	II 129TZ	C42	100-600 °C	3,0 K/s	100 s (o)	no	1503	OK
MANET II	cyldr.	FZK/II 96TZ/C43	II 96TZ	C43	100-600 °C	3,0 K/s	100 s (u)	no	2285	OK
MANET II	cyldr.	FZK/II 125TZ/C44-45	II 125TZ	C44-45	100-600 °C	3,0 K/s	-	yes	2625	irregularities
MANET II	cyldr.	FZK/II 86TZ/C46-47	II 86TZ	C46-47	100-500 °C	3,0 K/s	-	yes	74890	no fracture
MANET II	cyldr.	FZK/II 64TZ/D33-36	II 64TZ	D33-36	100-500 °C	5,8 K/s	100 s (o+u)	yes	43957	irregularities
MANET II	cyldr.	FZK/II 133TZ/D37-38	II 133TZ	D37-38	100-550 °C	3,0 K/s	100 s (o+u)	yes	1696	irregularities
MANET II	cyldr.	FZK/II 114TZ/D39-40	II 114TZ	D39-40	100-500 °C	3,0 K/s	100 s (u)	yes	70085	no fracture
MANET II	cyldr.	FZK/II 148TZ/D41-42	II 148TZ	D41-42	100-450 °C	3,0 K/s	100 s (o)	yes	69770	no fracture
MANET II	cyldr.	FZK/II 23TZ/D29	II 23TZ	D29	100-550 °C	5,8 K/s	100 s (o)	no	17593	OK
MANET II	cyldr.	FZK/II 27TZ/D31-32	II 27TZ	D31-32	100-550 °C	5,8 K/s	-	yes	30256	irregularities
MANET II	cyldr.	FZK/II 161TZ/E60	II 161TZ	E60	200-600 °C	5,8 K/s	-	no	2000	irregularities
MANET II	cyldr.	FZK/II 142TZ/E46	II 142TZ	E46	250-600 °C	5,8 K/s	-	no	70147	no fracture
MANET II	cyldr.	FZK/II 151TZ/E47-48	II 151TZ	E47-48	350-600 °C	5,8 K/s	-	yes	107836	no fracture

Material identifier	Shape identifier	Specimen/Test identifier	Specimen identifier	Test identifier	Condition identifier	heating rate identifier	Hold time identifier	Interrupted identifier	N_{Break}-identifier	Remark identifier
MANET II	cyldr.	FZK/II 25TZ/E35-37	II 25TZ	E35-37	100-550 °C	5,8 K/s	-	yes	69090	no fracture
MANET II	cyldr.	FZK/II 84TZ/E38-40	II 84TZ	E38-40	200-550 °C	5,8 K/s	-	yes	83932	no fracture
MANET II	cyldr.	FZK/II 54TZ/E41-45	II 54TZ	E41-45	100-450 °C	5,8 K/s	100 s (o+u)	yes	87659	no fracture
MANET II	cyldr.	FZK/II 145TZ/F14	II 145TZ	F14	200-650 °C	5,8 K/s	1000 s (o+u)	no	119	irregularities
MANET II	cyldr.	FZK/II 146TZ/F15	II 146TZ	F15	200-650 °C	5,8 K/s	1000 s (u)	no	2152	OK
MANET II	cyldr.	FZK/II 32TZ/F1	II 32TZ	F1	200-650 °C	5,8 K/s	100 s (o+u)	no	576	OK
MANET II	cyldr.	FZK/II 60TZ/F2	II 60TZ	F2	200-650 °C	5,8 K/s	100 s (o)	no	1498	OK
MANET II	cyldr.	FZK/II 36TZ/F3	II 36TZ	F3	200-650 °C	5,8 K/s	100 s (u)	no	2467	irregularities
MANET II	cyldr.	FZK/II 81TZ/F4	II 81TZ	F4	200-650 °C	5,8 K/s	1000 s (o+u)	no	114	OK
MANET II	cyldr.	FZK/II 80TZ/F5-6	II 80TZ	F5-6	100-550 °C	5,8 K/s	100 s (o)	yes	21855	irregularities
MANET II	cyldr.	FZK/II 67TZ/F7	II 67TZ	F7	100-550 °C	5,8 K/s	100 s (o)	no	12306	OK
MANET II	cyldr.	FZK/II 57TZ/F8-10	II 57TZ	F8-10	100-500 °C	5,8 K/s	-	yes	56425	irregularities
MANET II	cyldr.	FZK/II 112TZ/F11-12	II 112TZ	F11-12	100-550 °C	5,8 K/s	100 s (o)	yes	3555	irregularities
MANET II	cyldr.	FZK/II 140TZ/F13	II 140TZ	F13	100-550 °C	3,0 K/s	100 s (o)	no	9694	OK
MANET II	cyldr.	FZK/II 61TZ/G15	II 61TZ	G15	200-600 °C	5,8 K/s	100 s (o+u)	no	6269	OK
MANET II	cyldr.	FZK/II 56TZ/G16	II 56TZ	G16	200-700 °C	5,8 K/s	100 s (o+u)	no	215	OK
MANET II	cyldr.	FZK/II 12TZ/G17-18	II 12TZ	G17-18	200-700 °C	5,8 K/s	100 s (o)	yes	296	irregularities
MANET II	cyldr.	FZK/II 85TZ/G19	II 85TZ	G19	200-700 °C	5,8 K/s	100 s (u)	no	422	OK
MANET II	cyldr.	FZK/II 74TZ/G21	II 74TZ	G21	100-550 °C	5,8 K/s	100 s (o+u)	no	3868	OK
MANET II	cyldr.	FZK/II 59TZ/G25-28	II 59TZ	G25-28	100-450 °C	5,8 K/s	-	yes	80822	no fracture
MANET II	cyldr.	FZK/II 134TZ/G29-30	II 134TZ	G29-30	100-500 °C	3,0 K/s	100 s (o+u)	yes	69804	no fracture
MANET II	cyldr.	FZK/II 37TZ/H18	II 37TZ	H18	200-600 °C	5,8 K/s	100 s (o)	no	6546	OK
MANET II	cyldr.	FZK/II 68TZ/H20	II 68TZ	H20	200-650 °C	5,8 K/s	1000 s (o)	no	493	OK
MANET II	cyldr.	FZK/II 20TZ/H21	II 20TZ	H21	200-650 °C	5,8 K/s	1000 s (u)	no	1809	OK
MANET II	cyldr.	FZK/II 31TZ/H22-26	II 31TZ	H22-26	100-500 °C	5,8 K/s	100 s (o)	yes	73659	no fracture
MANET II	cyldr.	FZK/II 136TZ/H27-28	II 136TZ	H27-28	100-500 °C	5,8 K/s	100 s (o)	yes	70328	no fracture

Material identifier	Shape identi-fier	Specimen/Test identi-fier	Specimen identifier	Test iden-tifier	Condition identifier	heating rate identifier	Hold time identifier	Interrupted identifier	N_{Break}-identifier	Remark identifier
MANET II	cyldr.	FZK/II 63TZ/I11-12	II 63TZ	I11-12	200-600 °C	5,8 K/s	100 s (u)	yes	15662	irregularities
MANET II	cyldr.	FZK/II 24TZ/I13	II 24TZ	I13	100-550 °C	5,8 K/s	-	no	7953	irregularities
MANET II	cyldr.	FZK/II 34TZ/I14-17	II 34TZ	I14-17	100-450 °C	5,8 K/s	100 s (o)	yes	70319	no fracture
MANET II	cyldr.	FZK/II 152TZ/I18-19	II 152TZ	I18-19	100-500 °C	3,0 K/s	100 s (o)	yes	70593	no fracture

no storage

Tab. 8-10: TMF data of MANET II

MANET II	cylindrical	5.8 K/s	without HT				
Nf Krit. [-]	d Sigma t [MPa]	d Eps t,m [%]	d Eps p,m [%]	Nf Krit. [-]	d Sigma t [MPa]	d Eps t,m [%]	d Eps p,m [%]
100-600 °C				**100-500 °C**			
6461	663	0.375	0.0188	56425	443.9	0.315	0.049
8195	658	0.406	0.015	**100-450 °C**			
100-550 °C				80822	476.4	0.26	0.015
30071	625.4	0.362	0.019				
69090	616	0.331	0.019				

Tab. 8-11: Specific TMF values of MANET II at 100°C lower temperature without hold times

MANET II	cylindrical	5.8 K/s	with 100 s HT						
Nf Krit. [-]	d Sigma t [MPa]	d Eps t,m [%]	d Eps p,m [%]	Mode	Nf Krit. [-]	d Sigma t [MPa]	d Eps t,m [%]	d Eps p,m [%]	Mode
100-600 °C					**100-500 °C**				
2935	706	0.475	0.0975	HTL	71190	595.5	0.332	0.051	HTL
2193	658	0.475	0.1088	HTH	73659	584.7	0.297	0.027	HTH
1292	701	0.6	0.204	HTHL	43957	652.3	0.395	0.025	HTHL
100-550 °C					**100-450 °C**				
17864	663	0.338	0.013	HTL	70454	511	0.264	0.019	HTL
12000	573.8	0.353	0.009	HTH	70319	487.2	0.302	0.064	HTH
17390	644	0.413	0.0313	HTH	87659	586.9	0.268	0.024	HTHL
9105	701	0.363	0.031	HTHL					
3856	682	0.438	0.044	HTHL					

HTH = Hold Time at High temperature
HTL = Hold Time at Low temperature
HTHL = Hold Time at both temperatures

Tab. 8-12: Specific TMF values of MANET II at 100°C lower temperature with 100s hold times

MANET II	cylindrical	5.8 K/s	without HT				
Nf Krit. [-]	d Sigma t [MPa]	d Eps t,m [%]	d Eps p,m [%]	Nf Krit. [-]	d Sigma t [MPa]	d Eps t,m [%]	d Eps p,m [%]
200-700 C				**200-600 C**			
400	578	0.556	0.25	17389	540	0.331	0.035
452	587	0.563	0.238	20655	531	0.319	0.0125
200-650 C				24854	540	0.3	0.0125
2387	573	0.375	0.044	**200-550 C**			
1480	583	0.394	0.09	83932	470.9	0.269	0.023

Tab. 8-13: Specific TMF values of MANET II at 200°C lower temperature without hold times

MANET II	cylindrical	5.8 K/s	with 100 s HT						
Nf Krit. [-]	d Sigma t [MPa]	d Eps t,m [%]	d Eps p,m [%]	Mode	Nf Krit. [-]	d Sigma t [MPa]	d Eps t,m [%]	d Eps p,m [%]	Mode
200-700 °C					**200-600 °C**				
412	587	0.619	0.294	HTL	15638	550	0.331	0.0338	HTL
275	540	0.75	0.463	HTH	6535	559	0.331	0.0125	HTH
208	550	0.938	0.613	HTHL	6251	493	0.35	0.035	HTHL
200-650 °C					**200-550 °C**				
2442	616	0.419	0.025	HTL	72143	519.7	0.275	0.007	HTL
1475	559	0.4	0.044	HTH	70441	511	0.263	0.011	HTH
565	587	0.575	0.225	HTHL	40754	568.4	0.241	0.019	HTHL

HTH = Hold Time at High temperature
HTL = Hold Time at Low temperature
HTHL = Hold Time at both temperatures

Tab. 8-14: Specific TMF values of MANET II at 200°C lower temperature with 100s hold times

MANET II	cylindrical	**3.0 K/s**	without HT
Nf Krit. [-]	d Sigma t [MPa]	d Eps t,m [%]	d Eps p,m [%]
100-600 °C			
2350	703.7	0.48	0.017
100-550 °C			
19497	632.3	0.345	0.019
100-500 °C			
74890	561.9	0.316	0.04

Tab. 8-15: Specific TMF values of MANET II at 100°C lower temperature and 3 K/s without hold times

MANET II	cylindrical	**3.0 K/s**	with 100 s HT						
Nf Krit. [-]	d Sigma t [MPa]	d Eps t,m [%]	d Eps p,m [%]	Mode	Nf Krit. [-]	d Sigma t [MPa]	d Eps t,m [%]	d Eps p,m [%]	Mode
100-600 °C					**100-500 °C**				
2230	695.1	0.426	0.044	HTL	70085	601	0.313	0.013	HTL
1447	674.5	0.469	0.074	HTH	69804	621.5	0.329	0.02	HTHL
1221	686.4	0.609	0.191	HTHL	**100-450 °C**				
100-550 °C					65889	520	0.29	0.04	HTL
16570	660.4	0.371	0.009	HTL	69770	522.1	0.253	0.019	HTH
6833	662.6	0.401	0.009	HTH	69973	558.3	0.266	0.027	HTHL
1676	714.6	0.451	0.073	HTHL					

HTH = Hold Time at High temperature
HTL = Hold Time at Low temperature
HTHL = Hold Time at both temperatures

Tab. 8-16: Specific TMF values of MANET II at 100°C lower temperature and 3 K/s with 100s hold times

8.3.4 OPTIFER IV

Material identifier	Shape identifier	Specimen/Test identifier	Specimen identifier	Test identifier	Condition identifier	heating rate identifier	Hold time identifier	Interrupted identifier	N_{Break}-identifier	Remark identifier
OPTIFER IV	cyldr.	FZK/OIV-24/A50	OIV-25	A50	200-650 °C	5,8 K/s	-	no	662	OK
OPTIFER IV	cyldr.	FZK/OIV-27/A51	OIV-27	A51	200-650 °C	5,8 K/s	-	no	679	OK
OPTIFER IV	cyldr.	FZK/OIV-18/A53	OIV-18	A53	200-600 °C	5,8 K/s	100 s (o+u)	no	567	OK
OPTIFER IV	cyldr.	FZK/OIV-22/A54	OIV-22	A54	200-550 °C	5,8 K/s	100 s (u)	no	22371	OK
OPTIFER IV	cyldr.	FZK/OIV-7/A36	OIV-7	A36	200-550 °C	5,8 K/s	-	no	27345	OK
OPTIFER IV	cyldr.	FZK/OIV-12/A39	OIV-12	A39	100-600 °C	5,8 K/s	-	no	1066	OK
OPTIFER IV	cyldr.	FZK/OIV-13/A40	OIV-13	A40	100-600 °C	5,8 K/s	-	no	853	OK
OPTIFER IV	cyldr.	FZK/OIV-14/A41-42	OIV-14	A41-42	100-550 °C	5,8 K/s	-	yes	3761	OK
OPTIFER IV	cyldr.	FZK/OIV-15/A43	OIV-15	A43	100-550 °C	5,8 K/s	-	no	3201	OK
OPTIFER IV	cyldr.	FZK/OIV-25/B43	OIV-25	B43	200-600 °C	5,8 K/s	-	no	3138	OK
OPTIFER IV	cyldr.	FZK/OIV-19/B44	OIV-19	B44	200-600 °C	5,8 K/s	100 s (o)	no	1180	OK
OPTIFER IV	cyldr.	FZK/OIV-23/B45	OIV-23	B45	200-550 °C	5,8 K/s	100 s (o)	no	10893	OK
OPTIFER IV	cyldr.	FZK/OIV-10/B37-38	OIV-10	B37-38	200-550 °C	5,8 K/s	-	yes	118667	no fracture
OPTIFER IV	cyldr.	FZK/OIV-4/C54-55	OIV-4	C54-55	200-600 °C	5,8 K/s	-	yes	29321	irregularities
OPTIFER IV	cyldr.	FZK/OIV-8/C58	OIV-8	C58	200-650 °C	5,8 K/s	-	no	1050	OK
OPTIFER IV	cyldr.	FZK/OIV-9/C59	OIV-9	C59	200-600 °C	5,8 K/s	-	no	2560	OK
OPTIFER IV	cyldr.	FZK/OIV-20/C66	OIV-20	C66	200-600 °C	5,8 K/s	100 s (u)	no	1791	OK
OPTIFER IV	cyldr.	FZK/OIV-28/D57	OIV-28	D57	200-600 °C	5,8 K/s	-	no	1745	OK
OPTIFER IV	cyldr.	FZK/OIV-3/D43-44	OIV-3	D43-44	200-600 °C	5,8 K/s	-	yes	31599	irregularities
OPTIFER IV	cyldr.	FZK/OIV-6/D47	OIV-6	D47	200-650 °C	5,8 K/s	-	no	1260	irregularities
OPTIFER IV	cyldr.	FZK/OIV-5/D48	OIV-5	D48	200-600 °C	5,8 K/s	-	no	2219	OK
OPTIFER IV	cyldr.	FZK/OIV-16/D51	OIV-16	D51	100-500 °C	5,8 K/s	-	no	36119	OK

Material identifier	Shape iden-tifier	Specimen/Test identi-fier	Specimen identifier	Test iden-tifier	Condition identifier	heating rate identifier	Hold time identifier	Interrupted identifier	N_{Break}-identifier	Remark identifier
OPTIFER IV	cyldr.	FZK/OIV-2/E49	OIV-2	E49	200-650 °C	5,8 K/s	-	no	4942	OK
OPTIFER IV	cyldr.	FZK/OIV-17/E50	OIV-17	E50	100-500 °C	5,8 K/s	-	no	42936	irregularities
OPTIFER IV	cyldr.	FZK/OIV-26/E55	OIV-26	E55	200-550 °C	5,8 K/s	-	no	7484	OK
OPTIFER IV	cyldr.	FZK/OIV-29/E56	OIV-29	E56	200-550 °C	5,8 K/s	-	no	19211	OK
OPTIFER IV	cyldr.	FZK/OIV-1/H29	OIV-1	H29	200-650 °C	5,8 K/s	-	no	10001	OK
OPTIFER IV	cyldr.	FZK/OIV-21/I29	OIV-21	I29	200-550 °C	5,8 K/s	100 s (o+u)	no	2753	OK
OPTIFER IV	950°C/30 min + 750°C/2h		no storage	data loss						
OPTIFER IV	1075°C/30 min + 750°C/2h									

Tab. 8-17: TMF data of OPTIFER IV

OPTIFER IV	cylindrical	5.8 K/s	without HT
Nf Krit. [-]	d Sigma t [MPa]	d Eps t,m [%]	d Eps p,m [%]
100-600 °C			
1020	566.9	0.517	0.223
812	566.9	0.502	0.221
100-550 °C			
3664	563	0.418	0.029
2980	559.1	0.377	0.041

Tab. 8-18: Specific TMF values of OPTIFER IV cold rolled at 100°C lower temperature without hold times

OPTIFER IV	cylindrical	5.8 K/s	without HT
Nf Krit. [-]	d Sigma t [MPa]	d Eps t,m [%]	d Eps p,m [%]
200-650 °C			
9909	649.8	0.43	0.025
4696	624.8	0.302	0.022
200-600 °C			
31452	575.5	0.172	0.025
29142	613.5	0.287	0.021

Tab. 8-19: Specific TMF values of OPTIFER IV cold rolled at 200°C lower temperature without hold times

OPTIFER IV	cylindrical	5.8 K/s	without HT				
Nf Krit. [-]	d Sigma t [MPa]	d Eps t,m [%]	d Eps p,m [%]	Nf Krit. [-]	d Sigma t [MPa]	d Eps t,m [%]	d Eps p,m [%]
200-650 °C				**200-550 °C**			
980	496.9	0.455	0.164	26486	473.7	0.262	0.031
807	504.7	0.473	0.253				
200-600 °C							
2008	511	0.353	0.061				
2387	504.7	0.381	0.052				

Tab. 8-20: Specific TMF values of OPTIFER IV tempered at 200°C lower temperature without hold times

OPTIFER IV	cylindrical	5.8 K/s	without HT				
Nf Krit. [-]	d Sigma t [MPa]	d Eps t,m [%]	d Eps p,m [%]	Nf Krit. [-]	d Sigma t [MPa]	d Eps t,m [%]	d Eps p,m [%]
200-650 °C				**200-550 °C**			
630	505	0.338		7052	474	0.263	
645	497	0.507		18776	467	0.321	
200-600 °C							
3041	497	0.329					
1707	514	0.346					

Tab. 8-21: Specific TMF values of OPTIFER IV annealed at 200°C lower temperature without hold times

8.3.5 F82H mod.

Material identifier	Shape identifier	Specimen/Test identifier	Specimen identifier	Test identifier	Condition identifier	heating rate identifier	Hold time identifier	Interrupted identifier	N_{Break}-identifier	Remark identifier
F82Hmod.	cyldr.	FZK/J-43/A52	J-43	A52	200-550 °C	5,8 K/s	1000 s (o)	no	4109	OK
F82Hmod.	cyldr.	FZK/J-68/A55	J-68	A55	100-500 °C	5,8 K/s	1000 s (o+u)	no	197	OK
F82Hmod.	cyldr.	FZK/J-70/A56	J-70	A56	100-550 °C	5,8 K/s	1000 s (u)	no	6079	OK
F82Hmod.	cyldr.	FZK/J-18/A37	J-18	A37	100-600 °C	5,8 K/s	-	no	1115	OK
F82Hmod.	cyldr.	FZK/J-21/A38	J-21	A38	100-550 °C	5,8 K/s	-	no	5209	OK
F82Hmod.	cyldr.	FZK/J-69/B46	J-69	B46	100-500 °C	5,8 K/s	1000 s (o)	no	10012	OK
F82Hmod.	cyldr.	FZK/J-24/B39	J-24	B39	200-600 °C	5,8 K/s	100 s (o)	no	1516	OK
F82Hmod.	cyldr.	FZK/J-29/B40	J-29	B40	200-550 °C	5,8 K/s	100 s (o+u)	no	3490	OK
F82Hmod.	cyldr.	FZK/J-30/B41-42	J-30	B41-42	100-450 °C	5,8 K/s	100 s (o)	yes	69459	irregularities
F82Hmod.	cyldr.	FZK/J-53/C67	J-53	C67	100-500 °C	5,8 K/s	100 s (o+u)	no	5900	OK
F82Hmod.	cyldr.	FZK/J-57/C68	J-57	C68	100-450 °C	5,8 K/s	100 s (o+u)	no	70012	no fracture
F82Hmod.	cyldr.	FZK/J-9/C56	J-9	C56	200-600 °C	5,0 K/s	-	no	1555	OK
F82Hmod.	cyldr.	FZK/J-16/C57	J-16	C57	200-550 °C	5,0 K/s	-	no	70074	no fracture
F82Hmod.	cyldr.	FZK/J-22/C60-61	J-22	C60-61	100-500 °C	5,8 K/s	-	yes	71569	no fracture
F82Hmod.	cyldr.	FZK/J-25/C62	J-25	C62	200-600 °C	5,8 K/s	100 s (u)	no	1733	OK
F82Hmod.	cyldr.	FZK/J-62/C63	J-62	C63	200-600 °C	5,0 K/s	-	no	1760	OK
F82Hmod.	cyldr.	FZK/J-64/C64	J-64	C64	200-600 °C	5,0 K/s	-	no	1576	OK
F82Hmod.	cyldr.	FZK/J-4/C50	J-43	C50	200-650 °C	5,8 K/s	-	no	500	OK
F82Hmod.	cyldr.	FZK/J-5/C51	J-5	C51	200-600 °C	5,8 K/s	-	no	1771	OK
F82Hmod.	cyldr.	FZK/J-6/C52-53	J-6	C52-53	200-550 °C	5,8 K/s	-	yes	75216	no fracture
F82Hmod.	cyldr.	FZK/J-44/D58	J-44	D58	200-550 °C	5,8 K/s	1000 s (u)	no	18947	OK
F82Hmod.	cyldr.	FZK/J-58/D64	J-58	D64	200-600 °C	5,8 K/s	-	no	2000	no fracture

Material identifier	Shape iden-tifier	Specimen/Test identi-fier	Specimen identifier	Test iden-tifier	Condition identifier	heating rate identifier	Hold time identifier	Interrupted identifier	N_{Break}-identifier	Remark identifier
F82Hmod.	cyldr.	FZK/J-10/D45	J-10	D45	200-600 °C	5,0 K/s	-	no	1391	OK
F82Hmod.	cyldr.	FZK/J-17/D46	J-17	D46	200-550 °C	5,0 K/s	-	no	70675	no fracture
F82Hmod.	cyldr.	FZK/J-19/D49	J-17	D49	100-600 °C	5,8 K/s	-	no	945	OK
F82Hmod.	cyldr.	FZK/J-20/D50	J-20	D50	100-550 °C	5,8 K/s	-	no	3383	OK
F82Hmod.	cyldr.	FZK/J-26/D52	J-26	D52	200-600 °C	5,8 K/s	100 s (o+u)	no	759	OK
F82Hmod.	cyldr.	FZK/J-61/D53	J-61	D53	200-600 °C	5,0 K/s	-	no	1633	OK
F82Hmod.	cyldr.	FZK/J-63/D54	J-63	D54	200-600 °C	5,0 K/s	-	no	1829	OK
F82Hmod.	cyldr.	FZK/J-34/D55-56	J-34	D55-56	100-450 °C	5,8 K/s	100 s (o+u)	yes	65256	no fracture
F82Hmod.	cyldr.	FZK/J-27/E51-52	J-27	E51-52	200-550 °C	5,8 K/s	100 s (o)	yes	7168	irregularities
F82Hmod.	cyldr.	FZK/J-37/E53	J-37	E53	200-600 °C	5,8 K/s	100 s (o+u)	no	787	OK
F82Hmod.	cyldr.	FZK/J-40/E54	J-40	E54	200-550 °C	5,8 K/s	100 s (o+u)	no	2198	OK
F82Hmod.	cyldr.	FZK/J-49/E57	J-49	E57	200-550 °C	5,8 K/s	1000 s (u)	no	7940	OK
F82Hmod.	cyldr.	FZK/J-56/E58	J-56	E58	100-500 °C	5,8 K/s	100 s (u)	no	15931	OK
F82Hmod.	cyldr.	FZK/J-67/E59	J-67	E59	100-450 °C	5,8 K/s	100 s (u)	no	71015	no fracture
F82Hmod.	cyldr.	FZK/J-2/G31	J-2	G31	200-600 °C	5,8 K/s	-	no	2169	OK
F82Hmod.	cyldr.	FZK/J-3/G32	J-3	G32	200-650 °C	5,8 K/s	-	no	499	OK
F82Hmod.	cyldr.	FZK/J-8/G33	J-8	G33	200-550 °C	5,8 K/s	-	no	48805	OK
F82Hmod.	cyldr.	FZK/J-82/H56	J-82	H56	100-550 °C	5,8 K/s	-	no	1849	irregularities
F82Hmod.	cyldr.	FZK/J-83/H57	J-83	H57	100-550 °C	5,8 K/s	-	no	1725	irregularities
F82Hmod.	cyldr.	FZK/J-51/H42	J-51	H42	200-600 °C	5,8 K/s	1000 s (o)	no	842	OK
F82Hmod.	cyldr.	FZK/J-55/H43	J-55	H43	200-600 °C	5,8 K/s	1000 s (u)	no	1573	OK
F82Hmod.	cyldr.	FZK/J-66/H44	J-66	H44	100-450 °C	5,8 K/s	100 s (o)	no	70579	no fracture
F82Hmod.	cyldr.	FZK/J-35/H36	J-35	H36	200-600 °C	5,8 K/s	100 s (o)	no	976	OK
F82Hmod.	cyldr.	FZK/J-38/H37	J-38	H37	200-550 °C	5,8 K/s	100 s (o)	no	8978	OK
F82Hmod.	cyldr.	FZK/J-42/H38	J-42	H38	200-600 °C	5,8 K/s	1000 s (u)	no	1329	OK
F82Hmod.	cyldr.	FZK/J-46/H39	J-46	H39	200-550 °C	5,8 K/s	1000 s (o+u)	no	235	OK

Material identifier	Shape identifier	Specimen/Test identifier	Specimen identifier	Test identifier	Condition identifier	heating rate identifier	Hold time identifier	Interrupted identifier	N_{Break}-identifier	Remark identifier
F82Hmod.	cyldr.	FZK/J-47/H40	J-47	H40	200-550 °C	5,8 K/s	1000 s (o+u)	no	344	OK
F82Hmod.	cyldr.	FZK/J-50/H41	J-50	H41	200-600 °C	5,8 K/s	1000 s (o+u)	no	129	OK
F82Hmod.	cyldr.	FZK/J-36/I24	J-36	I24	200-600 °C	5,8 K/s	100 s (u)	no	1980	OK
F82Hmod.	cyldr.	FZK/J-39/I25	J-39	I25	200-550 °C	5,8 K/s	100 s (u)	no	25290	OK
F82Hmod.	cyldr.	FZK/J-41/I26	J-41	I26	200-600 °C	5,8 K/s	1000 s (o)	no	739	OK
F82Hmod.	cyldr.	FZK/J-45/I27	J-45	I27	200-600 °C	5,8 K/s	1000 s (o+u)	no	119	OK
F82Hmod.	cyldr.	FZK/J-48/I28	J-48	I28	200-550 °C	5,8 K/s	1000 s (o)	no	2226	OK
F82Hmod.	cyldr.	FZK/J-54/I30	J-54	I30	100-500 °C	5,8 K/s	100 s (o)	no	12997	irregularities
F82Hmod.	cyldr.	FZK/J-65/I31	J-65	I31	100-500 °C	5,8 K/s	100 s (o)	no	18087	OK
F82Hmod.	cyldr.	FZK/J-23/I20-21	J-23	I20-21	100-500 °C	5,8 K/s	-	yes	70448	no fracture
F82Hmod.	cyldr.	FZK/J-28/I22-23	J-28	I22-23	200-550 °C	5,8 K/s	100 s (o)	yes	28092	irregularities

Data loss

no storage

Tab. 8-22: TMF data of F82H mod.

F82H mod.	cylindrical	5.8 K/s	without HT
Nf Krit. [-]	d Sigma t [MPa]	d Eps t,m [%]	d Eps p,m [%]
100-600 °C			
967	578.5	0.493	0.185
891	570.7	0.475	0.207
100-550 °C			
5005	570.7	0.381	0.018
3261	563	0.369	0.065

Tab. 8-23: Specific TMF values of F82H mod. as received at 100°C lower temperature without hold times

F82H mod.	cylindrical	5.8 K/s	with 100 s HT	
Nf Krit. [-]	d Sigma t [MPa]	d Eps t,m [%]	d Eps p,m [%]	Mode
100-500 °C				
17658	551	0.313	0.006	HTH
15064	580	0.349	0.021	HTL
5651	600	0.444	0.09	HTHL
100-450 °C				
69459	494	0.263	0.035	HTH
69409	522	0.288	0.013	HTL
64482	584	0.349	0.015	HTHL

HTH = Hold Time at High temperature
HTL = Hold Time at Low temperature
HTHL = Hold Time at both temperatures

Tab. 8-24: Specific TMF values of F82H mod. as received at 100°C lower temperature with 100s hold times

F82H mod.	cylindrical	5.8 K/s	with 1000 s HT	
Nf Krit. [-]	d Sigma t [MPa]	d Eps t,m [%]	d Eps p,m [%]	Mode
100-500 °C				
9686	573	0.331	0.033	HTH
5776	576	0.329	0.012	HTL
173	681	1.059	0.599	HTHL

HTH = Hold Time at High temperature
HTL = Hold Time at Low temperature
HTHL = Hold Time at both temperatures

Tab. 8-25: Specific TMF values of F82H mod. as received at 100°C lower temperature with 1000s hold times

F82H mod.	cylindrical	5.8 K/s	without HT				
Nf Krit. [-]	d Sigma t [MPa]	d Eps t,m [%]	d Eps p,m [%]	Nf Krit. [-]	d Sigma t [MPa]	d Eps t,m [%]	d Eps p,m [%]
200-650 °C				**200-550 °C**			
500	506.84	0.525	0.231	75216	466	0.252	0.014
470	492.63	0.425	0.3125	48271	463.5	0.298	0.025
200-600 °C							
2100	492.62	0.337	0.0625				
1541	508.6	0.384	0.108				
1363	508.6	0.338	0.111				
1750	502.1	0.363	0.11				

Tab. 8-26: Specific TMF values of F82H mod. as received at 200°C lower temperature without hold times

F82H mod. cylindrical 5.8 K/s with 100 s HT

Nf Krit. [-]	d Sigma t [MPa]	d Eps t,m [%]	d Eps p,m [%]	Mode	Nf Krit. [-]	d Sigma t [MPa]	d Eps t,m [%]	d Eps p,m [%]	Mode
200-600 °C					**200-550 °C**				
1381	491	0.363	0.112	HTH	6855	491	0.25	0.031	HTH
1148	522	0.385	0.09	HTL	27175	498	0.288	0.009	HTL
720	510	0.584	0.309	HTHL	3195	535	0.34	0.049	HTHL
905	504	0.416	0.136	HTH	8721	484	0.319	0.01	HTH
1840	519	0.349	0.062	HTL	24385	485	0.312	0.008	HTL
758	522	0.473	0.204	HTHL	2095	522	0.321	0.093	HTHL

HTH = Hold Time at High temperature
HTL = Hold Time at Low temperature
HTHL = Hold Time at both temperatures

Tab. 8-27: Specific TMF values of F82H mod. as received at 200°C lower temperature with 100s hold times

F82H mod. cylindrical 5.8 K/s with 1000 s HT

Nf Krit. [-]	d Sigma t [MPa]	d Eps t,m [%]	d Eps p,m [%]	Mode	Nf Krit. [-]	d Sigma t [MPa]	d Eps t,m [%]	d Eps p,m [%]	Mode
200-600 °C					**200-550 °C**				
651	487	0.488	0.185	HTH	3804	491	0.311	0.012	HTH
1235	518	0.349	0.086	HTL	7286	506	0.278	0.021	HTL
111	549	1.181	0.821	HTHL	213	565	0.805	0.442	HTHL
765	502	0.429	0.113	HTH	2093	506	0.329	0.012	HTH
1469	491	0.375	0.087	HTL	18198	506	0.339	0.049	HTL
123	557	1.171	0.771	HTHL	328	619	0.758	0.372	HTHL

HTH = Hold Time at High temperature
HTL = Hold Time at Low temperature
HTHL = Hold Time at both temperatures

Tab. 8-28: Specific TMF values of F82H mod. as received at 200°C lower temperature with 1000s hold times

8.3.6 EUROFER 97

8.3.6.1 EUROFER 1

Material identifier	Shape identifier	Specimen/Test identifier	Specimen identifier	Test identifier	Condition identifier	heating rate identifier	Hold time identifier	Interrupted identifier	N_{Break}-identifier	Remark identifier
EUROFER 1	cyldr.	FZK/E-1/A57	E-1	A57	100-600 °C	5,8 K/s	-	no	712	OK
EUROFER 1	cyldr.	FZK/E-3/A58	E-3	A58	100-500 °C	5,8 K/s	-	no	9800	irregularities
EUROFER 1	cyldr.	FZK/E-7/A59	E-7	A59	100-550 °C	5,8 K/s	1000 s (o+u)	no	504	OK
EUROFER 1	cyldr.	FZK/E-10/A60	E-10	A60	100-500 °C	5,8 K/s	1000 s (o+u)	no	1723	OK
EUROFER 1	cyldr.	FZK/E-11/A61	E-11	A61	100-500 °C	5,8 K/s	1000 s (u)	no	5418	OK
EUROFER 1	cyldr.	FZK/E-23/A62-64	E-23	A62-64	100-450 °C	5,8 K/s	1000 s (o)	yes	38435	OK
EUROFER 1	cyldr.	FZK/E-58/A65	E-58	A65	100-600 °C	5,8 K/s	1000 s (o+u)	no	238	OK
EUROFER 1	cyldr.	FZK/E-60/B57	E-60	B57	100-450 °C	5,8 K/s	-	no	70143	no fracture
EUROFER 1	cyldr.	FZK/E-12/B47	E-12	B47	100-500 °C	5,8 K/s	100 s (o)	no	9009	OK
EUROFER 1	cyldr.	FZK/E-20/B48	E-20	B48	100-450 °C	5,8 K/s	100 s (u)	yes	68924	no fracture
EUROFER 1	cyldr.	FZK/E-39/B49	E-39	B49	100-450 °C	5,8 K/s	100 s (u)	yes	69506	no fracture
EUROFER 1	cyldr.	FZK/E-45/B50	E-45	B50	100-550 °C	5,8 K/s	-	no	1830	irregularities
EUROFER 1	cyldr.	FZK/E-47/B51	E-47	B51	100-550 °C	5,8 K/s	-	no	819	irregularities
EUROFER 1	cyldr.	FZK/E-48/B52	E-48	B52	100-550 °C	5,8 K/s	-	no	2140	irregularities
EUROFER 1	cyldr.	FZK/E-49/B53	E-49	B53	100-600 °C	5,8 K/s	100 s (o)	no	421	OK
EUROFER 1	cyldr.	FZK/E-52/B54	E-52	B54	100-600 °C	5,8 K/s	100 s (o)	no	383	OK
EUROFER 1	cyldr.	FZK/E-57/B55	E-57	B55	100-600 °C	5,8 K/s	100 s (u)	no	541	OK
EUROFER 1	cyldr.	FZK/E-19/C69	E-19	C69	100-450 °C	5,8 K/s	100 s (o)	no	68306	no fracture
EUROFER 1	cyldr.	FZK/E-43/C70-71	E-43	C70-71	100-450 °C	5,8 K/s	1000 s (u)	yes	24475	irregularities
EUROFER 1	cyldr.	FZK/E-89/D71-72	E-89	D71-72	100-450 °C	5,8 K/s	1000 s (u)	yes	20294	irregularities
EUROFER 1	cyldr.	FZK/E-2/D59	E-2	D59	100-550 °C	5,8 K/s	-	no	1909	OK

Material identifier	Shape identifier	Specimen/Test identifier	Specimen identifier	Test identifier	Condition identifier	heating rate identifier	Hold time identifier	Interrupted identifier	N_{Break}-identifier	Remark identifier
EUROFER 1	cyldr.	FZK/E-4/D60	E-4	D60	100-600 °C	5,8 K/s	-	no	558	OK
EUROFER 1	cyldr.	FZK/E-5/D61	E-5	D61	100-550 °C	5,8 K/s	-	no	1455	OK
EUROFER 1	cyldr.	FZK/E-6/D62	E-6	D62	100-500 °C	5,8 K/s	-	no	11386	OK
EUROFER 1	cyldr.	FZK/E-9/D63	E-9	D63	100-550 °C	5,8 K/s	100 s (u)	no	1168	OK
EUROFER 1	cyldr.	FZK/E-15/D65	E-15	D65	100-550 °C	5,8 K/s	1000 s (u)	no	919	OK
EUROFER 1	cyldr.	FZK/E-17/D66	E-17	D66	100-500 °C	5,8 K/s	1000 s (o)	no	2876	OK
EUROFER 1	cyldr.	FZK/E-24/D67-70	E-24	D67-70	100-450 °C	5,8 K/s	1000 s (u)	yes	42940	irregularities
EUROFER 1	cyldr.	FZK/E-21/E62	E-21	E62	100-450 °C	5,8 K/s	100 s (o+u)	no	38059	OK
EUROFER 1	cyldr.	FZK/E-37/E63-65	E-37	E63-65	100-450 °C	5,8 K/s	100 s (o+u)	yes	31489	OK
EUROFER 1	cyldr.	FZK/E-42/E66	E-42	E66	100-450 °C	5,8 K/s	1000 s (o)	no	11057	OK
EUROFER 1	cyldr.	FZK/E-51/E67	E-51	E67	100-600 °C	5,8 K/s	100 s (o+u)	no	212	OK
EUROFER 1	cyldr.	FZK/E-54/E68	E-54	E68	100-600 °C	5,8 K/s	100 s (o+u)	no	325	OK
EUROFER 1	cyldr.	FZK/E-56/E69	E-56	E69	100-600 °C	5,8 K/s	100 s (o)	no	406	OK
EUROFER 1	cyldr.	FZK/E-14/E61	E-14	E61	100-550 °C	5,8 K/s	1000 s (o)	no	730	OK
EUROFER 1	cyldr.	FZK/E-38/H55	E-38	H55	100-450 °C	5,8 K/s	100 s (o)	no	70148	OK
EUROFER 1	cyldr.	FZK/E-22/H45	E-22	H45	100-450 °C	5,8 K/s	1000 s (o+u)	no	1589	OK
EUROFER 1	cyldr.	FZK/E-25/H46	E-25	H46	100-550 °C	5,8 K/s	100 s (o+u)	no	439	OK
EUROFER 1	cyldr.	FZK/E-26/H47	E-26	H47	100-550 °C	5,8 K/s	100 s (o)	no	701	OK
EUROFER 1	cyldr.	FZK/E-27/H48	E-27	H48	100-550 °C	5,8 K/s	100 s (u)	no	938	OK
EUROFER 1	cyldr.	FZK/E-28/H49	E-28	H49	100-500 °C	5,8 K/s	100 s (o+u)	no	1600	OK
EUROFER 1	cyldr.	FZK/E-30/H50	E-30	H50	100-500 °C	5,8 K/s	100 s (u)	no	6701	OK
EUROFER 1	cyldr.	FZK/E-31/H51	E-31	H51	100-550 °C	5,8 K/s	1000 s (o+u)	no	69	OK
EUROFER 1	cyldr.	FZK/E-33/H52	E-33	H52	100-550 °C	5,8 K/s	1000 s (u)	no	939	OK
EUROFER 1	cyldr.	FZK/E-35/H53-54	E-35	H53-54	100-500 °C	5,8 K/s	1000 s (o)	yes	3381	irregularities
EUROFER 1	cyldr.	FZK/E-32/I37	E-32	I37	100-550 °C	5,8 K/s	1000 s (o)	no	464	OK
EUROFER 1	cyldr.	FZK/E-34/I38	E-34	I38	100-500 °C	5,8 K/s	1000 s (o+u)	no	211	OK

Material identifier	Shape identifier	Specimen/Test identifier	Specimen identifier	Test identifier	Condition identifier	heating rate identifier	Hold time identifier	Interrupted identifier	N_{Break}-identifier	Remark identifier
EUROFER 1	cyldr.	FZK/E-36/I39-41	E-36	I39-41	100-500 °C	5,8 K/s	1000 s (u)	yes	6444	irregularities
EUROFER 1	cyldr.	FZK/E-41/I42	E-41	I42	100-450 °C	5,8 K/s	1000 s (o+u)	no	1918	OK
EUROFER 1	cyldr.	FZK/E-61/I44	E-61	I44	100-500 °C	5,8 K/s	-	no	5101	irregularities
EUROFER 1	cyldr.	FZK/E-50/I45	E-50	I45	100-600 °C	5,8 K/s	100 s (u)	no	477	OK
EUROFER 1	cyldr.	FZK/E-53/I46	E-53	I46	100-600 °C	5,8 K/s	100 s (u)	no	420	OK
EUROFER 1	cyldr.	FZK/E-59/I49	E-59	I49	100-450 °C	5,8 K/s	-	no	71000	no fracture
EUROFER 1	cyldr.	FZK/E-8/I32	E-8	I32	100-550 °C	5,8 K/s	100 s (o)	no	710	OK
EUROFER 1	cyldr.	FZK/E-13/I33	E-13	I33	100-550 °C	5,8 K/s	1000 s (o+u)	no	69	OK
EUROFER 1	cyldr.	FZK/E-16/I34	E-16	I34	100-500 °C	5,8 K/s	1000 s (o+u)	no	251	OK
EUROFER 1	cyldr.	FZK/E-18/I35	E-18	I35	100-500 °C	5,8 K/s	1000 s (u)	no	5666	OK
EUROFER 1	cyldr.	FZK/E-29/I36	E-29	I36	100-500 °C	5,8 K/s	100 s (o)	no	10637	OK

Data loss

no storage

Tab. 8-29: TMF data of EUROFER 97, as received (EUROFER 1)

EUROFER 97	cylindrical	5.8 K/s	without HT				
Nf Krit. [-]	d Sigma t [MPa]	d Eps t,m [%]	d Eps p,m [%]	Nf Krit. [-]	d Sigma t [MPa]	d Eps t,m [%]	d Eps p,m [%]
100-600 °C				**100-500 °C**			
662	561	0.54	0.21	10947	537	0.34	0.013
510	572	0.56	0.23	9469	529	0.37	0.023
100-550 °C				**100-450 °C**			
1800	568	0.41	0.14	70143	461.3	0.25	0.043
1375	565	0.41	0.095	70000	450.4	0.288	0.064

Tab. 8-30: Specific TMF values of EUROFER 97 as received at 100°C lower temperature without hold times

EUROFER 97	980°C	cylindrical	5.8 K/s	with 100 s HT					
Nf Krit. [-]	d Sigma t [MPa]	d Eps t,m [%]	d Eps p,m [%]	Mode	Nf Krit. [-]	d Sigma t [MPa]	d Eps t,m [%]	d Eps p,m [%]	Mode
100-600 °C					**100-500 °C**				
398	537.3	0.658	0.364	HTH	8671	525.9	0.324	0.037	HTH
391	538.5	0.657	0.372	HTH	10297	529.7	0.352	0.0046	HTH
373	565.3	0.573	0.266	HTH	6512	572.2	0.344	0.027	HTL
445	584	0.678	0.315	HTL	5068	580	0.379	0.012	HTL
497	577.7	0.584	0.325	HTL	1270	603.2	0.389	0.049	HTHL
405	583.2	0.659	0.316	HTL	1474	603.2	0.381	0.036	HTHL
199	584	0.812	0.467	HTHL	**100-450 °C**				
224	565.3	0.845	0.597	HTHL	68306	502.7	0.263	0.029	HTH
290	570.4	0.807	0.452	HTHL	70148	491	0.325	0.041	HTH
100-550 °C					67652	510.4	0.26	0.037	HTL
650	564	0.421	0.113	HTH	69505	498	0.442	0.031	HTL
671	603.2	0.398	0.073	HTH	37574	549	0.315	0.039	HTHL
999	588	0.516	0.165	HTL	30569	549	0.344	0.016	HTHL
885	572	0.5	0.171	HTL					
452	599.6	0.596	0.253	HTHL					
396	587.7	0.602	0.252	HTHL					

HTH = Hold Time at High temperature
HTL = Hold Time at Low temperature
HTHL = Hold Time at both temperatures

Tab. 8-31: Specific TMF values of EUROFER 97 as received at 100°C lower temperature with 100s hold times

EUROFER 97	980°C	cylindrical	5.8 K/s	with 1000 s HT					
Nf Krit. [-]	d Sigma t [MPa]	d Eps t,m [%]	d Eps p,m [%]	Mode	Nf Krit. [-]	d Sigma t [MPa]	d Eps t,m [%]	d Eps p,m [%]	Mode
100-600 °C					**100-500 °C**				
677	568.4	0.471	0.129	HTH	38300	503.2	0.289	0.018	HTH
379	548.9	0.471	0.136	HTH	10730	521.7	0.288	0.023	HTH
885	607.3	0.563	0.195	HTL	42869	521.8	0.304	0.013	HTL
903	591.8	0.482	0.117	HTL	24438	475.2	0.25	0.037	HTL
52	642.4	1.619	1.076	HTHL	1608	693	0.639	0.184	HTHL
53	642.4	1.465	0.975	HTHL	1286	696.9	0.639	0.143	HTHL
100-500 °C									
3320	556.7	0.37	0.015	HTH					
2811	545.1	0.416	0.066	HTH					
5460	552.8	0.361	0.039	HTL					
6390	584	0.427	0.067	HTL					
200	700.8	0.928	0.471	HTHL					
187	704.7	0.904	0.42	HTHL					

HTH = Hold Time at High temperature
HTL = Hold Time at Low temperature
HTHL = Hold Time at both temperatures

Tab. 8-32: Specific TMF values of EUROFER 97 as received at 100°C lower temperature with 1000s hold times

8.3.6.2 EUROFER 2

Material identifier	Shape identifier	Specimen/Test identifier	Specimen identifier	Test identifier	Condition identifier	heating rate identifier	Hold time identifier	Interrupted identifier	N_{Break}-identifier	Remark identifier
EUROFER 2	cyldr.	FZK/E-82/A70	E-82	A70	100-500 °C	5,8 K/s	1000 s (o+u)	no	155	OK
EUROFER 2	cyldr.	FZK/E-83/A71	E-83	A71	100-500 °C	5,8 K/s	1000 s (o)	no	1606	OK
EUROFER 2	cyldr.	FZK/E-88/A72	E-88	A72	100-500 °C	5,8 K/s	1000 s (o)	no	1456	OK
EUROFER 2	cyldr.	FZK/E-62/A73-74	E-62	A73-74	100-450 °C	5,8 K/s	1000 s (o)	yes	20537	irregularities
EUROFER 2	cyldr.	FZK/E-71/A66	E-71	A66	100-550 °C	5,8 K/s	-	no	2192	OK
EUROFER 2	cyldr.	FZK/E-76/A67	E-76	A67	100-550 °C	5,8 K/s	-	no	3134	OK
EUROFER 2	cyldr.	FZK/E-74/A68	E-74	A68	100-450 °C	5,8 K/s	-	no	70175	no fracture
EUROFER 2	cyldr.	FZK/E-81/A69	E-81	A69	100-550 °C	5,8 K/s	1000 s (o+u)	no	85	OK
EUROFER 2	cyldr.	FZK/E-72/B56	E-72	B56	100-500 °C	5,8 K/s	-	no	43927	OK
EUROFER 2	cyldr.	FZK/E-85/B58	E-85	B58	100-450 °C	5,8 K/s	1000 s (o+u)	no	885	OK
EUROFER 2	cyldr.	FZK/E-61/B60	E-61	B60	100-450 °C	5,8 K/s	1000 s (o+u)	no	536	OK
EUROFER 2	cyldr.	FZK/E-64/B61	E-64	B61	100-500 °C	5,8 K/s	1000 s (o+u)	no	201	OK
EUROFER 2	cyldr.	FZK/E-65/B62	E-65	B62	100-550 °C	5,8 K/s	1000 s (o+u)	no	86	OK
EUROFER 2	cyldr.	FZK/E-66/B63	E-66	B63	100-550 °C	5,8 K/s	1000 s (o)	no	494	OK
EUROFER 2	cyldr.	FZK/E-67/B64	E-67	B64	100-550 °C	5,8 K/s	1000 s (u)	no	983	OK
EUROFER 2	cyldr.	FZK/E-73/E70	E-73	E70	100-450 °C	5,8 K/s	-	no	70691	no fracture
EUROFER 2	cyldr.	FZK/E-80/E71	E-80	E71	100-550 °C	5,8 K/s	1000 s (o)	no	667	OK
EUROFER 2	cyldr.	FZK/E-84/E72	E-84	E72	100-500 °C	5,8 K/s	1000 s (u)	no	3690	OK
EUROFER 2	cyldr.	FZK/E-63/E73	E-63	E73	100-500 °C	5,8 K/s	1000 s (u)	no	3693	OK
EUROFER 2	cyldr.	FZK/E-68/E74-75	E-68	E74-75	100-450 °C	5,8 K/s	1000 s (u)	yes	15752	irregularities
EUROFER 2	cyldr.	FZK/E-78/H58	E-78	H58	100-500 °C	5,8 K/s	-	no	30974	OK
EUROFER 2	cyldr.	FZK/E-79/H59	E-79	H59	100-550 °C	5,8 K/s	1000 s (u)	no	696	OK

Material identifier	Shape identifier	Specimen/Test identifier	Specimen identifier	Test identifier	Condition identifier	heating rate identifier	Hold time identifier	Interrupted identifier	N_{Break}-identifier	Remark identifier
EUROFER 2	cyldr.	FZK/E-87/H60-61	E-87	H60-61	100-450 °C	5,8 K/s	1000 s (u)	yes	23293	irregularities
EUROFER 2	cyldr.	FZK/E-86/I50-52	E-86	I50-52	100-450 °C	5,8 K/s	1000 s (o)	yes	23150	irregularities
EUROFER 2	cyldr.	FZK/E-75/I47	E-75	I47	100-600 °C	5,8 K/s	-	no	861	OK
EUROFER 2	cyldr.	FZK/E-77/I48	E-77	I48	100-600 °C	5,8 K/s	-	no	814	OK

Data loss

no storage

Tab. 8-33: TMF data of EUROFER 97, annealed (EUROFER 2)

EUROFER 97 1040°C cylindrical 5.8 K/s with 1000 s HT

Nf Krit. [-]	d Sigma t [MPa]	d Eps t,m [%]	d Eps p,m [%]	Mode	Nf Krit. [-]	d Sigma t [MPa]	d Eps t,m [%]	d Eps p,m [%]	Mode
100-550 °C					**100-500 °C**				
464	559.1	0.504	0.148	HTH	1375	547.4	0.378	0.029	HTH
625	532.7	0.561	0.221	HTH	1483	542.8	0.371	0.049	HTH
653	569.2	0.515	0.239	HTL	3555	550.5	0.423	0.039	HTL
967	566.1	0.61	0.252	HTL	3380	557.5	0.387	0.046	HTL
78	556.8	1.642	1.432	HTHL	191	646.1	1.166	0.714	HTHL
81	596.4	1.687	1.193	HTHL	138	646.1	1.24	0.768	HTHL

HTH = Hold Time at High temperature
HTL = Hold Time at Low temperature
HTHL = Hold Time at both temperatures

Tab. 8-34: Specific TMF values of EUROFER 97 annealed at 100°C lower temperature with 1000s hold times

9 TMF data on the enclosed CD

9.1 FZK-IMF II-TMF-tests; Description of the delivered data sets

1. File: "**Result Files**"

   - Type of file "**TMx000nn.dat**": (with “x” as the test facility number, i.e. the letter A to I, and “nn” the current number in the column “Test identifier” of Tabs. 7-3; 7-6; 7-10; 7-17; 7-22; 7-29 and 7-33.)

   This type of files e.g. of test A65 contains data sheets and diagrams:

   a. **TMA00065Gefiltertorigin**: The initial TMF-data of FZK in ASCII-format.
   b. **TMA00065Gefiltertbearbeitet**: Transfer of the TMF-data of FZK in ASCII-format into columns.
   c. **Minimalwerte**: The minimum values of the cycles are shown.
   d. **Maximalwerte**: The maximum values of the cycles are shown.
   e. **StressStrainDiffs**: Calculation of strain-, stress- and temperature-values are performed (according to the recommendations of the TMF-STANDARD Project and the Mat-DB). Data of these tables will be used to generate diagrams showing the cyclic dependency of the above quantities.
   f. **Geradenpunkte**: Data values generated by the linear slope regression calculation for 5%, 10%, 20%, 50% reduction in stress. Each intersection of this line with the stress vs. cycles curve gives an N_f result at a deviation of 95%, 90%, 80% and 50%. This value is set to zero if no intersection exists.
   g. **Ergebnisse**: Listing of the N_f results from f.
   h. **THM_ADB_VorReduktion**: Table as e. after prefiltering.
   i. **THM_ADB_NachReduktion**: As table h. after a second filtering. This table contains additional information for the specimen identifier, i.e. path: "cyclic data files".
   j. **TAx-FileNames**: All existing TA-Files without duplication.
   k. **Diagr.StressRangeversusCycles**: Diagram of stress range vs. cycles.
   l. **Diagr.StrainRangeversusCycles**: if existing, diagram of strain range vs. cycles.
   m. **Diagr.InelStrainRangevsCycles**: if existing, diagram of inelastic strain range vs. cycles.

   - Type of file "**TMx000nn-ADB_Reduktion.xls**":

     This type of data contains data of selected hysteresis of the individual TMF tests with all additional information.

2. File "**HystereseDateien**":

   - Type of file "**TAx000nn\ Hyst_TAx000nn_Zmmm.xls**": (with “x” as the test facility number, i.e. the letter A to I, and “nn” the current number in the column “Test identifier” of Tabs. 7-3; 7-6; 7-10; 7-17; 7-22; 7-29 and 7-33. ”Zmmm” denominates the selected cycle number.)

   This type of file contains data for selected hysteresis of individual specimens with full identification. For clearer view each test has its own file named: "TAx000nn".

   Beside the individual data sheets "TabHyst_TAx000nn_Zmmm" additional information is available in form of diagrams:

   1.) Diagram "**ChartHystStressStrain**" => Diagram of hysteresis of the specimen in cycle "Zmmm" as well as

   2.) Diagram "**ChartHystStressTime**" => Diagram of time dependence of stress of the specimen in cycle "Zmmm".

10 EFDA Task Sheet

REPORT for TASK of the EFDA Technology Programme			
Reference:	Field: Tritium Breeding and Materials Area: Materials Development Task: TW2-TTMS-002a (formarly TW1-TTMS 002) RAFM Steels: Metallurgical and Mechanical Characterisation Deliverable No. 19		
Document:	Thermo mechanical fatigue testing on EUROFER 97 and selected Reduced Activation Ferritic Martensitic (RAFM) Steels		
Level of confidentiality	Free distribution ☐ Confidential ☐ Restricted distribution **X**		
Author(s):	Claus Petersen, Forschungszentrum Karlsruhe (FZK)		
Date:	24. June 2009		
Distribution list:	Rainer Laesser (Field Co-Ordinator/) Eberhard Diegele (Responsible Officer) Farhad Tavassoli (Project Leader)		
Abstract:	Blanket Modules of a future nuclear fusion reactor are subjected during service to alternating thermal and mechanical stresses as a consequence of the pulsed reactor operation. Therefore the Thermo-Mechanical Fatigue (TMF) behaviour of ferrite/martensite stainless steels, as its structural material, is examined. After the development of the testing method and the setup of the facilities for TMF testing a series of different materials had been examined. After a peer selection process evaluated data of about 350 TMF-experiments, with and without hold times, performed in the last 15 years, have been transferred into the Mat-DB, the data bank system of the Joint Research Center, Petten. TMF results of examined steels show a remarkable reduction in life time compared to isothermal low cycle fatigue (LCF) tests. The application of hold times in TMF-experiments leads to different damage reaction than during LCF loading. Micro structural evaluation during both cyclic loading procedures is very similar and gives no indication of the different damage behaviour.		
Revision No: 0	Changes:		
	Written by:	Revised by:	Approved by:
	C. Petersen	Dr. J. Aktaa	Prof. Dr. O. Kraft